CHEMICAL REVIEWS

pubs.acs.org/CR

Review

Open Access

This article is licensed under CC-BY 4.0

The Chemistry of CO_2 Conversion: A Review

R. Gary Grim,* Alex Badgett, Wade A. Braunecker, Michael T. Guarnieri, Susan E. Habas, Christopher Hahn, Kenneth Neyerlin, Aditya Prajapati, Daniel A. Ruddy, and Roxanne Z. Walker

Cite This: *Chem. Rev.* 2026, 126, 5028−5082

Read Online

ACCESS | Metrics & More | Article Recommendations | Supporting Information

ABSTRACT: For much of the past century, carbon dioxide (CO_2) has received little attention scientifically outside of its role as a byproduct in the industrialization of the global economy. This trend has recently been upended where, due to mounting environmental concerns, CO_2 has been brought squarely into the public consciousness. This surge in activity has contributed to a once unimaginable idea now pervading the scientific community: could CO_2, a highly stable byproduct of hydrocarbon combustion, be recycled and converted back into useful chemicals and fuels? Owing to its ubiquitous nature and availability at truly massive quantities, it is thought that CO_2-based products could offer a meaningful pathway toward lowering the environmental impact of many of the top industrial products while also enhancing supply chain diversification and resilience. In this manuscript we provide a holistic review of the pathways for CO_2 conversion, the underlying chemistry and challenges involved in the transformation to products, and considerations for commercialization.

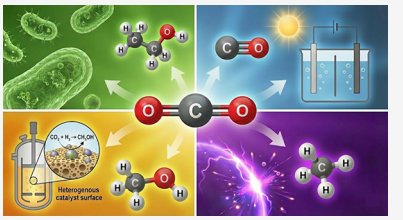

Downloaded via ACS Test Institution on June 17, 2026 at 16:05:52 (UTC).
See https://pubs.acs.org/sharingguidelines for options on how to legitimately share published articles.

CONTENTS

1. Introduction 5028
2. Electron-Mediated CO_2 Conversion 5030
  2.1. Low-Temperature Electrolysis 5030
  2.2. High-Temperature Electrolysis 5036
  2.3. Non-Thermal Plasma 5039
  2.4. Photochemical Reduction 5040
  2.5. Microbial Electrosynthesis 5042
3. H_2-Mediated CO_2 Conversion 5044
  3.1. CO_2 Hydrogenation 5044
  3.2. Nonthermal Plasma CO_2 Hydrogenation 5047
  3.3. CO_2 Fermentation 5049
4. Emerging Trends in CO_2 Conversion 5050
  4.1. Reacting Bound States of CO_2 via Reactive Carbon Capture (RCC) 5050
  4.2. Synthetic CO_2 Assimilation Pathways 5052
5. Cross-Comparison of CO_2 Conversion Pathways 5054
  5.1. Energy Efficiency 5054
  5.2. Carbon Conversion Efficiency 5055
  5.3. Product Selectivity 5056
  5.4. Pathway Strengths, Active Research Areas, and Scalability 5056
    5.4.1. Microbial Electrosynthesis 5056
    5.4.2. Photocatalysis 5056
    5.4.3. Non-Thermal Plasma 5056
    5.4.4. Low-Temperature Electrolysis 5057
    5.4.5. High-Temperature Electrolysis 5058
    5.4.6. Biochemical Conversion 5058
    5.4.7. Thermocatalysis 5058
6. Logistics for CO_2 Conversion Chemistry and Barriers to Scale Up 5059
  6.1. Sourcing Electricity 5059
  6.2. Sourcing H_2 5062
  6.3. Sourcing CO_2 5063
  6.4. Economics and Scale Up of CO_2 Conversion 5064
  6.5. Environmental Impacts of CO_2 Conversion at Scale 5067
7. Conclusions and Outlook 5068
Associated Content 5068
  Supporting Information 5068
Author Information 5069
  Corresponding Author 5069
  Authors 5069
  Author Contributions 5069
  Notes 5069
  Biographies 5069
Acknowledgments 5070
References 5070

1. INTRODUCTION

Over the past decade, estimates suggest nearly 360 billion tonnes of carbon dioxide (CO_2) were emitted as a result of human activities, pushing atmospheric concentrations in excess of 419 ppm, a level not seen on Earth in some three million years.[1,2] As concerns over the impact of rising CO_2 emissions continue to grow, policymakers and scientists around the globe are being called into action to pursue strategies for mitigation.[3]

Received: April 30, 2025
Revised: March 16, 2026
Accepted: April 9, 2026
Published: April 21, 2026

© 2026 The Authors. Published by American Chemical Society

Once unimaginable, one of the prevailing ideas now receiving widespread international attention is the concept using the CO_2 molecule itself as a carbonaceous resource for producing the chemicals and fuels consumed in everyday life.[4−8] Specifically, in processes colloquially referred to as "Power-to-X", "e-fuels", or "e-products", by pairing electrons or other electricity-sourced energy carriers (e.g., H_2) with novel conversion pathways across electrochemistry, photochemistry, plasma science, biology, and thermochemistry, recent studies have shown proof of concept for the transformation of CO_2 into a variety of species spanning a range of chemical functionalities.[4,9−11] Comprising predominantly lower molecular weight species such as carbon monoxide (CO), methanol (MeOH), methane (CH_4), ethanol (EtOH), and ethylene (C_2H_4), it is proposed that many of the top industrial products could be synthesized from these platform molecules as e-products through technically mature routes such as Fischer−Tropsch (FT), methanol-to-olefins (MTO), and other established chemical pathways currently utilized across industry.[12]

Within the past several years support for CO_2 conversion and e-products has moved from a fringe concept relegated to academic laboratories to now entering the mainstream where some companies are actively pursuing and/or operating pilot and commercial scale operations based around CO_2 conversion. Governments worldwide have also begun to show support for CO_2 conversion, highlighted by recent policies from the United States (e.g., SAF Grand Challenge, 45Z credits)[13] and in the European Union. As part of the recently announced ReFuelEU aviation program, mandates are now in place that require fuel suppliers to gradually increase the amount of synthetic fuel (i.e., CO_2-based e-fuels) across EU airports from 1.2% of total fuel supplied in 2030 to 35% in 2050.[14]

The conversion of CO_2 is not without its challenges, however.[4] Shown in Table 1, the CO_2 molecule represents a significant departure from the conventional feedstocks on which current economies are based. Being itself a product of the hydrocarbon combustion reaction, CO_2 has no intrinsic energy content (i.e., heating value), exists in a highly stable and fully oxidized state, and is comprised predominately of oxygen (~73% by mass). By comparison, conventional feedstocks like crude oil and natural gas are comprised of less than 1.5% oxygen by mass and carry a significantly higher inherent energy content in the range of 42 − 47 MJ/kg, providing a favorable starting point for the synthesis of fuels and chemicals. Indeed, prior to 15−20 years ago, the idea of CO_2 conversion to hydrocarbon products would be considered by most as nonsensical. In addition to the uphill energetic challenges of rebuilding a CO_2 molecule, when powered by energy sources or reactants that are predominately fossil in origin, the conversion itself will, in most instances, be more energy intensive and costly and therefore generate even more CO_2 emissions than simply making the products directly from conventional resources.[15−18]

Table 1. Heating Values and Oxygen Content Across CO_2 and Common Feedstocks

	Lower Heating Value (MJ/kg)[a]	Oxygen Content (w/w %)
Carbon Dioxide	0.0	72.7
Natural Gas	47.1	0.01
Crude Oil	42.7	<1.5
Bituminous Coal	26.1	6−8
Corn Stover	16.4	41.5[b]
Sugar cane Bagasse	15.1	48.8[c]
Woody Biomass	19.6	41.2[d]
Hydrogen Gas	120.2	0.0

[a]Ref 19. [b]Ref 20. [c]Ref 21. [d]Ref 22.

However, as the rate of renewable energy deployment has increased dramatically in recent years and the cost has, in some areas of the world, reached a point lower than conventional fossil energy,[23] that paradigm is now beginning to shift. Some forward-looking analyses now find that despite being an inherently energy intensive process, if low carbon intensity electricity is made widely abundant at low enough cost, CO_2 conversion pathways could potentially produce products at a price point at, or even below, that of conventional fossil-based products with, in most cases, a significantly lower carbon emissions profile.[24−26] This realization combined with the explosive growth of renewable energy has led to a flurry of activity in CO_2 conversion research where over the past 15 years the number of publications referencing "CO_2 conversion" has increased exponentially from only ~ 300 in 2010 to now over 4,700 per year in 2024 (Figure 1).

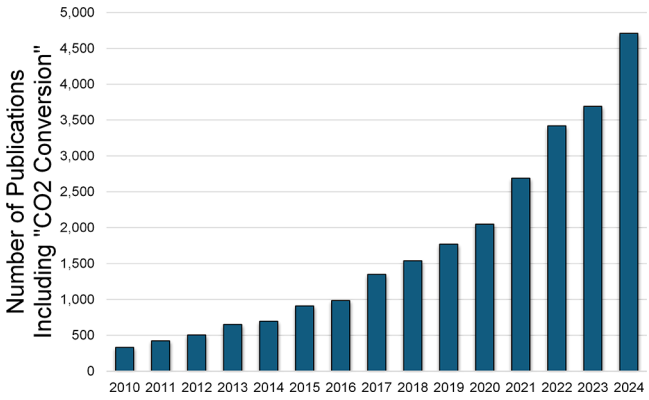

Figure 1. Number of publications by year mentioning the term "CO_2 Conversion" as indexed by Google Scholar.

This emerging intersection of low-cost and low-carbon intensity electricity with CO_2 conversion has significant potential implications for global carbon circularity and the future of sustainable products. Owing to its abundance in the carbon cycle, CO_2 represents a sustainable carbon resource available in truly massive quantities, sufficient to easily meet the entire global demand for carbon-based products many times over.[4] By reusing this abundant "waste" carbonaceous resource, it creates the opportunity for a closed-loop circular carbon economy whereby products with a near carbon-neutral footprint are possible. Another key differentiator of CO_2 is that it is not geographically constrained to any one region but rather is ubiquitous across the globe. This widespread availability combined with the ability to potentially source directly from the atmosphere via direct air capture (DAC) without the need for extensive transportation infrastructure creates unique opportunities in siting and colocation that may offer strong economic incentives. This potential for a self-contained feedstock-to-product design increases the inherent resiliency of supply chains which in the future could serve to

https://doi.org/10.1021/acs.chemrev.5c00361
Chem. Rev. 2026, 126, 5028−5082

ease or avoid entirely disruptions like those felt in the early 2020s (e.g., global pandemic, geopolitical conflicts).[27,28]

Ultimately, unlocking the future potential of CO_2 conversion and e-products will rely on solving two fundamental challenges: (1) the ability to source low-carbon intensity electricity at a sufficiently low price point and high capacity factor to provide compelling economic opportunities, and (2) the ability to efficiently and selectively channel that energy toward CO_2 conversion via carbon-carbon and carbon-hydrogen bond formation. While renewable energy deployment is accelerating,[29] conversion efficiencies remain a significant bottleneck.[30,31] Recent studies estimate the current energy return on energy invested (EROEI) for some CO_2-derived products at 0.33 or lower, meaning the net energy demand for synthesis, CO_2 capture, and energy infrastructure is triple that of the energy ultimately delivered by the product.[32] Compared to conventional products (e.g., system-level EROEI $\sim 11-14$ for SMR-sourced methanol), these low values represent a significant thermodynamic gap. Given that an EROEI of > 3 is generally cited as the minimum threshold to be "useful" for society,[32] low energy efficiency CO_2 conversion puts e-products at risk of being "energy sinks" at a time when energy demand worldwide continues to accelerate meaningfully.[8] While system-level EROEI of e-products is inextricably linked to the primary energy source—where high EROEI sources like nuclear power (>50) offer a robust baseline—this reality underscores a critical need in the field of CO_2 conversion is an improved fundamental understanding of the chemical mechanisms and challenges in efficiently utilizing the reducing potential of electrons and other energy carriers to boost system-level efficiency.

In this review we discuss the recent advancements in the fundamental understanding in CO_2 conversion chemistry across seven prominent conversion pathways and, importantly, assess how this knowledge contributes to the rational design of processes, improvements in technical performance, and ultimately the viability of CO_2 conversion. To focus the scope of this review, we consider only reports published in the last six years ($2020-2025$) and cover only the processes associated with the conversion of CO_2 to value-added products or intermediates. In other words, we highlight only the chemical pathways that directly convert CO_2 and do not include discussion on subsequent downstream upgrading steps (e.g., syngas chemistry, alcohol upgrading, etc.) which have been reviewed elsewhere.[33,34] Herein we structure the review based on the way in which energy is consumed. In the first part of the review, electron-mediated conversion chemistries such as electrolysis, photocatalysis, nonthermal plasma, and microbial electrochemical processes are reviewed. In the following section, we consider H_2-mediated chemistries including CO_2 hydrogenation via thermocatalysis and biological conversion of CO_2 via fermentation. In the final sections of the manuscript, we review emerging trends across CO_2 conversion chemistry, compare pathways using cross-cutting technical metrics, discuss the logistics and barriers to scaling up CO_2 conversion, and highlight future R&D priorities for CO_2 conversion technologies.

2. ELECTRON-MEDIATED CO_2 CONVERSION

2.1. Low-Temperature Electrolysis

Low-temperature electrolysis (LTE) for CO_2 is an electrochemical process that converts CO_2 into value-added chemical feedstocks using electrical energy.[35] This pathway typically operates between 25−80 °C and in a pressure regime of 1−20 bar.[35] These operating parameters distinguish it substantially from high-temperature solid-oxide electrolysis (SOEC), which requires temperatures in excess of 800 °C to utilize solid-state ion conductors.[35,36]

LTE presents a strategic pathway toward industrial decarbonization. It provides a direct electrochemical route to convert CO_2 into value-added fuels and chemicals, offering an alternative pathway to replace the traditional energy and emissions-intense thermocatalytic, fossil-fuel-based processes. Furthermore, LTE systems can function as a flexible electrical load, capable of utilizing surplus renewable electricity from intermittent sources such as solar and wind. This capability addresses the challenge of grid instability from renewable curtailment and enables greater penetration of clean energy.[35,37] The primary strengths of this pathway lie in its direct conversion of electrical energy into storable chemical bonds, its operation under mild conditions that are compatible with existing industrial infrastructure, its modularity that provides practical advantages for distribution site selection and operational flexibility, and its feedstock versatility in utilizing waste CO_2 as a carbon source. The overall process of LTE is driven by a full electrochemical cell, which comprises two distinct half-reactions. At the cathode, the negative electrode, CO_2 is reduced in the CO_2 reduction reaction (CO_2RR) to form a variety of chemical products such as CO, Formic acid, ethylene, etc. At the anode, the positive electrode, a corresponding oxidation reaction (typically, water oxidation) must occur to complete the electrical circuit.[38] Detailed half reactions on cathode and anode are provided in the Supporting Information.

Currently, the high-rate LTE research for CO_2RR is centered on the membrane electrode assembly (MEA), a zero-gap electrolyzer architecture adapted from fuel cell technology.[39] This design minimizes ohmic resistance, enabling the high current densities required for commercial viability. While a detailed breakdown of device components is available in the Supporting Information, the main chemistry of a CO_2 electrolyzer is centered at the cathode.[40] Cathode is fabricated as a porous gas diffusion electrode (GDE), a complex structure engineered to create a stable three-phase interface for gaseous CO_2 reactant, a liquid electrolyte or ionomer phase for ion transport, and the solid heterogeneous catalyst surface where the electrochemical reaction occurs. At the anode, oxygen evolution reaction (OER) occurs to complete the electrical circuit while an ion-conducting polymer membrane is positioned between the electrodes to transport ions and prevent reactant and product crossover.

To evaluate and compare the chemical performance of these systems, a set of key metrics is described here with further details on their calculations in Supporting Information. (1) Faradaic Efficiency (FE,%): This quantifies the selectivity of the process, defined as the fraction of total electrons that are used to form a specific, desired product. (2) Partial Current Density (j, mA/cm^2): This represents the productivity or rate of product formation per geometric electrode area. (3) Full-Cell Energy Efficiency (EE,%): The overall energy conversion efficiency, representing the ratio of the Gibbs free energy stored in the chemical product to the total electrical energy consumed by the cell. (4) Single-Pass Carbon Conversion (SPC): The fraction of CO_2 reactant converted into products in a single pass through the reactor.

https://doi.org/10.1021/acs.chemrev.5c00361
Chem. Rev. 2026, 126, 5028−5082

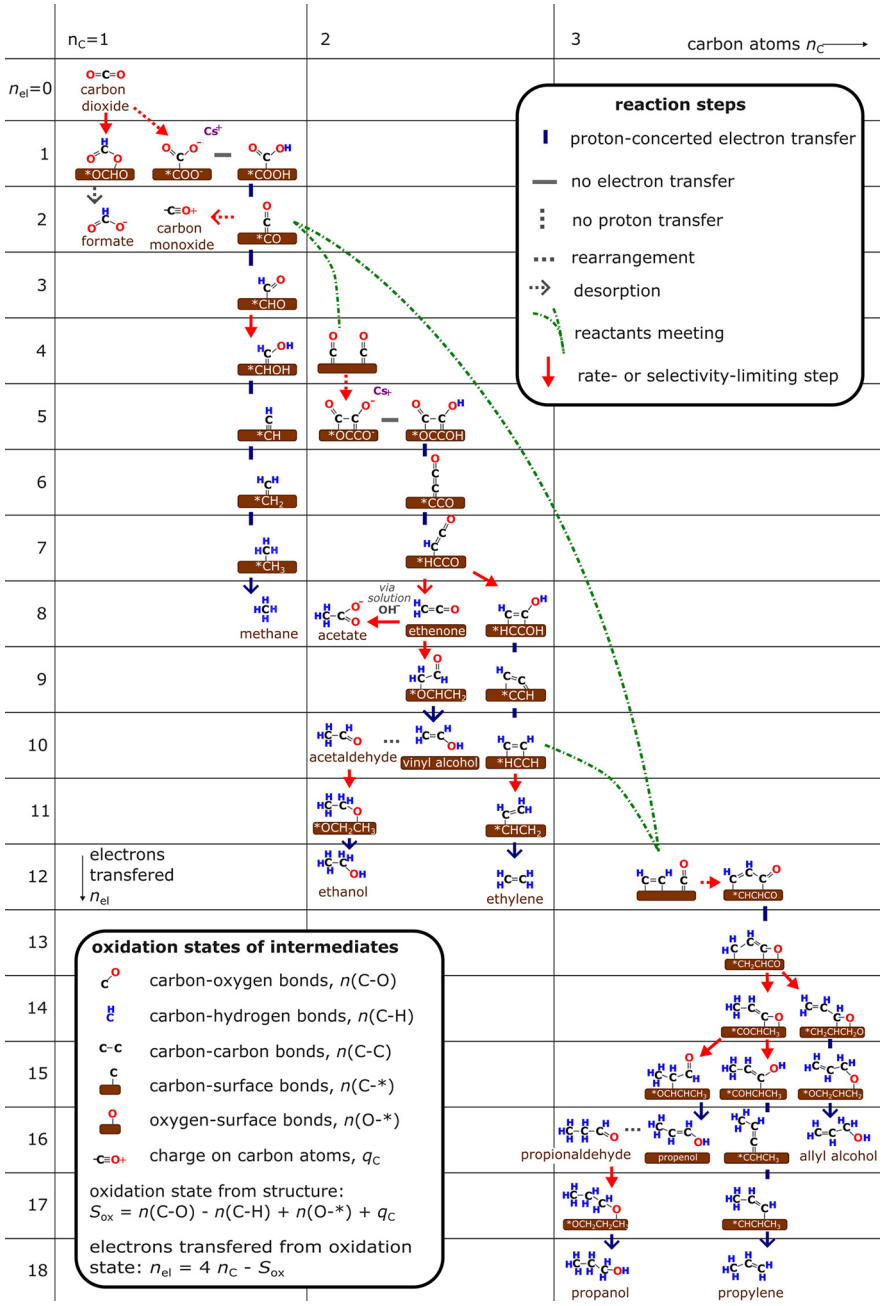

Figure 2. Proposed reaction network for the electrochemical reduction of CO_2 to various C_1, C_2, and C_{3+} products. The formation of the *CO intermediate is a key branching point for many reaction pathways. Adapted from ref 40. Copyright 2025 American Chemical Society. Although the figure reflects the consolidated, post-2020 understanding of CO_2RR pathways, many of the mechanistic elements that define this network originated from pre-2020 work as shown in ref 38.

The field CO_2RR is chemically broad, spanning multiple classes of catalysts.[38,41,42] We acknowledge that seminal advances in homogeneous catalysis using molecular catalysts (e.g., transition-metal complexes) dissolved in solution, and immobilized catalysis, have played a formative role in shaping the mechanistic understanding of CO_2 activation and product selectivity. Ligand-controlled electronic structure, hydride transfer chemistry, and site isolation, have directly influenced heterogeneous motifs including Co-complex–derived methanol catalysts, atomically dispersed M-N-C sites, and other hybrid architectures.[42] Consequently, heterogeneous catalysis, that utilizes solid-state materials such as metal nanoparticles (e.g., Cu, Ag, Sn), oxide-derived materials, and carbon-based catalysts,[38,39] has shown a clearer translation of the chemistry advances toward scalable, high-current-density electrolyzer systems has been achieved using heterogeneous materials. Therefore, this section of the review will bound its discussion and focus exclusively on the advances in the chemistry of heterogeneous catalysis for CO_2RR. We emphasize how reaction mechanisms, interfacial chemistry, and catalyst-ionomer interactions have guided the design of the modern design-principles of low temperature electrolyzers. In that framework, we have organized this discussion chronologically from foundational mechanistic insights prior to 2020, to the post-2020 advances in electrolyzer design and microenviron-

https://doi.org/10.1021/acs.chemrev.5c00361
Chem. Rev. 2026, 126, 5028−5082

ment control and concluded by identifying key opportunities that will define the field's trajectory.

Prior to 2020, foundational discoveries established the core principles of reaction mechanisms, the critical influence of catalyst restructuring and the local chemical environment, and the emergence of the scale-up bottleneck inclusive of an energy penalty related to carbonate crossover. This period saw the field grow from fundamental studies in aqueous H-cells to the first high-rate gas-phase electrolyzers. The pioneering work of Hori et al. established that product selectivity in CO_2RR is, to a first approximation, determined by the identity of the metal electrocatalyst.[43] The selectivity of these metal electrocatalysts for CO_2RR, later rationalized by computational density functional theory (DFT) studies,[38,44] identified distinct product classes. In the case of C_1 products (CO and Formate), the initial branching of CO_2 reduction is dictated by the binding of the first intermediate. Metals such as Au, Ag, and Zn weakly bind carbon. They are believed to stabilize CO_2 adsorption and the *COOH intermediate, which, after a second electron−proton transfer, desorbs as CO.[40] In contrast, oxophilic metals like Sn, Bi, and In preferentially stabilize the oxygen-bound *OCHO intermediate,[45] which is subsequently reduced to formate ($HCOO^-$).[38,40] For C_{2+} products, Cu is unique among elemental metals in its ability to catalyze the reduction of CO_2 to valuable multicarbon products, such as ethylene (C_2H_4) and ethanol (C_2H_5OH).[46] This multielectron ($12e^-$ for ethylene), multiproton pathway is vastly more kinetically complex than the $2e^-$ pathways to C_1 products.[44,47,48]

The activation of CO_2 and subsequent reduction steps were often described within the framework of proton-coupled electron transfer (PCET), where an electron transfer from the electrode and a proton transfer from solution occur in a concerted fashion.[49] While the PCET model is powerful, particularly for describing the initial CO_2-to-*COOH step, it is now understood to be an oversimplification for the entire complex reaction network.[38,40] A more nuanced understanding, developed through both computational and experimental work,[50] posits that many key transformations may proceed via decoupled sequential pathways (e.g., an electron transfer followed by a separate proton transfer step) or as pure chemical steps (e.g., protonation of a surface intermediate without a simultaneous electron transfer).[40] The dominant mechanism (concerted, sequential, or chemical) is highly dependent on the applied potential, local pH, and specific catalytic environment.[51] A representative reaction network based on the aggregate view that the field proposes is shown in Figure 2. An important mechanistic challenge that emerged is the bifurcation between the ethylene and ethanol pathways. Extensive computational and *operando* studies have proposed competing routes involving *HCCO, HCCHO, or H_2CCHO intermediates,[52−54] yet no conclusion has been reached on the precise branching point. This uncertainty mirrors the broader ambiguity surrounding C_{3+} formation mechanisms, where multiple multielectron, multiproton pathways remain kinetically and spectroscopically indistinguishable. Additionally, the challenge of sequential and multiple C-C coupling steps lead to low selectivity of C_{3+} hydrocarbons.[38,39] A more practical strategy, established in this period, is a two-step hybrid approach: (1) LTE is used to produce a simple, energy-dense building block like CO (or syngas) at high selectivity, and (2) this intermediate gas is then fed into established thermocatalytic processes like Fischer−Tropsch synthesis for upgrading.[38,55] CO reduction in tandem with CO_2RR emerged as another complementary route that enables higher selectivity for C_{3+} liquid products and oxygenates.[56] These parallel two-step strategies broaden the design space for producing more complex hydrocarbons from CO_2.

Research prior to 2020 also established that beyond just catalyst metal identity, CO_2RR is highly sensitive to more subtle factors such as the catalyst's physical structure and its local chemical environment. Surface-science studies demonstrated that CO_2RR on Cu is structure-sensitive.[57,58] The Cu(100) facet was shown to be more selective for ethylene, whereas Cu(111) preferentially produced methane. This was attributed to the different adsorption energies of key intermediates on these distinct atomic arrangements.[35] A breakthrough was the discovery of oxide-derived (OD) catalysts (e.g., Cu derived from Cu_2O reduction).[59−61] These high-surface-area, structured materials exhibited dramatically enhanced C_{2+} selectivity compared to their nanoparticle or foil counterparts.[39] This enhancement was hypothesized to be due to a combination of high porosity, stable grain boundaries, and a high density of active defect sites.[57] Similar structural engineering principle were observed in C_1 catalysts such as Ag[62] and Sn[63] for enhanced activity and selectivity.

For the local chemical environment, two factors were identified as major modulators of reactivity. First, the local pH at the catalyst surface, which can be significantly higher than the bulk electrolyte during reaction, was shown to suppress the competing HER.[64−66] Second, a strong promotional effect was identified for large alkali metal cations (e.g., Cs^+, K^+).[67,68] The consensus mechanism proposes that these large, weakly hydrated cations accumulate at the outer Helmholtz plane, creating an intense local electric field.[69] This field is believed to stabilize the negatively charged $*CO_2^-$ transition state, lowering the kinetic barrier for CO_2 activation, while also structuring interfacial water to suppress HER.

By 2020, the field's momentum for high FE and current density led to the widespread adoption of the Anion Exchange Membrane (AEM) electrolyzer.[35] The chemical rationale was to use AEMs to selectively transport anions (OH^-), creating a highly alkaline local environment at the cathode, thereby suppressing HER and promoting CO_2RR. However, the same alkaline environment drives the rapid reaction of CO_2 with OH^- to form carbonate: $CO_2 + 2OH^- \rightarrow CO_3^{2-} + H_2O$. This carbonate becomes the primary charge-carrying species and migrates across the AEM to the anode, where it is neutralized by protons from OER and rereleased as CO_2 gas: $CO_3^{2-} + 2H^+ \rightarrow CO_2 + H_2O$. This carbonate crossover problem establishes a stoichiometric limit on carbon conversion efficiency. For the 2-electron reduction to CO (which produces $2OH^-$), a 2-charge CO_3^{2-} must cross the membrane to balance the charge. Therefore, for every one mole of CO produced, one mole of CO_2 is wastefully transported and lost to the anode. This fixes a theoretical maximum SPC of 50% for CO (and a similarly derived 25% for ethylene).[70] It is important to note, however, that this theoretical limit is not universal. Under operating regimes where OH^- is a dominant charge carrier, the effective maximum SPC may exceed these constrained values. These observations remain anecdotal and system-dependent,[71,72] but they indicate that charge-carrier identity is a function of local chemistry rather than a fixed boundary condition. In any case, the CO_2 lost due to carbonate crossover to the anode must be separated from the oxygen stream (an energy-intensive process) and recycled, imposing a massive energy penalty

https://doi.org/10.1021/acs.chemrev.5c00361
Chem. Rev. 2026, 126, 5028−5082

that could undermine the entire economic viability of the technology. This realization was a critical inflection point, demonstrating that simply optimizing catalysts within the dominant AEM architecture was an insufficient and perhaps nonviable path to commercialization. It motivated the field to consider alternative electrolyzer designs where differences in ion transport and interfacial chemistry could open new pathways for improving performance in the coming years.

By 2020, increasing technological maturity and growing private-sector interest pushed the field toward more integrated MEA and device-level studies. This transition revealed a broader set of transport and interfacial challenges that emerge only under industrially relevant conditions. Research efforts rapidly diversified, moving beyond simple catalyst optimization in AEMs to two new, interconnected frontiers: 1) the rational design of novel electrolyzer architectures explicitly to mitigate or eliminate carbonate crossover,[73−75] and 2) a more fundamental investigation into the catalytic microenvironment[76,77] to gain new levers of control over reaction pathways. The primary response to the stoichiometric limitations of AEMs led to the development and optimization of systems based on bipolar and proton exchange membranes.

Bipolar Membranes (BPMs) are composite structures containing both an anion exchange layer (AEL) and a cation exchange layer (CEL). This structure acts as a physical barrier to anion transport from cathode to anode, chemically isolating the two compartments. In the reverse-bias configuration (with the CEL facing the cathode), the cathode becomes acidic, which reduces carbonate formation but introduces a substantial challenge: the high proton concentration favors HER, resulting in very low FE's for CO_2RR.[78,79] Conversely, the forward-bias configuration (with the AEL facing the cathode) maintains a kinetically favorable alkaline environment at the cathode. Here, H^+ from the anode and OH^- from the cathode migrate into the membrane junction where they recombine to form water, enabling a pure-water anolyte feed and avoiding salt precipitation and carbonate crossover. However, this architecture introduces a mechanical-integrity challenge of accumulation of CO_2 and water at the internal membrane junction can lead to delamination or catastrophic cell failure,[73,79,80] though recent approaches involving perforated layers incorporated into BPMs have the potential to mitigate these failure modes.[81] BPM systems mitigate carbonate crossover by introducing an internal water-dissociation junction, but this approach can impose additional energy and transport penalties. As a result, parallel efforts have been explored in proton exchange membrane (PEM)-based architecture to eliminate the formation of carbonate.

Running CO_2 electrolysis using a PEM eliminates carbonate formation but historically was considered impractical because the high H^+ concentration at the cathode favors HER.[82] Post-2020 work has shown that this limitation is not absolute: by engineering the local microenvironment, specifically introducing high concentrations of alkali metal cations into the acidic catalyst layer, the cation-effect can stabilize CO_2RR intermediates and suppress HER,[82,83] enabling meaningful CO_2RR activity even under acidic conditions. Although still emerging, this approach offers a promising path toward carbonate-free CO_2 electrolysis in proton-conducting architectures.

Since 2020, advances in device architecture have been accompanied by a more fundamental understanding of the catalytic interface where water activity, ionomer structure, and organic additives directly influence reaction pathways.[76,84] The field has begun to appreciate water not just as a passive solvent, but as a tunable reactant and mediator. A notable 2023 study demonstrated that tuning the activity of water, by adding hygroscopic solutes to the electrolyte, is a powerful and previously unrecognized lever for controlling selectivity.[85] The key finding was that lowering the water activity suppressed the formation of H_2 and CO, but promoted the formation of desirable C_{2+} multicarbon products.[85] Another study shows the deviations in water and solute activities within concentrated electrolytes alters reaction energetics and mass-transport profiles, directly influencing CO_2RR product distributions and validating water-activity tuning as a mechanistic control parameter.[86] This provides a novel strategy to modulate microenvironment to influence reaction selectivity.

A parallel strategy for engineering the microenvironment involves the use of organic additives or advanced polymer electrolytes.[87] Recent work has shown that tailored organic films can assemble on Cu surfaces and act as selective proton-transport barriers, attenuating the flux of H^+ to the catalytic interface and thereby suppressing HER even under acidic conditions.[88] Building on this, a 2024 study demonstrated that engineered organic thin films can stabilize otherwise transient Cu^+ species under CO_2RR conditions and reshape the interfacial ionic environment, leading to enhanced C_{2+} selectivity.[89] Collectively, these additive-based approaches provide a chemical route to modulate interfacial transport and reactivity, enabling > 70% FE to multicarbon products in environments that would otherwise be dominated by HER. Historically, the ionomer within the catalyst layer was viewed primarily as a structural binder and ionic conductor. However, a growing body of post-2020 literature has demonstrated that the ionomer has a direct and active influence on CO_2RR kinetics and selectivity.[90] Recent studies have shown that ionomer chemistry, including fixed charge, hydrophobicity, and molecular architecture, can substantially alter local solvation, interfacial pH, and the adsorption thermodynamics of key intermediates.[90−92] *Operando* spectroscopic measurements have been instrumental in establishing these effects. Using *operando* Raman, FTIR, and synchrotron-based techniques, researchers have shown that anionic fluorinated ionomers such as Nafion and cationic AEMs such as Sustainion produce measurably different *CO adsorption behaviors at Cu and Ag surfaces, leading to divergent selectivity between CO and C_{2+} products.[93] These measurements provide direct evidence that the ionomer controls local intermediate coverage rather than merely facilitating ion transport. In a notable recent study, the combination of operando Raman spectroscopy and differential electrochemical mass spectrometry yielded the first spectroscopic detection of a *CCO-type intermediate at the electrode/polyelectrolyte interface, confirming the role of the ionomer in stabilizing multicarbon pathways under realistic operating conditions.[94] The convergence of these insights such as ionomer-induced local pH gradients, cation-ionomer interactions, solvation structure, and interfacial conformational effects, marks a substantive evolution in the mechanistic understanding of CO_2RR. Rather than treating the electrode as immersed in a spatially uniform bulk electrolyte, current models recognize the reaction as occurring within a nanometer-scale, dynamic interphase governed by the specific arrangement of polymer chains, ions, and water molecules. This interphase-centric view has become foundational for the rational design of next-generation catalyst layers, ionomers, and MEAs optimized for high-rate, selective CO_2RR. Figure 3

https://doi.org/10.1021/acs.chemrev.5c00361
Chem. Rev. 2026, 126, 5028−5082

further shows the evidence that ionomer is not merely a passive binder but an active component that directly modulates the local environment.

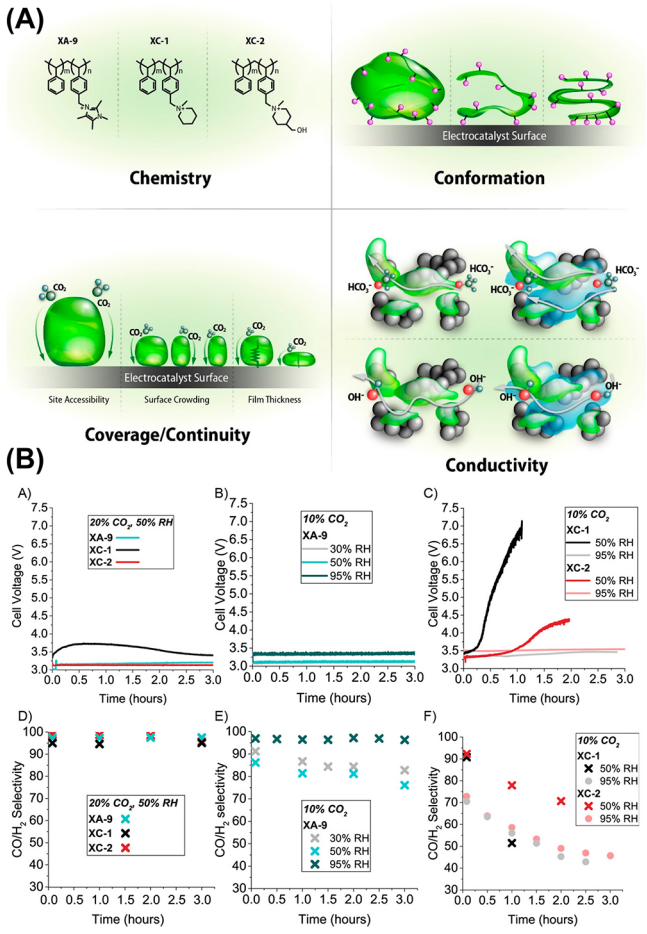

Figure 3. (A) A schematic illustrating the various impacts that ionomer properties such as chemistry, conformation, and coverage can have on the electrochemical properties of the electrode and the local reaction environment. (B) Effect of different ionomers on CO_2 electrolyzer performance. Adapted from ref 92. Copyright 2024 American Chemical Society.

The deeper understanding of interfacial chemistry has been crucial for reframing durability not as a late-stage engineering problem, but as a set of fundamental chemical challenges rooted in transport phenomena and materials stability that need to be addressed in early stage research.[95] Traditionally treated as an engineering problem, degradation is increasingly recognized as a chemically driven phenomenon governed by the stability and reactivity of interfaces under nonequilibrium conditions. The coupling of electrochemical potentials, local pH gradients, and reactive intermediates gives rise to self-evolving catalyst structures and complex transport failures. A major advance, driven by *operando* characterization studies,[96,97] highlights that catalysts are not static entities. Under the harsh, reducing potentials of CO_2RR, metal surfaces are dynamic. A key finding on Cu is that the reaction may not even occur on the as-synthesized perfect (100) or (111) facets. Instead, the strong adsorption of the *CO intermediate provides a thermodynamic driving force for the catalyst to reconstruct, forming a high density of active steps and kinks. The true active site is now believed to be a dynamic structure created during the reaction, often at sites adjacent to these defects.[98] This insight helps explain why disordered, high-defect materials like OD-Cu show such high C2+ selectivity.

A significant fraction of catastrophic cell failures in low-temperature CO_2 electrolyzers can be traced to chemical transport imbalances rather than mechanical failure modes. These degradation phenomena originate from the coupled migration of ions, water, and reactive species across porous and polymeric interfaces, which collectively determine the stability of the local reaction environment. Among the most pervasive chemical degradation pathways is salt precipitation, a consequence of ion crossover and carbonate accumulation. In AEM systems, cations such as K^+ from the anolyte migrate across the membrane and encounter the high local concentrations of carbonate and bicarbonate species generated at the cathode. $KHCO_3$ nucleates and grows within the GDL pores which obstructs gas pathways, impedes CO_2 access to active sites, and can lead to abrupt, irreversible cell failure.[78] The local water content (λ, or water molecules per ionic group) in the ionomer is a critical descriptor for designing an efficient catalyst.[91] Maintaining the appropriate λ requires balancing electro-osmotic drag, which pulls water from anode to cathode, with back-diffusion, which drives water in the opposite direction resulting in either flooding or dehydration of the GDE. Flooding (high λ) occurs when excess hydration leads to liquid water accumulation within GDL pores, blocking gaseous CO_2 transport and suppressing catalytic activity. Dehydration (low λ) takes place when insufficient hydration dries the membrane and ionomer, reducing ionic conductivity and inducing mechanical cracking due to differential swelling stresses. This balance of water uptake is not only a physical property but also a chemical descriptor of selectivity, as local water activity directly modulates CO adsorption strength and C-C coupling probability. A representative data set in Figure 4 illustrates this relationship, showing how ionomer hydration levels influence ethylene FE at 200 mA cm^{-2}. Advances in understanding these coupled transport phenomena have guided the rational design of hydrophobic GDL architectures and the implementation of controlled humidification and thermal management strategies, enabling sustained operation and improved long-term stability. A comparative summary of the degradation mechanisms, trade-offs, and mitigation strategies across state-of-the-art CO_2RR architectures is tabulated in the *Supporting Information*.

The fundamental chemical insights gained over the last five years have translated directly into tangible and, in some cases, transformative improvements in electrolyzer performance, durability, and viability. The progress is not the result of a single breakthrough but rather the synergistic effect of advancements in architecture, interfacial control, and materials design. Recent progress illustrates how a molecular-level understanding of electrochemical phenomena can yield system-level gains. The quantitative chemical analysis of the carbonate problem prompted the rapid emergence of BPM and PEM architectures, enabling CO_2 utilization efficiencies well beyond the ≈ 50% SPC values typically observed in anion-exchange systems, substantially lowering the carbon-recycle load and projected energy intensity of downstream separations. The mechanistic understanding of the cation effect resulted in a practical design strategy for acidic environments. By engineering high local alkali-cation concentrations at the cathode-electrolyte interface, researchers mitigated competitive HER,[83] and also developed PEM CO_2 electrolyzers with > 90%

https://doi.org/10.1021/acs.chemrev.5c00361
Chem. Rev. 2026, 126, 5028−5082

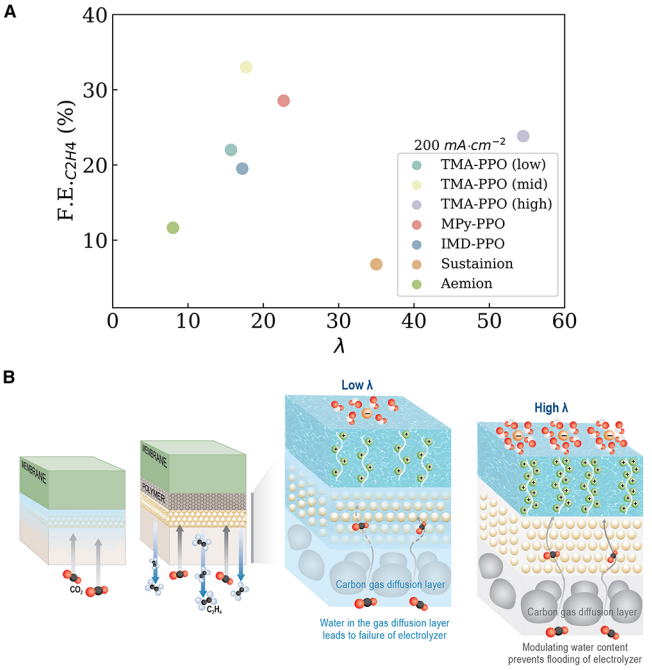

Figure 4. Influence of ionomer λ on selectivity and flooding behavior. (A) Ethylene F.E. at 200 mA/cm^2 for all ionomers in this study as a function of λ. (B) Schematic illustration of how GDL floods without an ionomer binder and when λ is low. Adapted with permission from ref 91. Copyright 2025 Elsevier.

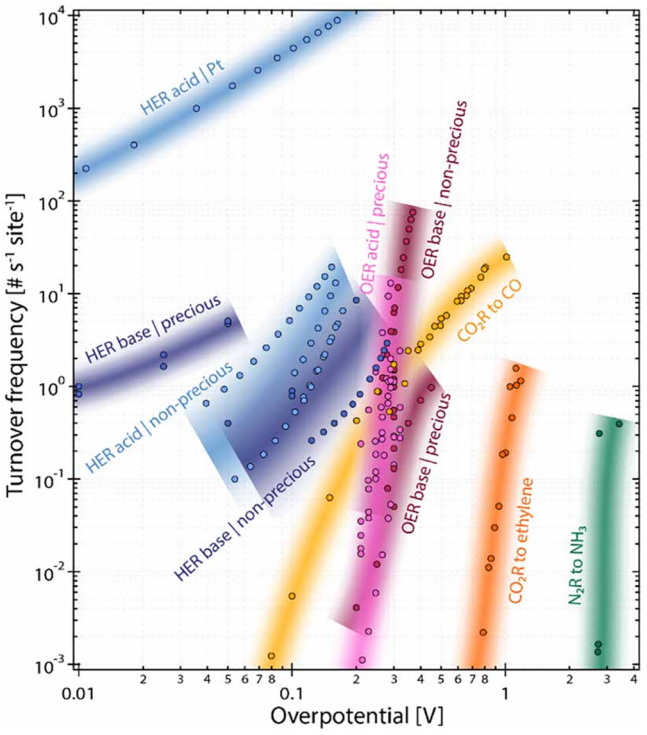

Figure 5. Turnover frequency (TOF) of state-of-the-art catalysts for CO_2RR to CO, CO_2RR to ethylene, and other significant electrocatalytic reactions plotted against the overpotential relative to the thermodynamically required potential for the respective reactions. Shadings are a guide to the eye. Reproduced with permission from ref 100. Copyright 2022 IOP Publishing Limited.

FE for formic acid and durability exceeding 5,000 h at > 600 mA cm^{-2} with hydrogen oxidation reaction (HOR) at the anode.[99] These results open avenues for exploring acidic systems for scale-up development as an industrially viable platform. Finally, recognition that ionomers actively mediate local reaction environments has spurred the development of bifunctional binders that couple ionic conductivity with catalytic modulation. Such materials have enabled CO_2 coelectrolysis at high current densities exceeding 300 mA cm^{-2} while retaining high selectivity, marking a pivotal advance toward economically scalable electrolyzer stacks.

Despite these achievements, the field now faces a new frontier of chemical stability and kinetic limitations. The durability of membranes and ionomers remains the critical bottleneck for commercialization. Each architecture faces distinct degradation pathways. In AEMs, nucleophilic attack by concentrated OH^- leads to backbone cleavage and quaternary-ammonium loss. PEMs suffer oxidative radical attack under high anodic potentials, while BPMs endure extreme electric-field gradients and gas-evolution stress at the cation/anion interface, often resulting in delamination. Within the GDE, the ionomer experiences compressive and shear stresses from gas evolution, swelling from water uptake, transient flooding, and salt crystallization, leading to pore collapse, loss of adhesion to catalyst particles, and degradation of the three-phase boundary. Although substantial progress has been made in identifying highly active catalysts for the CO_2-to-CO step, their turnover frequencies now approach those of state-of-the-art OER catalysts at comparable overpotentials that suggests that the kinetics of the first two-electron reduction step are no longer the primary bottleneck. In contrast, the formation of multicarbon products remains orders of magnitude slower. As highlighted in Figure 5, TOFs for ethylene remains far below those accessible for CO formation, reflecting the intrinsically more complex, multistep C-C coupling chemistry. This kinetic gap is further amplified by competing pathways and branching between ethylene, ethanol, and higher oxygenates, as well as the challenge in accessing routes to C_{3+} products under practical operating conditions. Slow C-C coupling kinetics, pathway bifurcation, and selectivity limitations lead to low FEs and necessitate higher overpotentials, both of which negatively impact overall energy efficiency. This emphasizes the need for catalysts and electrolytes that co-optimize charge transfer, solvation, and intermediate stabilization under industrial current densities.

Addressing these intertwined issues requires more than next-generation polymers and ionomers with high conductivity, tunable hydration, and long-term stability. An emerging priority is the science of device integration, which focuses on materials compatibility and interface behavior under industrially relevant conditions. This perspective shifts how fundamental studies should be conducted: even in H-cells or half-cells, researchers must consider the actual catalyst–polymer electrolyte interfaces and the reactive species, gradients, and chemical potentials present in MEA-based devices. Designing basic science experiments keeping this in mind ensures that mechanistic insights translate more reliably to full devices.

Moreover, another frontier to focus on is the science of scale-up. Practical reactors introduce down-the-channel gradients, catalytic nonuniformities, reactant distribution effects, and variations in water activity and local chemical potential that are often absent in benchtop systems. These emergent behaviors strongly influence selectivity, stability, and transport. Developing systematic model platforms that reproduce these

https://doi.org/10.1021/acs.chemrev.5c00361
Chem. Rev. 2026, 126, 5028−5082

mesoscale conditions will be essential for identifying mechanisms that only arise at high current densities and industrially relevant scales. Together, these aspects will be central to bridging laboratory advances with commercial CO_2 electrolysis technologies.

Low-temperature CO_2 electrolysis has evolved from a catalyst-centric discipline into a chemistry-informed systems science. The shift from searching for active metals to understanding interfacial chemistry, ion transport, and polymer stability has yielded tangible gains in carbon efficiency, selectivity, and durability. The next transformative step will significantly depend on rationally designed, stable polymer electrolytes that can withstand the coupled electrical, chemical, and mechanical stresses of continuous operation. Solving this challenge will close the gap between laboratory discovery and commercial deployment for electrochemical CO_2 conversion.

2.2. High-Temperature Electrolysis

High temperature electrolysis represents a fundamentally distinct pathway for electrochemical CO_2 conversion, unique both in its elevated operating temperature—generally ranging from 500 to 1000 °C—but also in the underlying CO_2 reduction chemistry.[101] The origins of high temperature solid oxide electrochemical cell (SOEC) application in CO_2 conversion are generally linked to work led by NASA beginning in the 1960s as a means of providing both life support and propellant in space.[102,103] In the time since, SOEC utilization has expanded to more recently include CO_2 conversion for applications in industrial chemicals and fuels production (i.e., Power-to-X).[104]

Shown in Figure 6, two primary reaction pathways have been considered for CO_2 electrolysis in SOECs, depending on

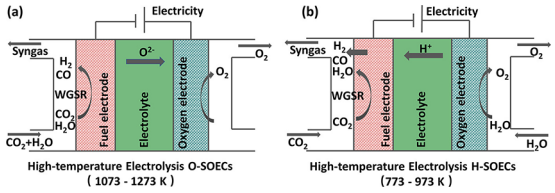

Figure 6. (a) Oxygen-conducting and (b) proton-conducting solid oxide electrochemical cells for CO_2 conversion. Reproduced from ref 101. Copyright 2024 American Chemical Society.

reactor design and operation. In oxygen-conducting configurations (O-SOECs) electrochemical reduction of CO_2 is performed at the negatively charged cathode (fuel electrode), forming carbon monoxide (CO) and oxygen ions (O^{2-}) shown in Equation 1. In the presence of H_2O (i.e., coelectrolysis mode) H_2O can similarly be converted to H_2 and O^{2-} (Equation 2). The oxygen ions generated from reduction on the cathode subsequently migrate through a porous ceramic-based solid electrolyte that isolates and conducts ions between the two electrodes, recombining at the positively charged anode (oxygen electrode) to form molecular oxygen (O_2, Equation 3).

Alternatively, in proton conducting SOECs (H-SOECs), H_2O is exclusively fed to the anode whereby molecular oxygen and protons (H^+) are formed (Equation 4). The generated protons then cross the electrolyte to the cathode, facilitating the reduction of CO_2 to products. Unlike in O-SOEC operation where products are limited to CO for pure CO_2 feeds or CO + H_2 in the presence of H_2O, the transfer of protons in H-SOEC combined with less extreme operating temperatures (500 − 700 °C) allows for a more diverse product set at the fuel electrode, including CO, CH_4, H_2O, and H_2 depending on specific reaction conditions and water-gas shift activity (Equation 5). These SOEC-derived products, in particular syngas, are viewed as promising feedstocks for the chemical industry to support a variety of high-volume applications such as methanol synthesis, Fischer−Tropsch liquids, or other industrially vetted catalytic processes to generate liquid fuels and valuable chemicals.

$$CO_2 + 2e^- \rightarrow CO + O^{2-} \quad (1)$$

$$H_2O + 2e^- \rightarrow H_2 + O^{2-} \quad (2)$$

$$2O^{2-} \rightarrow O_2 + 4e^- \quad (3)$$

$$2H_2O \rightarrow O_2 + 4H^+ + 4e^- \quad (4)$$

$$CO_2 + 4H^+ + 4e^- \rightarrow CO + H_2O + H_2 \quad (5)$$

As noted, a key defining attribute of SOECs is the elevated temperature regime at which they operate, offering a unique advantage in the way energy is sourced for CO_2 conversion. Indeed, as highlighted by the thermodynamics of direct conversion of CO_2 in Figure 7, although the total energy

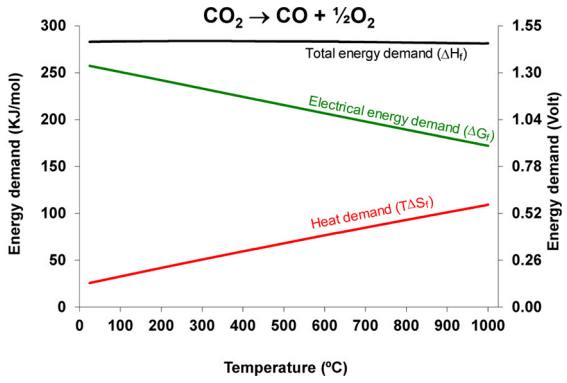

Figure 7. Thermodynamics of CO_2 electrolysis as a function of temperature. Reproduced from ref 105. Copyright 2014 American Chemical Society.

demand (i.e., enthalpy of formation ΔH_f) for the conversion to CO is nearly constant across the typical temperature SOEC range, thermodynamic principles state that the energy can be supplied either in the form of electrical energy (Gibbs free energy of formation, ΔG_f) or in the form of heat ($T\Delta S$) as shown in Equation 6.[30] Since the entropic term ΔS is positive, as reaction temperature, T, increases, the amount of electrical energy required decreases proportionally. For example, at 25 °C the electrical energy component ΔG comprises approximately 90% of the total energy demand ΔH_f, yet at 800 °C only 67%.[30]

Consequently, since heat can be significantly cheaper to source than electricity, this relationship between heat and electrical energy demand has important implications to SOEC operation and can be leveraged to the advantage of industry practitioners.[103] Specifically, through utilization of the joule heat produced internally from ohmic resistances during electrolysis and/or opportunities in utilizing colocated waste process heat (e.g., from a refinery or nuclear power plant), electrical energy demand can be significantly reduced often

https://doi.org/10.1021/acs.chemrev.5c00361
Chem. Rev. 2026, 126, 5028−5082

without the need for on-purpose external heat. Leveraging these principles, CO_2 conversion energy efficiency has been shown to exceed 95%,[105] a significant advantage compared to low temperature processes that meet the entirety of the energy demand through external electrical inputs. Further, at these elevated temperatures, SOEC chemistry benefits from thermally enhanced reaction kinetics, reducing the overpotentials required to drive CO_2 conversion at meaningful rates thereby improving productivity. However, a tradeoff of high temperature operation is C-C bond formation becomes thermodynamically unfavorable, translating to a product slate limited to only C_1 products (e.g., CO, CH_4) compared to the more diverse low temperature CO_2 electrolysis product set comprising a variety of C_1, C_2 and C_{3+} products.[9]

$$\Delta H = \Delta G + T\Delta S \tag{6}$$

As the potential use cases and general interest in SOECs has expanded in recent years to include CO_2 conversion for fuels and chemicals synthesis, the field has largely consolidated R&D efforts around two central themes: (1) materials development for high performance electrodes and electrolytes, and (2) understanding and overcoming degradation mechanisms to improve long-term system durability.[104] Indeed, there is a large body of work and published reviews covering both topics falling outside the intended scope of this review. For a comprehensive summary of pre-2020 literature, we direct readers to the following reviews.[103−106] Key takeaways from this early work across the three primary components of the SOEC (e.g., electrolyte, fuel electrode, oxygen electrode) and their respective stability are discussed below.

A functional electrolyte for SOECs must exhibit negligible electronic conductivity to prevent short-circuiting, high ionic conductivity to facilitate rapid transport of O^{2-} or H^+ species, and strong chemical resistance to oxidizing and reducing environments. Additionally, electrolytes must also match the thermal expansion properties of the adjacent fuel and oxygen electrodes and possess sufficient mechanical strength to resist embrittlement and fracturing, all while being as thin as possible to reduce ohmic losses.[103] Early testing of electrolyte materials and respective dopants has identified Z_rO_2 stabilized with Y_2O_3 or "yttria-stabilized zirconia" (YSZ) as the leading electrolyte choice in O^{2-} conducting O-SOECs. Specifically, earlier studies commonly cited electrolytes comprising a 8 mol% blend of Y_2O_3 with ZrO_2 or (8YSZ), providing a strong blend of high ionic conductivity and performance across the target SOEC operating temperature range and harsh reducing environment.[105] H-SOEC research has similarly consolidated around the use of barium cerate-zirconate (BCZY) based electrolytes and other metal doped variants to balance proton conductivity, chemical stability against CO_2 and H_2O, and mechanical strength.[105]

The purpose of the fuel electrode is to provide thermally stable active sites that facilitate the reduction of CO_2 into value-added products. High-performing electrodes are typically comprised of porous media designed to facilitate the simultaneous transport of electrons, ions, and CO_2 gas to active catalyst sites at the "triple phase boundary" (TPB)—the critical junction where these three phases intersect. The most common material architecture used in fuel electrodes is a metal ceramic composite known as a "cermet", with Ni-YSZ representing the benchmark for much of the pre-2020 era. The widespread adoption of Ni-YSZ electrodes is motivated by its combination of synergistic properties including high electronic conduction without the use of rare earth metals, high activity toward C = O bond cleavage, and rigid structural properties. Indeed, the use of cermets is a key to the mechanical stability of the entirety of the electrode stack as the ratio of metal to ceramic can be tuned to match the thermal expansion coefficient of the electrolyte, minimizing thermal stress and risk of delamination or cracking during operation and cycling.

On the oxygen electrode, materials compatible with high operating temperatures in a highly oxidizing environment are required. Most early studies investigated the use of mixed-conducting $ABO_{3-\delta}$ perovskites.[105] The $ABO_{3-\delta}$ nomenclature contains key structural information about the perovskite materials and its electronic properties. Specifically, the A-site is characterized by a large-radius ion coordinated by 12 oxygen ions, often comprised of elements La^{3+}, Sr^{2+}, or Ba^{2+}. The B-site cation is smaller in radius and coordinated by 6 oxygen ions usually comprised of a transition metal ion like Co^{3+}, Fe^{3+}, or Mn^{3+}.[107] The "O" term denotes oxygen sites in the crystal structure and $-\delta$ reflects the oxygen nonstochiometric nature (i.e., intentional oxygen vacancies) created by substituting ions of different valency into the lattice structure.

These oxygen vacancies are deliberately induced during synthesis to create the highly desirable property of mixed ionic and electronic conductivity (MIEC). Unlike the Ni-YSZ cermets on the fuel electrode which is a composite of separate electronic and ionic conducting phases, the MIEC $ABO_{3-\delta}$ perovskite does both in a single material. This significantly expands the electrochemical reaction zone beyond the TPB to instead effectively cover the entire surface of the electrode.[104] Commonly cited oxygen electrode compositions include lanthanum-based materials such as lanthanum strontium manganite (LSM) or lanthanum strontium cobalt ferrite (LSCF), both known for their high catalytic activity for oxygen evolution and compatibility with the electrolyte.[108,109] In applications involving LSCF, a small buffer layer of gadolinium-doped ceria (GDC) is also typically inserted as a thin reaction barrier between the YSZ electrolyte and the oxygen electrode to prevent unwanted reactions between the two layers at high temperature.[104]

Despite the relatively high initial performance of these early benchmark materials (e.g., Ni-YSZ | YSZ | GDC-LSCF), fundamental challenges surrounding long-term stability and degradation have slowed commercialization and scale-up. While the baseline Ni-YSZ fuel electrode demonstrated excellent conduction properties, the high partial pressures of CO present on the fuel electrode in turn made it prone to carbon deposition (coking) from the Boudouard reaction ($2CO \rightleftarrows C_{(S)} + CO_2$).[110] Further, at temperatures required to maintain conductivity (e.g., 800 − 850 °C), nickel was also shown to be susceptible to redox instability leading to particle aggregation and "coarsening".[111] Both phenomena, coking and aggregation, contribute to the blocking of TPB active sites and progressively deteriorate the performance of the SOEC over time. Indeed, the fuel electrode has been shown to be the primary source of degradation across SOEC experiments.[107,110]

On the oxygen electrode, high partial pressures of gases (e.g., oxygen) have similarly been linked to stability issues whereby O_2 bubble formation at the electrolyte-electrode interface was observed to lead to delamination and long-term irreversible damage and increase in ohmic resistance.[103] Additionally, during long-term stability studies cation migration in the perovskite structure and formation of secondary insulating

https://doi.org/10.1021/acs.chemrev.5c00361
Chem. Rev. 2026, 126, 5028−5082

phases were shown to further dampen performance. These issues combined with stack-level challenges of accumulation of contaminants (e.g., Cr, Si, B, S),[103] interconnected corrosion, glass crystallization has motivated the next phase of SOEC research and shift from emphasis on initial performance metrics to sustained long-term durability.[104]

In attempt to address some of these noted challenges, recent advancements (2020−2025) have emphasized materials development as a means to overcome performance limitations and tradeoffs between catalytic activity vs stability. Specifically, in the benchmark Ni-YSZ fuel electrode, the metallic and ceramic phases are physically mixed as a composite resulting in metal particles adhered to the surface of the support material via weak physical interactions. As revealed by earlier studies, this form of physical metal−support interaction and lack of strong bonding leads to high surface mobility of nickel and eventual aggregation at high temperatures.[105,112] Consequently, recent research has investigated alternative cathode materials with enhanced long-term stability. Perovskite oxides—like those used on the oxygen electrode—have gained attention as a potential replacement for Ni-YSZ due to their excellent stability, structural tunability, and thermal compatibility with commercial electrolytes.[113] However, the use of perovskites alone is hindered by their intrinsically low catalytic activity toward CO_2 reduction relative to the metallic nickel baseline.[113,114] To overcome this activity-stability tradeoff, emerging cathode development has centered around different pathways for modifying the parent perovskite framework to increase the number of reaction sites and their activity toward CO_2 conversion. These efforts typically fall within three categories: lattice doping, composites of two or more electrode materials, or surface engineering modifications (see: Figure 8).[107]

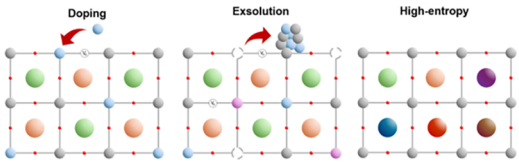

Figure 8. Illustrations of perovskite enhancements via doping, exsolution, or high-entropy synthesis. Adapted with permission from ref 107. Copyright 2025 John Wiley and Sons.

Perovskite doping is the intentional exchange of ions within the parent lattice. A-site doping involves the substitution of A-site cations (e.g., La^{3+}) with divalent cations (e.g., Ca^{2+}, Ce^{2+}, Sr^{2+}) to change the local valency within the crystal lattice and drive the creation of oxygen vacancies to maintain charge neutrality.[115] A common example is the transition of $LaFeO_3$ → $La_{1-x}Sr_xFeO_3$ (LSF) where a fraction (x) of La^{3+} is replaced with Sr^{2+}. Not only do oxygen vacations play a critical role in CO_2 conversion chemistry by providing sites for CO_2 adsorption and conversion to CO but depending on the specific dopants used, ionic conductivity, thermal stability, and durability properties may also be enhanced (see: Figures 9 and 10). Similarly, B-site doping is the deliberate substitution of catalytically active transition metals (e.g., Ni, Fe, Co, etc.) into the B-site of the perovskite crystal lattice to maximize electronic conductivity and provide the necessary active sites to drive CO_2 reduction chemistry.

In an extension of traditional A/B-site doping strategies, other emerging research has focused on the development of

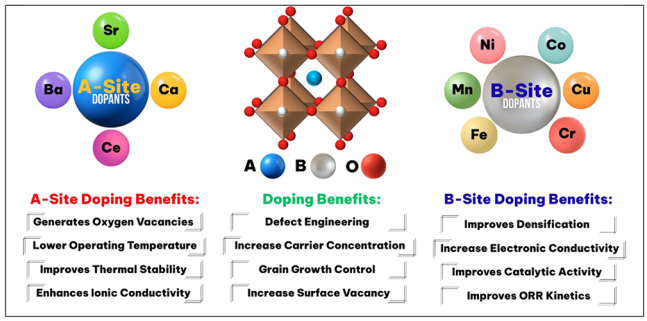

Figure 9. A-site and B-site doping of ABO3 perovskites in SOEC electrodes. Reproduced with permission from ref 115. Copyright 2026 Elsevier.

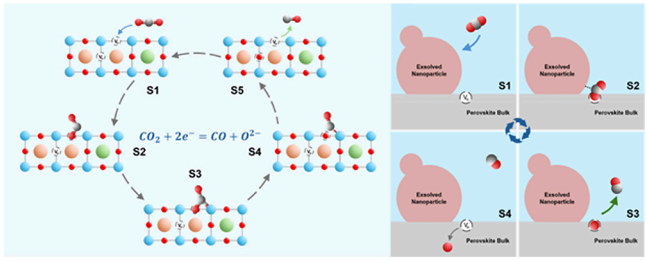

Figure 10. Mechanisms of CO_2 conversion over exsolved-based perovskite cathodes. Reproduced with permission from ref 107. Copyright 2025 John Wiley and Sons.

"high-entropy perovskites" (HEP) as another means of overcoming the stability-activity tradeoffs of conventional electrodes. Unlike in conventional doping where a relative minor fraction of the host lattice undergoes cation substitution (e.g., La^{3+} for Sr^{2+}), HEPs incorporate multiple cations (5+) at near equimolar ratios to induce radical changes inside the host lattice and maximize configuration entropy (Figure 8). Increasing the lattice entropy acts to thermodynamically stabilize the perovskite structure, suppressing the formation of secondary phases or cation migration at elevated temperatures that are often observed in lower entropy configurations. Further, in addition to enhanced stability, the presence of multiple cationic species and the associated lattice distortion contributes to a diverse set of active sites that facilitates CO_2 adsorption and reduction to CO.[116] Recent promising examples of materials tested for CO_2 conversion include $Sr_2Fe_{1.0}Ti_{0.2}Cr_{0.2}Mn_{0.2}Mo_{0.2}Ni_{0.2}O_{6-\delta}$,[116,117] $La_{0.2}Sr_{0.2}Pr_{0.2}Ba_{0.2}Ca_{0.2}FeO_{3-\delta}$,[118] and $La_{0.2}Pr_{0.2}Sm_{0.2}Sr_{0.2}Ca_{0.2}Fe_{0.9}Ni_{0.1}O_{3-\delta}$,[119] reporting current densities in excess of 1.5 A cm^{-2} while also showing durability in excess of 100h.

As a complement to these bulk lattice modification strategies, active research has also been devoted to developing "exsolution" synthesis techniques to modify the perovskite surface structure for long-term stability. Specifically, if A/B-doped perovskites are treated with a reducing atmosphere (e.g., H_2, CO), the formation of oxygen vacancies destabilizes the perovskite framework, causing the reducible metal ions (e.g., Ni^{2+}) at the B-sites to migrate from the bulk to the surface where they undergo chemical reduction into their metallic state (e.g., Ni^{2+} → Ni^0) to maintain thermodynamic equilibrium in the lattice (Figure 10). With the metal particles "growing" from within the lattice, they become effectively socketed and chemically anchored within the perovskite skeleton thereby strengthening the integrity of the TPB. This

https://doi.org/10.1021/acs.chemrev.5c00361
Chem. Rev. 2026, 126, 5028−5082

is fundamentally different and a critical distinction from conventional synthesis techniques whereby the metal nanoparticles are more weakly bound on the surface. Thus, the exsolution method offers a pathway to preserve the high initial catalytic activity of the metal while suppressing a known degradation mechanism.[120]

Indeed, as highlighted by Han and co-workers in Figure 11,[107] activity in perovskite-based fuel electrodes has garnered

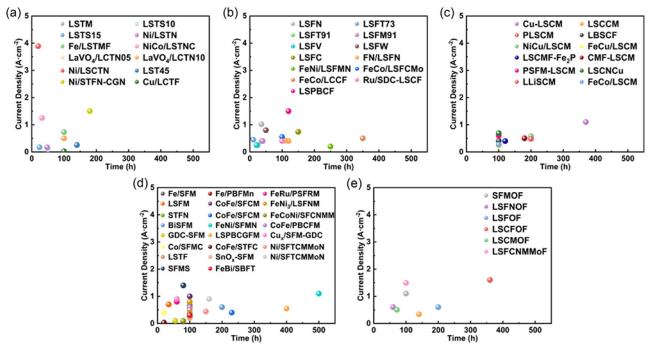

Figure 11. Electrochemical stability summary of (a) LST-based perovskites, (b) LSF-based perovskites, (c) LSCM-based perovskites, (d) double perovskites, and (e) anion-site modified cathodes. Reproduced with permission from ref 107. Copyright 2025 John Wiley and Sons.

significant interest in recent years. While research is still ongoing to pinpoint the optimal combinations of A/B-site dopants, material blends, and surface modifications, data published to date paints an optimistic picture for overcoming the initial activity-stability tradeoff issue. A compilation of reported data highlights relatively low impedance of doped perovskites is possible at commercially relevant current densities while also showing stability in lab scale testing in excess of 100h.[107]

Although SOEC energy efficiency remains excellent and is a standout across CO_2-conversion pathways, further future research is needed. Despite these recent strides in perovskite tuning and initial performance gains, the mechanistic link between dopant chemistry, lattice distortion, vacancy energetics, and long-term kinetics remain poorly understood and should be a focus of ongoing R&D.[115] Extended long-term stability testing beyond the 100−300 h commonly cited and into the thousands of hours will be another critical next step to demonstrating the potential for these novel materials in commercial applications. Advances in in-situ characterization techniques and computational modeling will be essential in guiding the rational design of next generation solid oxide electrolysis cells. With continued innovation to develop more robust and cost-effective materials, improved reactor designs, and integrating SOEC systems with existing industrial processes to test systems under real-world conditions, high temperature CO_2 electrolysis has the potential to become a key technology for sustainable carbon utilization, enabling the production of renewable fuels and chemicals while contributing to global decarbonization efforts.

2.3. Non-Thermal Plasma

Nonthermal plasma (NTP) technologies provide an electron-mediated approach to activate and convert the stable CO_2 molecule. NTP is generated by applying an electromagnetic field to a gas which energizes electrons that activate ground-state gas molecules through excitation, ionization, and dissociation processes.[121] The resulting partially ionized gas includes reactive species such as electrons, ions, radicals, and vibrationally and electronically excited species that can promote thermodynamically and kinetically unfavorable gas-phase and surface reactions under conditions far from those accessible by conventional thermal catalytic chemistry.[122] NTP is characterized by its deviation from local thermodynamic equilibrium, wherein the electron temperatures are higher than those of the bulk gas ions and neutral species. Consequently, NTP is exceptionally suited for driving thermodynamically unfavorable reactions of CO_2 at more mild conditions. The highly energetic electrons (1−10 eV range) can break the C = O bond or reduce energy barriers for reaction without substantially heating the bulk gas as in thermal methods or requiring other reactants, although additional reactants can lead to dramatic changes in chemistry as will be discussed in Section 3.2. In this contribution, we will focus on NTP, from cold to warm discharges, rather than thermal plasmas that are in local thermodynamic equilibrium, to take advantage of the deviations from equilibrium and the interesting chemistry that arises, as well as to enable integration with a catalyst to promote selectivity within the chemical pathways.

Depending on the electrode geometry and configuration as well as power source, multiple NTP reactor types can be created including dielectric barrier discharges (DBDs), gliding arc (GA), and microwave (MW) plasmas which are most studied for CO_2 conversion, although other types have been investigated as well (e.g., radio frequency, atmospheric pressure glow, corona, spark, and nanosecond pulsed discharges).[123] Catalysts are readily integrated within the plasma zone of DBD reactors that have gas temperatures ranging from 300 to 400 K,[124] enabling increased selectivity control through plasma catalysis, although, despite high conversion, the energy efficiency of DBD plasmas is lower compared to other plasma systems such as GA or MW.[125] These reactors, while still considered nonthermal due to their nonequilibrium nature, have higher average gas temperatures ranging from 1000−3000 K for MW and 1000−1500 K for GA,[124] which affect CO_2 reactivity. MW and GA also have extreme temperature gradients, with core temperatures that can exceed 6000 and 3000 K, respectively, in the core region, with significantly cooler temperatures in the afterglow region.[126,127] The details of these NTP systems in reference to CO_2 conversion have been extensively covered in the literature,[125,128−132] so here we will focus on conveying key aspects salient to understanding the chemistry of NTP CO_2 conversion. For direct CO_2 splitting, there are three primary plasma-mediated reaction pathways. These processes are covered in greater detail elsewhere,[133] but they include (i) CO_2 splitting by electronic excitation which is not very efficient due to the mismatch between the lowest electronic level of CO_2 and the dissociation enthalpy of CO_2 (5.5 eV), (ii) CO_2 splitting via vibrational excitation which is more energy efficient, and (iii) CO_2 splitting by thermal dissociation at high plasma temperature. Electronic excitation is prevalent in DBD processes with the proportion of vibrationally excited species increasing in warmer plasmas such as GA or MW, due to different reduced electric fields (i.e., electric field divided by gas number density (E/N), expressed in Td) of the different discharge types. Typical E/N values in DBDs are above 100 Td, yielding electron impact dissociation, while vibrational excitation requires lower E/N (below 50 Td), like in warm

https://doi.org/10.1021/acs.chemrev.5c00361
Chem. Rev. 2026, 126, 5028−5082

plasmas.[134] While the energy efficiency of CO_2 splitting by vibrational excitation is higher than that of splitting by electronic excitation, the higher temperature of plasmas with larger vibrationally excited populations can change the options for integration with materials such as catalysts which have the potential to improve the selectivity of NTP catalysis processes,[134−137] especially those with additional reactants, as will be discussed in Section 3.2. An example of the reaction pathways for CO_2 splitting based on kinetic modeling by Mohanan et. al is shown in Figure 12 for a gas phase discharge

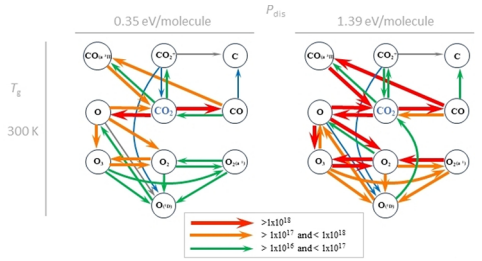

Figure 12. CO_2 conversion pathways in an NTP reactor at 300 K at two different input energies, with production pathway magnitudes as gray < blue < green < orange < red. Reproduced with permission from ref 138. Copyright 2024 Chemistry Europe.

at 300 K, with two different specific energy inputs (SEIs), demonstrating how much influence energy input can have on the reaction rates of different conversion pathways. Mohanan[138] also showed how reaction pathways are modified at higher gas temperatures (up to 1050 K) highlighting the differences in mechanisms between cold and warm discharges.

Many excellent studies have evaluated the impact of operational parameters such as reactor configuration, electrode material, dielectric material, discharge gap, applied frequency, applied power, gas flow rate, dilution gas (e.g., Ar, He), and reactor temperature and pressure on NTP-assisted CO_2 splitting and others have highlighted the role of packing media including catalysts, and these are collectively reviewed and discussed in the literature.[137,139,140] Integration of catalyst materials in DBD reactors is of particular interest as it provides opportunities to overcome the inverse relationship between energy efficiency and conversion and enhance both concurrently,[141] for example by providing stable surface oxygen vacancies in Mo-doped CeO_2 that can promote CO_2 dissociative adsorption to improve conversion.[142] Gao, et al., describe the integration of a NiCo-CuO catalyst into a DBD plasma system to enhance the uniformity of the discharge and the energy distribution of discharge filaments, highlighting the impact of the catalyst material on the plasma environment.[143]

Warm plasmas, including GA and MW discharges, are capable of much higher conversions and energy efficiencies, initially ascribed to the primary CO_2 vibration splitting pathway. More recently, it has been suggested that the high temperatures and accompanying thermal CO_2 decomposition rather than electron-mediated reactions drive the high efficiencies.[138] However, vibrational excitation may be important for very low pressure MWs at limited conversions.[144] Nonetheless, some researchers argue that particular reactor geometries, such as a modified GA with vortex flow (GA plasmatron) have reached conversion and energy efficiency limits.[145] Therefore, strategies for further performance improvements include limiting back reactions to CO_2.[133] In contrast to in-plasma catalysis that is suitable for the lower temperatures of DBD reactors, catalyst integration directly in the warm (1000 K+) plasma zone is not compatible with traditional catalyst materials, as the high temperatures can cause catalyst deactivation.[132] However, materials that can quench back reactions by reacting oxygen species with a postplasma carbon bed or reduced metal oxide may be introduced in the postplasma region to improve the conversion and efficiency.[146] For example, Girard-Sahun et. al demonstrated nearly double conversion (7.6% to 12.6%) with energy efficiency increasing from 27.9% to 45.4% by introducing a postdischarge carbon bed in a GA plasmatron system.[147] Other approaches to limit back reactions in warm plasmas include quenching the high temperature gas,[148,149] the utilization of pulsed systems,[150] or the integration of membranes.[151,152]

While progress has been made in improving conversion and efficiency of NTP based CO_2 splitting, there are still many challenges to scale these reactors to higher TRL. While details are provided in Figure 20 and Figure 21, the primary challenges faced by cold DBDs and warm GA/MW are inherently different due to the various CO_2 dissociation mechanisms (electronic vs vibrational). Additionally, the opportunities to integrate (catalyst) materials directly into the plasma are different due to the local temperatures produced. Researchers have pointed out that while improvements through geometry modifications or catalyst integration could be impactful, they are not necessarily critical to commercial success given that plasma processes may not compete in the same markets as existing large-scale processes as they are more suited to modular distributed systems.[153] However, another promising avenue for NTP upgrading of CO_2 targets higher value products such as C1 hydrocarbons. These products are formed in conjunction with secondary reactants such as H_2, hydrocarbons, or water and will be discussed in Section 3.2.[125,128]

2.4. Photochemical Reduction

Photochemistry provides a distinct route to CO_2 conversion by using photons to access excited-state pathways that are not available under purely thermal or electrochemical conditions.[154] Light absorption enables these catalysts to stabilize certain reactive intermediates that steer selectivity, opening novel routes to value-added fuels and chemicals—including emerging C_2 + products[155,156]—powered by photons. Light can further be used to lower apparent activation energies,[157] allowing reactions to proceed under comparatively mild conditions—an especially valuable advantage for endothermic processes such as dry reforming of methane or the reverse-water gas shift (RWGS). Recent years have shifted the field from broad materials exploration toward a sharper focus on structure−property relationships, defect chemistry, and microenvironment design that enable selective, efficient, and durable CO_2 conversion.

At its core, photochemical CO_2 conversion couples light absorption with catalytic chemistry that enable photons to activate charge carriers rather than thermally excite reactants. In practice, this typically occurs in liquid slurries or gas−solid photoreactors, where for example a semiconductor or plasmonic catalyst is irradiated by simulated or natural sunlight. In liquid-phase systems, CO_2 is sparged or dissolved into an aqueous or mixed solvent containing a suspension of photocatalyst powder, allowing photogenerated electrons and holes to drive reduction and oxidation half-reactions at the solid−liquid interface. In gas-phase systems, CO_2 flows over a

https://doi.org/10.1021/acs.chemrev.5c00361
Chem. Rev. 2026, 126, 5028−5082

fixed or fluidized photocatalyst bed under illumination, often co−fed with H_2 or CH_4.[158] Photoelectrochemical (PEC) cells combine light absorption with applied bias. Many incorporate membrane-separation analogous to electrolyzers but are driven primarily by sunlight rather than electricity. Across all architectures, the key commonality is the generation of photogenerated charge carriers that migrate to the catalyst surface to activate and reduce CO_2, often through intermediates such as $*CO_2^-$, *COOH, or *CO.

The mechanistic foundations of photocatalytic CO_2 reduction were firmly established well before 2020, encompassing several major classes of materials. Classical semiconductors such as TiO_2, $SrTiO_3$, g-C_3N_4, and GaP operate by promoting electrons from the valence to the conduction band upon light absorption, where photoexcited electrons reduce adsorbed CO_2 and holes drive complementary oxidation reactions (Figure 13a).[159,160] Single-atom catalysts based on transition-

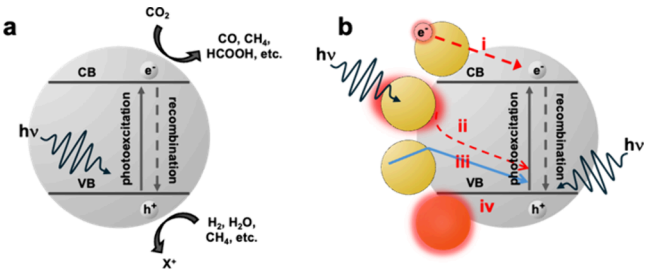

Figure 13. (a) Activation of a semiconductor photocatalyst. (b) Activation of a semiconductor with plasmonic metal NP. Potential mechanisms driving plasmon-mediated semiconductor photocatalysis include (i) hot electron transfer, (ii) near-field enhancement, (iii) resonant scattering, and (iv) local heating. Adapted with permission from ref 165. Copyright 2025, Springer Nature.

metal complexes and photosensitizer−catalyst dyads,[161] in both homogeneous and heterogeneous forms, offer precise control over coordination environments and have proven highly effective in tuning product selectivity.[162] More recently, plasmonic nanostructures, particularly those based on Au, Ag, and Cu, have gained attention for their exceptional ability to harvest light and open new activation channels through localized surface plasmon resonance (LSPR)—the collective oscillation of conduction electrons under optical excitation. These pathways include hot-carrier injection into antibonding orbitals of adsorbed CO_2, near-field effects that can induce carrier separation at interfaces, and multielectron transfer accelerated by photothermal heating (Figure 13b). Although the relative contributions of these effects remain challenging to deconvolute experimentally,[163] their interplay can produce reactivity and selectivity patterns distinct from both thermal catalysis and conventional semiconductor photocatalysis.[164]

What has evolved since 2020 is not a wholesale reinvention of the field, but rather a continued refinement of the underlying chemistry and an ever-sharper ability to pinpoint reactive intermediates and mechanisms that drive selectivity. For example, in semiconductor photocatalysts, defect chemistry has emerged as a deliberate design lever. Oxygen vacancies in metal oxides—once viewed as detrimental—are now recognized for trapping photogenerated electrons, promoting charge separation, and suppressing recombination.[166] Although full reduction of CO_2 to CH_4 is thermodynamically favored, kinetic limitations often bias selectivity toward partial reduction and CO desorption. Electrons stabilized at TiO_2 oxygen vacancies, however, were recently observed to persist for *minutes* after illumination, extending their lifetime for multielectron transfer and substantially enhancing methane production.[167] A related study coupled oxygen-deficient TiO_2 with gold quantum dots to enable the oxidative coupling of methane (OCM) using CO_2 as a soft oxidant.[168] Mechanistic analysis suggested that CO_2 adsorbed at Au−V_0−Ti interfacial sites through dual Au−C and Ti−O coordination simultaneously facilitated CO_2 reduction to *COOH while also lowering the barrier for C−H bond activation in methane. This synergy between CO_2 activation and methane oxidation illustrates how tailoring defect and interface chemistry can direct complex photoredox cycles.

In recent years, efforts to exert finer chemical control over photocatalytic microenvironments have intensified, with covalent[169] and metal−organic frameworks[170] (COFs and MOFs) emerging as versatile platforms for integrating light absorption, charge transport, and catalysis within a single architecture. Their modular composition enables systematic variation of linker conjugation, metal−ligand geometry, and pore polarity—parameters that directly influence CO_2 adsorption strength, charge separation, and intermediate stabilization. Single-atom[171] and bimetallic sites[172] confined within these frameworks have proven especially powerful for probing structure−function relationships: changes in coordination number or ligand field can shift reduction potentials, stabilize key *COOH or *CO intermediates, and steer selectivity toward CO, formate, or methanol. Operando spectroscopy and DFT studies increasingly show that site symmetry and electronic coupling between light-harvesting linkers and catalytically active nodes control the balance between electron delocalization and localization, defining both activity and product distribution. Collectively, this growing body of work demonstrates how tailoring local coordination environments and framework electronic structure provides a rational, molecular-level route to tune photocatalytic reactivity and selectivity.[173]

A major advance in photocatalytic CO_2 reduction—particularly in tunability and scalability—has been the emergence of heterometallic plasmonic antenna−reactor (AR) architectures.[174] In these systems, earth-abundant plasmonic "antenna" nanoparticles (e.g., Cu, Al) harvest light and transfer the resulting electromagnetic energy or hot carriers to adjacent catalytic "reactor" sites (e.g., Ru, Pd, Ni) that mediate bond activation (Figure 14).[175] By decoupling light absorption from active-site chemistry, the AR concept enables independent optimization of optical and catalytic properties—a key step toward rational photocatalyst design. Mechanistically, the plasmonic antenna concentrates the local electromagnetic field and generates energetic charge carriers that migrate to nearby metal or oxide reactor sites, where they drive reactions such as CO_2 reduction, C−H activation, and H_2 evolution. In addition to promoting activity, these energetic carriers can also enhance catalyst stability by facilitating the desorption of poisoning species and mitigating sintering—limitations that often plague thermocatalytic systems.[176] Representative Cu−Ru AR catalysts, for example, have demonstrated selective light-driven dry reforming of methane ($CH_4 + CO_2 \rightarrow 2CO + 2H_2$) with near-quantitative syngas yields and minimal coking under conditions where purely thermal operation typically deactivates and consumes H_2 via

https://doi.org/10.1021/acs.chemrev.5c00361
Chem. Rev. 2026, 126, 5028−5082

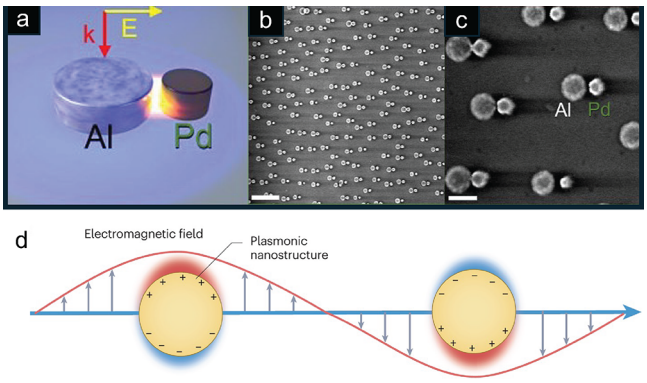

Figure 14. Planar nanodisk heterodimer complexes for plasmonic photocatalysis. (a) Schematics of forced plasmon modes excited on Al−Pd dimer; red and yellow arrows represent the wave vector and electrical field of the incident light, respectively. (b,c) SEM images of Al−Pd heterodimers, all with small gaps (~5 nm on average) between the Al antenna and Pd reactors. Scale bars: (b) 500 nm and (c) 100 nm. Reproduced from ref 175. Copyright 2024 American Chemical Society. (d) Excitation of surface plasmons gives rise to near-fields in a plasmonic nanoparticle. Adapted with permission from ref 178. Copyright 2023, Springer Nature.

RWGS.[177] The resulting light-assisted reforming cycle cleaves C−H bonds more efficiently, continuously removes surface carbon, and channels photogenerated electrons into productive syngas formation rather than unselective side reactions.

The same principles have been extended to other transformations of CO_2, including methanation,[179] RWGS,[180,181] and selective C_2 product formation.[182] Across these chemistries, AR systems consistently demonstrate higher selectivity and lower onset temperatures compared to their thermal counterparts. Beyond the laboratory, these advances have translated to early pilot demonstrations: industrial-scale photoreactors employing AR catalysts have achieved continuous syngas production and ammonia-cracking operation at throughputs exceeding 200 kg day^{-1},[183] underscoring the potential of AR designs as a scalable route to light-driven chemical manufacturing.

Coupling plasmonic photocatalysis with an applied electrochemical bias in photoelectrochemical (PEC) configurations merges the advantages of photochemical excitation and electrocatalytic control. By integrating optical energy input with electronic driving force, these hybrid systems lower kinetic barriers while maintaining steady-state currents and tunable redox environments. In CO_2 electroreduction (CO_2ER), sluggish CO_2 activation and high overpotentials often limit efficiency, while competing hydrogen evolution (HER) suppresses selectivity. Plasmonic excitation directly addresses these challenges by generating energetic hot electrons that populate antibonding orbitals of $*CO_2$, thereby reducing the barrier for $*CO_2^{\bullet-}$ formation and accelerating proton-coupled electron-transfer (PCET) steps.[184] Under constant potential, illumination can modulate product distributions—shifting selectivity toward deeper reduction pathways such as methanol[185] or favoring C_2^+ coupling reactions otherwise inaccessible under dark electrolysis conditions.[186]

Beyond performance gains, these light-biased electrochemical systems also serve as a mechanistic bridge between purely photochemical and electrocatalytic regimes, allowing direct interrogation of photoinduced charge-transfer dynamics under controlled potential.[187] Collectively, PEC platforms highlight how optical excitation can be used not only to reduce overpotentials and expand product scope, but to actively shape electron-transfer kinetics and interfacial energetics—providing a unifying framework for integrating light harvesting with catalytic selectivity control.

Taken together, these advances mark a decisive maturation in our molecular understanding of photocatalytic CO_2 conversion. Over the past few years, increasingly sophisticated mechanistic tools—spanning ultrafast spectroscopy, operando surface probes, and theory-driven modeling—have illuminated how light absorption, charge transfer, and catalytic chemistry can be coherently coupled to steer reactivity. This deeper insight has begun to translate into measurable improvements: higher apparent efficiencies, tunable product distributions through defect and interface engineering, and mechanistic data sets now guiding machine-learning−assisted discovery.[188] At the same time, early pilot demonstrations indicate that photochemical systems are beginning to transition from laboratory-scale discovery toward practical, light and solar-driven chemical manufacturing.

Still, fundamental chemical challenges persist. At the heart of photocatalytic CO_2 conversion lies the need to orchestrate multielectron, multiproton transfer reactions across heterogeneous interfaces where carrier lifetimes are short and recombination pathways numerous. Disentangling the intertwined roles of hot carriers, photothermal effects, and defect states under dynamic illumination remains a major frontier, as these processes can evolve on ultrafast timescales and shift with surface reconstruction. Precise control over band alignment, and interfacial dipoles is required to modulate electron transfer energetics and suppress side reactions such as hydrogen evolution or partial CO desorption. Equally critical is understanding how local coordination, adsorbate geometry, and solvation can shape reaction intermediates—from $*CO_2^-$ and *COOH to C−C coupling motifs—and how these evolve under real operating potentials and photon flux. Catalyst deactivation through oxidative passivation or metal migration continues to constrain durability in real world systems, while structure−property relationships governing long-term photochemical stability are only beginning to be understood. Addressing these issues will continue to require deep integration of *in situ* spectroscopy, electronic-structure theory, and synthetic chemistry to establish quantitative correlations between surface composition, excited-state dynamics, and product selectivity.

2.5. Microbial Electrosynthesis

Microbial electrosynthesis (MES) is a hybrid bioelectrochemical technology that harnesses the metabolic capabilities of electroactive microorganisms to convert electrical energy and carbon dioxide into value-added organic compounds (for extensive review, please refer to (Rabaey, 2010).[189] Operating at the interface of microbiology, electrochemistry, and environmental engineering, MES offers a sustainable platform for carbon capture and conversion, with potential applications in renewable energy storage, bioremediation, and biomanufacturing. MES employs chemolithoautotrophic microbes, often from the *Geobacter* or *Clostridium* genera, coupled with electrical energy to enable cathodic CO_2 reduction into target products, ranging from short chain fatty acids (SCFAs) to alcohols.

https://doi.org/10.1021/acs.chemrev.5c00361
Chem. Rev. 2026, 126, 5028−5082

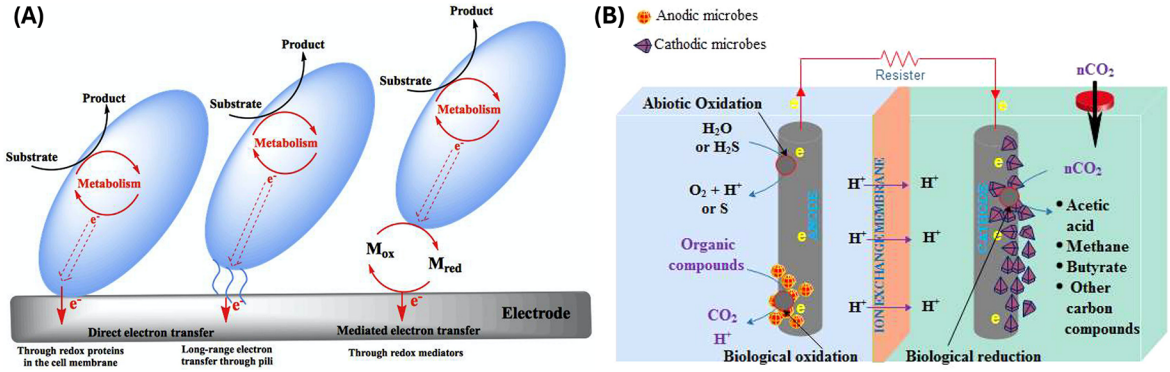

Figure 15. MES electron transfer mechanisms and potential product suite. (A) Mechanisms of electron transfer in microbial cells include (1) direct contact via cell membrane bound c-type cytochromes, (2) mediated electron transfer via extracellular redox-active electron shuttles (mediators), and (3) long-range electron transfer though pili in a bacterial microorganism. Reproduced from ref 190. Copyright 2020 American Chemical Society. (B) Schematic diagram of the microbial electrosynthesis carbon dioxide sequestration process and synthesis of value-added products. Reproduced from ref 191. Copyright 2023 American Chemical Society.

MES has conventionally faced several key challenges that currently limit its scalability and efficiency, and in turn, economic viability and sustainability. From a biological perspective, the mechanisms of direct and mediated extracellular electron transfer (EET) at the cathode − wherein cells accept electrons from the cathode via physical contact using outer membrane redox proteins (e.g., cytochromes), conductive appendages ("nanowires"), or redox active biofilm matrices (Figure 15)− are slow, due to low exchange current densities at biocathodes, limited turnover of redox enzymes, poor biofilm conductivity, long electron transport distances through heterogeneous biofilms, mass transfer constraints for CO_2 and nutrients, and/or competition with abiotic reactions. Further, these mechanisms remain incompletely understood; dominant routes of electron entry across the cell envelope under different conditions are unknown and there remains uncertainty surrounding the identity and regulation of key redox proteins in cathodic uptake. Additional uncertainties surround the rate limiting steps from the cathode surface to cytoplasmic ferredoxin/NAD(P)H and the conditions under which direct electron transfer outcompetes mediated (H_2/formate) pathways.

Additionally, MES systems often rely on complex microbial consortia; however, maintaining stable, selective, and productive communities over long time periods can prove challenging. Unwanted metabolic pathways can divert electrons and carbon flux toward competitive pathways, such as excessive abiotic H_2 evolution, preferential biomass accumulation rather than product formation, and chain elongation to nontarget SCFAs/alcohols. The above challenges lead to poor production rates and low concentrations of target compounds (e.g., current densities ∼ 0.1−10 A/m^2, with productivities often in the tens to hundreds of mg/L/day) relative to conventional sugar bioconversion pathways. Additionally, current electrode materials − such as graphite, modified surfaces with graphene, and carbon nanotubes − have high fabrication costs due to high surface area, biocompatibility, and corrosion resistance requirements. Gas−liquid mass transfer presents further hurdles to efficient nutrient and substrate delivery for MES deployment. Combined, these uncertainties currently cap achievable current densities and space-time yields, complicate scale-up and control of selectivity, and often force operation in regimes that favor H_2/formate mediation rather than true direct EET.

Over the past five years, significant advancements have been made to address these challenges, including enhanced production rates of various chemicals (e.g., acetate), establishment of new microbial catalysts, and optimization of operational conditions (e.g., enhanced biofilm permeability and stabilization) to improve MES performance. For example, substantial improvement in acetate production rates and electron transfer have been achieved in recent years via biofilm modulation. Increasing the cell permeability of biofilms via enzymatic treatment enabled > 2X enhancement to electron transfer efficiency and acetate production.[192] Similarly, biofilm stabilization into 3D-printed cathodes successfully enabled process intensification resulting in nearly 5X enhancement to acetate production in an algal-mediated MES system.[193] Indeed, optimizing factors such as pH, temperature, and electrode materials has been crucial in enhancing MES efficiency. For example, studies have identified that neutral to slightly acidic pH levels (5.5−7.0) are optimal for CO_2 conversion to acetic acid, while lower pH levels may be necessary to suppress unwanted methanogenesis.[194] These enhancements are hypothesized to be mediated by a series of potential mechanisms including shortened electron transfer distances and improved contact density increase effective electron flux to cells; enhanced conductivity and redox active surfaces (graphene/composites) that facilitate charge transport through biofilms and better coupling to outer membrane cytochromes; and surface functionalization (e.g., polydopamine) promoting cell adhesion, biofilm stabilization, and/or chelation of metals that aid redox enzyme function. Biofilm permeability and optimized thickness can also reduce diffusion barriers for substrates/products, lowering internal mass transfer resistances and increasing overall reaction rates.

Advancements in novel electrode materials have also led to improved MES systems performance in recent years. Incorporation of carbonaceous materials into electrodes has the potential to increase the surface area and electrical conductivity thereof (please refer to Lekshmi, 2023 for extensive review[195]). For example, electrosynthetic formate production was recently achieved by photoassisted MES system by integrating a photoanode and an activated carbon fiber biocathode, enabling production of > 0.5 g/L formate.[196] Additional advances in carbonaceous electrodes have been demonstrated via the utilization of graphene as a mediator, which has been shown to enhance cell growth and electron

https://doi.org/10.1021/acs.chemrev.5c00361
Chem. Rev. 2026, 126, 5028−5082

transfer rate in myriad microbial systems.[197] For example, polydopamine-coated graphene aerogel anodes were recently demonstrated to achieve > 30% reduction in system start-up time and > 2X increases in maximum power density in *Geobacter*-mediated systems.[198]

Genetic modification of MES biocatalysts has also proved effective in enhancing system productivity (reviewed extensively in Klein, 2023[199]). Overexpression of nanowire proteins in *G. sulfurreducens* led to nearly 3-fold enhancement in in power density relative.[200] Additional advances in *Geobacter* and *Shewanella* spp. systems have been achieved via isolation and development of novel microbial variants. For example, genetic engineering of *S. carassii*-D_5 isolated from activated sludge achieved > 1.5X power densities relative to wild-type and > 5X higher than that achieved with the model electroactive microbe, *S. oneidensis* MR-1.[201] The identification and deployment of new MES biocatalysts hold promise to both electrochemical parameters and expand the range of obtainable products.

While MES holds great long-term potential, outstanding challenges remain (please refer to Prevoteau, 2020 and Jourdin 2021 for extensive review), and the near-term promise of MES is likely in specific niches rather than bulk commodity production due to current limitations in rate, energy efficiency, electrode cost, and scale-up.[202,203] Indeed, improving the efficiency of CO_2 reduction, effectively scaling MES technologies, and achieving viable economics remain among the key hurdles facing this technology. Further, maintaining stable microbial communities over long periods can prove challenging, necessitating frequent "catalyst regeneration" cycles. Continued efforts to optimize operational parameters (e.g., temperature, pH, pressure), develop novel reactor and electrode designs, and identify novel microbes with enhanced native or engineered deployment characteristics, present numerous opportunities to continue to improve MES technology.

3. H_2-MEDIATED CO_2 CONVERSION

3.1. CO_2 Hydrogenation

Thermocatalytic CO_2 hydrogenation has been employed to generate hydrocarbon and oxygenate products. Hydrocarbon products of varying chain length have been targeted in single-reactor approaches, from the simplest, methane, through lower olefins (C_2-C_3), across the range of liquid fuel range products (C_5-C_{20+}), and to aromatics. In contrast to the range of C-C coupling chemistry observed for hydrocarbons, the most common oxygenate products retain the C_1 fragment, methanol, dimethyl ether (DME, via dehydration of methanol), formic acid, and dimethyl carbonate (DMC). This section will summarize recent reports of high performing single-reactor approaches using tandem or multifunctional catalyst systems, highlight new catalyst materials where an understanding of how catalyst active site structure effects C-O bond breaking and C-C bond forming chemistry, and introduce a re-emerging target product, higher alcohol synthesis, that requires new catalysts to breakthrough traditional barriers. Notably, this section will not cover traditional reverse water-gas shift catalysis as an approach to generate carbon monoxide, since catalyst development and process considerations have been recently reviewed.[204−207] However, approaches that initiate hydrocarbon production using RWGS will be highlighted. Similarly, standalone CO_2 methanation and CO_2 to methanol have been recently reviewed,[208−211] including catalyst and process development aspects, and therefore, reports highlighted in this review with figures of merit to compare across emerging technologies will focus on alternative approaches to traditional processes (see Section 4). In line with the overarching theme for this review article, this section will focus on recent reports that build an understanding of the chemical mechanism for activating the CO_2 molecule, rather than reviewing the chemistry and catalyst development to direct the reactive intermediate to hydrocarbon or oxygenate products.

Single-reactor approaches to C_{2+} hydrocarbon products via CO_2 hydrogenation over tandem or multifunctional catalysts fall into two major categories based on the type of intermediate generated from CO_2: (a) a CO intermediate followed by FT chemistry to light olefins (CO_2-FT), and (b) a MeOH intermediate. Both the light olefins and the MeOH intermediates can be directed to a variety of hydrocarbon products, including fuel-range molecules and aromatics, typically through acid-catalyzed zeolite/zeotype carbon-pool chemistry. For historical context and advancements in this field made prior to 2020, which is before the scope of this review, the interested reader is directed to a comprehensive review of syngas and CO_2 conversion to hydrocarbons.[212] Since 2020, additional perspectives, review articles, and book chapters have also been published, focusing on specific catalyst combinations or products of interest.[213−219]

Of initial interest to the scope of this section is a summary of recent reports that have achieved high per-pass yield, high selectivity, or selectivity to a unique product slate using traditional FT catalyst metals for CO_2-FT, and systems where these FT catalysts were combined with acidic catalysts to access higher hydrocarbons. Using traditional metals for FT catalysts, Fe and Co, a series of Na-modified bimetallic FeCo catalysts were explored by Li et al. for light olefin production from CO_2.[220] At 340 °C and 4.0 MPa, the optimized composition of $Na_{0.02}Fe_1Co_1$ exhibited 56.9% CO_2 conversion with just 3.6% CO selectivity, and 40.5% light olefins selectivity, giving a remarkable 22.2% light olefin yield.

An attractive alternative target product to light olefins (C_{2-4}) is C_{4+} linear alpha-olefins (LAOs), which are valuable chemical precursors due to the terminal C = C bond. Xu et al. reported a ternary Fe-Zn-Al spinel catalyst based on an Fe FT catalyst that gave 88.7% LAOs among the C_{4+} products (53.5% selectivity to C_{4+}) at 350 °C, 1.5 MPa, and 39.1% CO_2 conversion.[221] The ternary catalyst also exhibited 24.7% selectivity to C_2-C_3 olefins under these conditions, with a high overall olefin-to-paraffin ratio of 9.9. Modified Fe catalysts have also been studied for direct liquid fuels and aromatics production from CO_2 hydrogenation. A Na and Cu modified Fe_2O_3 catalyst combined with hierarchical nanocrystalline HZSM-5 zeolite reached an aromatic selectivity of 57.7% at 33.3% CO_2 conversion (320 °C, 3.0 MPa), highlighted further by 94.8% of the liquid product being aromatics.[222] Building on a previous report demonstrating C_{4+} olefins from CO_2 hydrogenation with a delafossite $CuFeO_2$ catalyst,[223] Cheng et al. coupled it with HZSM-5 to exhibit aromatics selectivity of 56.4% at high CO_2 conversion (>50%) and with < 12% combined CO and CH_4 selectivity.[224]

Finally, improvements in the production rate of liquid fuels from CO_2 hydrogenation and subsequent acid catalysis has been the focus of recent work. Li et al. investigated the direct hydrogenation of CO_2 to gasoline-range hydrocarbons and

https://doi.org/10.1021/acs.chemrev.5c00361
Chem. Rev. 2026, 126, 5028−5082

olefins over a series of bifunctional, K-modified FeMn catalysts paired with zeolites and operated at high temperatures, 300−400 °C.[225] The optimized FeMnK+H-ZSM-5 catalyst provided 70% selectivity to an isoparaffin- and aromatic-rich C_5-C_{11} hydrocarbon product at 320 °C at approximately 30% CO_2 conversion. As expected, the hydrocarbon distribution was mainly a function of the micropore size of the zeolite, where the MFI structure gave the desired product slate for liquid fuels. Perhaps the most complex composition for a CO_2-FT catalyst based on Fe, NaFeGaZr, was reported by Wang and co-workers.[226] When combined with a hollow HZSM-5 zeolite and operated at 380 °C and 3.0 MPa, an aromatic-rich gasoline was produced with CO_2 conversion near 45% for 200 h time-on-stream. An overarching theme for the development of these modified Fe-based FT catalysts is the use of an additional metal or metals that affects the formation of the active iron carbide phase, resulting in a composition that produces the light olefins more readily or shifts the selectivity to longer chain olefins, for subsequent conversion to the product of interest.

Similar to the CO_2-FT approach, here we seek to summarize high selectivity and/or high yield to hydrocarbons from CO_2 hydrogenation through MeOH using the traditional methanol synthesis catalyst, $Cu/ZnO/Al_2O_3$ "CZA", and acid catalysts. It is worth noting that due to the mismatch in reaction temperature for MeOH synthesis using CZA (220−250 °C) and subsequent MTH chemistry (320 − 380 °C), many recent reports have utilized the Cu-free mixed oxide, $ZnZrO_x$, to initiate methanol production at higher temperatures, and these reports have been recently reviewed.[211] However, CZA still has its utility to be coupled with hydrocarbon production routes that are active below 300 °C. One report since 2020 stands out that builds upon initial reports that used 2-stage reactors,[227−229] and extends a catalyst system that demonstrated CO_2 coconversion with syngas.[230] To et al. employed a stacked-bed composite catalyst of CZA with acidic alumina positioned above a Cu-modified BEA zeolite (Cu/BEA) for hydrocarbon synthesis in a single reactor. Relatively mild conditions of 210 °C and 3 MPa provided 13% CO_2 conversion with high selectivity to C_{4+} hydrocarbons (96.4% within the hydrocarbon product, 35.3% overall) suitable for liquified petroleum gas (LPG) and gasoline fuels.[231]

The second topic of interest to this section is novel catalyst compositions for CO_2 activation that are challenging the traditional wisdom by directing the chemistry through alternative mechanisms, leading to breakthrough performance for activity and/or selectivity. In CO_2-FT, Co catalysts are a natural choice based on their known activity and selectivity for long carbon-chain products from analogous CO conversion. The particle size, oxidation state, crystal phase, and support are known to influence FT catalysis performance for Co catalysts,[232,233] and interestingly, the rock salt phase of cobalt oxide on TiO_2, CoO/TiO_2, was identified to be more active than its metallic counterpart in 2014.[234] In 2022, ten Have and co-workers uncovered the mechanistic aspects of CoO/TiO_2 that differentiate it from metallic Co.[235] The authors studied both CoO and metallic Co on reducible (TiO_2, CeO_2) and nonreducible (SiO_2, Al_2O_3) supports. Only for the TiO_2 support was CoO found to be more active than its metallic Co counterpart. Using sophisticated operando spectroscopy techniques, modulated excitation (ME) diffuse reflectance infrared Fourier transform spectroscopy (DRIFTS) with phase-sensitive detection (PSD), enabled the authors to differentiate the mechanism for CO_2 activation. For metallic Co catalysts, the direct dissociation mechanism was followed, where CO_2 dissociates to CO, which is the primary intermediate for either desorption or further dissociation to C_{ads} and subsequent chain-growth. On the contrary, CoO/TiO_2 proceeded through the H-assisted mechanism, where CO_2 forms carbonates, formates, or formyl intermediates followed by subsequent hydrogenation and chain-growth. Further, the authors investigated kinetic parameters, and an opposite relationship with H_2 partial pressure was found, where CoO/TiO_2 had a + 1.24 H_2 reaction order and Co/TiO_2 had a − 1.15 H_2 reaction order. This reaction order analysis supports the H-assisted mechanism for the CoO/TiO_2 catalyst. Finally, the authors used the mechanistic understanding to demonstrate that the CoO/TiO_2 catalyst could outperform traditional metallic Co analogues and that H-assisted mechanism is a more favorable pathway to produce long-chain hydrocarbons than the direct dissociation mechanism. Feeding a mixture of CO and CO_2, which may be expected in an industrial CO_2 hydrogenation process that utilizes a recycle stream, a 2.8× increase in overall C_{2+} yield was achieved over the CoO/TiO_2 catalyst compared to its reduced analog.

As presented above, Fe catalysts are similarly well-studied for CO_2-FT to hydrocarbon products. Identifying that high CO selectivity was a limiting factor for Fe-based CO_2-FT catalysts, Song and co-workers hypothesized that promotion of the catalyst with Cu could address this shortcoming. Targeting aromatics production, a composite catalyst of Cu-promoted Fe_2O_3 and HZSM-5 was developed, termed $Cu\text{-}Fe_2O_3$/HZSM-5. Meeting its intended goals, FT chemistry was enhanced over $Cu\text{-}Fe_2O_3$, decreasing CO selectivity to just 3.15% while achieving 56.61% selectivity to aromatics at high CO_2 conversion of 57.30%. Through mechanistic studies, the authors identified a cooperative effect between the $Cu\text{-}Fe_2O_3$ catalyst component and the zeolite to effect the observed high selectivity to aromatics. They proposed a "H recycling" mechanism, where the dehydrogenation that must occur in the zeolite during aromatization generates "H species", which could be H_2 or could be a carbon-based reactive H-carrier. These H species can diffuse to the $Cu\text{-}Fe_2O_3$ surface and react with bound CO_2. Thus, CO_2 is both the overall reactant and a critical "H consumer" that enables the aromatization chemistry to proceed with high selectivity.

Taking the concept of Fe-oxide based catalysts to initiate CO_2 conversion in a new direction, Tian and co-workers studied the perovskite, $LaFeO_3$, as an alternative to traditional iron oxides paired with HZSM-5 zeolite for aromatics production.[236] They hypothesized that uncontrolled C-C coupling on the Fe catalyst during FT chemistry complicated the subsequent aromatics chemistry occurring in the zeolite catalyst, limiting aromatics selectivity to < 70% within the hydrocarbon product slate. A critical design parameter for $LaFeO_3$ over traditional Fe oxides was the resistance to carburization, where the Fe_5C_2 phase resulting from carburization of Fe oxides is a known active phase in FT chemistry for hydrocarbon production. Rather, the structure and energetics of $LaFeO_3$ create a high barrier for carburization but still enable efficient CO_2 hydrogenation. Indeed, when CO_2 hydrogenation was conducted over the $LaFeO_3$ catalyst alone (no zeolite), iron carbide was not formed and the catalyst exhibited little C-C coupling activity, giving 92.5% methane selectivity. Optimizing $LaFeO_3$:HZSM-5 mass ratio (2:1) and

https://doi.org/10.1021/acs.chemrev.5c00361
Chem. Rev. 2026, 126, 5028−5082

Si/Al ratio (14) of the zeolite provided an extraordinary aromatics selectivity of nearly 85% at 61.4% CO_2 conversion, and with CO selectivity of just 9.3%. Further, the catalyst system maintained high activity with extremely low deactivation rate over 1000 h time-on-stream. The mechanistic reasons for the enhanced performance was elucidated using in situ DRIFTS spectroscopy with cofed CO_2 and H_2 at 350 °C, where the $LaFeO_3$ catalyst exhibited an oxygenate-rich surface comprised of formate, methoxy, and formyl species. In contrast, iron carbide catalysts displayed characteristic peaks for C = C and C-H species in their spectra under the same conditions. A computational assessment indicated that the mechanism through the formate species was more kinetically accessible than through bound CO*, supporting the alternative mechanism offered by the $LaFeO_3$ compared to traditional Fe catalysts.

In line with our interest to highlight approaches that challenge the traditional wisdom, here we present reports that look beyond methanol as an intermediate from CO_2 to fuels and chemicals, and rather, seek to develop catalysts that proceed through value-added higher alcohols (HAs), such as ethanol, propanol, and butanol. HA synthesis is a re-emerging field, where current researchers seek to breakthrough limitations identified in literature as far back as the 1980s that identified sulfide materials as active catalysts for syngas to HAs and a Mo-based catalyst for CO_2 to HAs.[237] Near the beginning of the time window of interest to this review, Xu et al. authored a comprehensive review article that outlined the thermodynamics of HA synthesis, the 4 main groups of catalysts being developed, effects of promoters and supports, and importantly, critical aspects of the mechanism that set stage for the past 5 years of research.[238] Considering the thermodynamics, many CO_2 hydrogenation reactions in the HA reaction network (RWGS, methanol synthesis, methanation, higher alcohols, higher alkanes) are exothermic, including alkane and alcohol synthesis, and notably excluding RWGS. Alkane products are more thermodynamically favored than alcohols from CO_2 hydrogenation, setting the overarching HA catalysis challenge: it is truly a "catalyst problem", necessitating the development of materials to control selectivity through a complex reaction network. Toward that goal, the 4 main categories of catalysts under development are modified MeOH synthesis catalysts (Cu-based), modified FT catalysts (Co, Fe based), noble metal catalysts (mostly Rh-based), and Mo-based catalysts (e.g., MoS_2, Mo_2C). Xu summarized the state of technology in 2020 as catalysts based on Cu > noble metals > Co for HA yield, and specifically noted an upper limit of HA selectivity of 35% as a limitation in traditional fixed-bed reactors. Across the types of catalysts, mechanistic considerations outline the challenge to balance the surface population of CO* and CH_x* to balance chain-growth and hydrogenation to make C_{2+} alcohols instead of making methanol or alkanes. Constructing a catalyst necessitates structural control over (at least) two active sites for CO nondissociative (forming CO*) and dissociative adsorption coupled with balanced hydrogenation activity (forming *CH_x, but not just CH_4), and of course, the sites must be colocated (Figure 16). The role of promoters was somewhat unclear, and typically understood on a catalyst-by-catalyst basis, for example, the effect being different for Cu vs Co catalysts. Similarly, the opportunity to explore modulation of the intermediate binding strength, whether through promoters or strong metal−support interaction (SMSI) was identified.

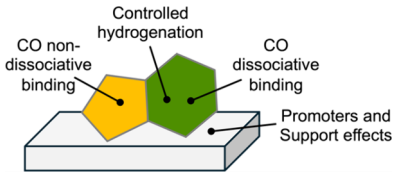

Figure 16. Schematic of the catalyst design challenge for higher alcohols synthesis.

In the 5 years since this review set the stage, the role of promoters remains linked to each type of catalyst, but a few reports provide an understanding of how specific elements act. For example, Na has a structural effect on Co catalysts, where the dispersion of the Co_2C active phase increased with moderate Na loadings (up to 5 wt%).[239] The Na sites also affected CO binding strength, and high Na loadings decreased CO binding energy, leading to high CO selectivity in the reaction. For a Rh catalyst, moderate loadings of Na also increased HA selectivity, and as expected, the promotion was deleterious at high Na loadings due to high surface coverage of Na.[240] Na helped form Rh^+ sites, which are important catalytic sites that work with Rh^0 to affect the desired HA synthesis. Co-promotion with Na and Fe on a Rh/CeO_2 catalyst was also found to be effective, especially for EtOH selectivity (reaching nearly 30%).[241] Similar to Co_2C, the promoters enhanced Rh dispersion and affected CO binding strength. For K on a multimetallic catalyst based on Cu and Fe (CuMgZnFe), again a moderate K loading (4.6 wt%) improved HA selectivity and catalyst activity.[242] Here, the role of K was to achieve the desired balance of CO* and CH_x* by controlling hydrogenation activity of the catalyst. For another CuFe-based catalyst, the role of Cr and K was investigated.[243] Rather than attributing the modulated hydrogenation activity to K, the authors showed that Cr modification balanced hydrogenation activity and CO adsorption strength, decreasing CO dissociation and the associated Fe-carbide formation from activated C* species. These reports highlight that although detailed information about the role of promoters can be elucidated, the effects are often multifunctional and intertwined, and thus, design principles for each promoter element do not apply across all catalyst types of interest. Continued research to understand promoters and attempt to build unifying design rules across catalysts, or in contrast understand the different effects across catalyst types, would be a valuable area of research to advance this field.

A review by Tan et al. summarizes notable performance improvements over the past 5 years for the four types of catalysts noted above.[244] Interestingly, despite recent reports for syngas to HAs over Mo-based catalysts, typically Mo_2C, only one recent report studied CO_2 hydrogenation over these promising catalysts.[245−251] Ye et al. showed that Mo_2C nanowires having exposed (101) surfaces were active for CO_2 hydrogenation to methanol in a batch reactor at surprisingly low temperature of 150 °C using 1,4-dioxane solvent and a pressure of 6.0 MPa. The required dual active site for HA synthesis was prepared by depositing atomic Rh sites on the Mo_2C nanowires, resulting in 44.6% selectivity to ethanol. Through detailed characterization of the Rh/Mo_2C catalyst, the authors determined that additional modification with K was necessary to balance hydrogenation activity. Optimizing the reaction conditions for the RhK/Mo_2C catalyst resulted in excellent ethanol selectivity of 72.1% at 150 °C,

https://doi.org/10.1021/acs.chemrev.5c00361
Chem. Rev. 2026, 126, 5028−5082

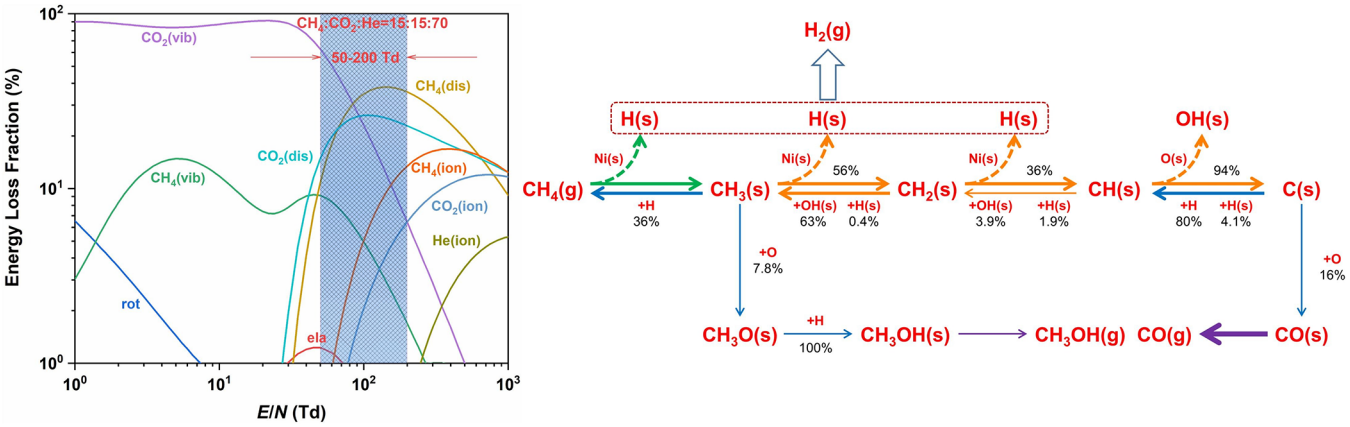

Figure 17. (Left) Fraction of plasma energy deposited into different excitation modes. (Right) Network of surface reaction pathways for carbon deposition C(s) and elimination for plasma-catalytic DRM over a Ni-based catalyst. Reproduced with permission.[279] Copyright 2024 Elsevier.

albeit with low ethanol yield (33.7 umol g^{-1} h^{-1}) in the batch reaction.[252] Given the emerging reports of more mild synthesis methods for Mo-carbide catalysts, including nanomaterials,[253,254] these represent a promising scaffold to rationally construct the necessary active phases for HA synthesis from CO_2 by depositing metals and promoters inspired by reports converting syngas.

3.2. Nonthermal Plasma CO_2 Hydrogenation

In addition to direct CO_2 splitting using NTP, indirect approaches for CO_2 conversion with secondary reactants such as H_2, CH_4, C_{2+} hydrocarbons, H_2O, etc. are advantageous in that they open the possibility of forming higher value products in a single step, which can help to mitigate the currently limited energy efficiency of common NTP approaches using DBD reactors.[125] These types of reactions also frequently benefit from catalyst introduction to help guide the reaction pathways. Much of the work thus far has been focused on the synthesis of simple gas phase products such as syngas ($CO + H_2$) and CH_4, as well as low carbon number liquid products including acids, aldehydes, and alcohols, especially over thermochemically inspired catalysts based on transition metals on high surface area metal oxide supports.[124,255−257]

In addition to hydrogenation of CO_2 via methanation ($CO_2 + 4H_2 \rightarrow CH_4 + 2H_2O$) and reverse water gas shift (RWGS, $CO_2 + H_2 \rightarrow CO + H_2O$),[124,258−260] direct methanol synthesis from CO_2 hydrogenation stands out as a reaction of interest for NTP catalysis, which has been primarily studied in DBD reactors with catalysts due to the prevalence of syngas formation in warm plasmas.[124,261,262] Although the reaction is favored at low temperature and high pressure, the kinetic limitation in CO_2 activation at low temperature and high energy cost for high pressure operation provide an opportunity for NTP. In fact, in contrast to many multistep thermal processes, NTP approaches have demonstrated direct conversion of CO_2 to methanol under ambient conditions.[263,264] Many NTP investigations have focused on Cu-based catalysts predicated on those used for thermal reactions, seeking to understand the role of NTP generated species on the reaction pathways, specifically predicting a transition toward the formate route.[265] Cui et al., have demonstrated a synergistic effect between a 4 wt% Cu/γ-Al_2O_3 catalyst and CO_2/H_2 plasma, leading to increased methanol selectivity particularly with H_2O addition.[266] The combined experimental and computational study highlighted the role of Eley−Rideal (E-R) mechanism in enabling the reaction to occur under atmospheric conditions.

Dry reforming of methane (DRM, $CO_2 + CH_4 \rightarrow 2CO + 2H_2$) and other reactions of CO_2 with CH_4, which are relevant for biogas ($CO_2 + CH_4$) conversion, for example, have been well studied by the NTP catalysis community,[256,267,268] The formation of syngas is the most energy efficient in warm plasmas,[269,270] with improvements arising from implementation of heat management strategies and postplasma catalyst integration,[271−273] although catalysts can suffer from deactivation due to sintering and carbon deposition.[269,271−276] Carbon particles have also been shown to impact the plasma characteristics when formed in the plasma region.[277,278] Selective production of high value oxygenates with DBD plasma-catalyst combinations can overcome the limitations of energy efficiency, and multiple examples of synergistic effects between the NTP and catalyst have been reported[279,280] giving rise to syngas, as well as other oxygenated hydrocarbons such as alcohols and aldehydes. These complex multireactant/product reactions have begun to benefit from mechanistic insight through both thoughtfully designed catalytic investigations, computational modeling, and in situ gas phase and catalyst surface spectroscopic characterization. A recent combined experimental and chemical kinetics modeling investigation by Qin, et al., provided insight into the gas and surface chemistry occurring in DRM over a Ni/SiO_2 catalyst as the applied electric field increases to gas breakdown (and thus, plasma formation).[281] In comparison to thermal catalysis at 500 °C, the application of external fields, both an electric field and NTP, increased the CH_4 and CO_2 conversion to syngas and hydrocarbons via the nonequilibrium excitation of the gas molecules. In the case of electric field catalysis, vibrationally excited CO_2 facilitates dissociative adsorption, whereas in the NTP, reactive radicals, ions, and electronically excited species promote gas-phase and E-R reactions. Similarly, Sun et al., have shown through a combined experimental and computational investigation that both radicals and vibrational species present at the reduced electric field of 50−200 Td (Figure 17, left) accelerate dissociative desorption and E-R reactions in DBD DRM over a Ni/SiO_2 catalyst.[279] Furthermore, the E-R reactions enhanced by NTP generated H and O atoms consume carbon deposited on the catalyst surface by stepwise dehydrogenation of CH_4 as shown in Figure 17 (right). Increased resistance of catalysts to coking during NTP catalysis has been noted as a beneficial feature of these processes.[282]

https://doi.org/10.1021/acs.chemrev.5c00361
Chem. Rev. 2026, 126, 5028−5082

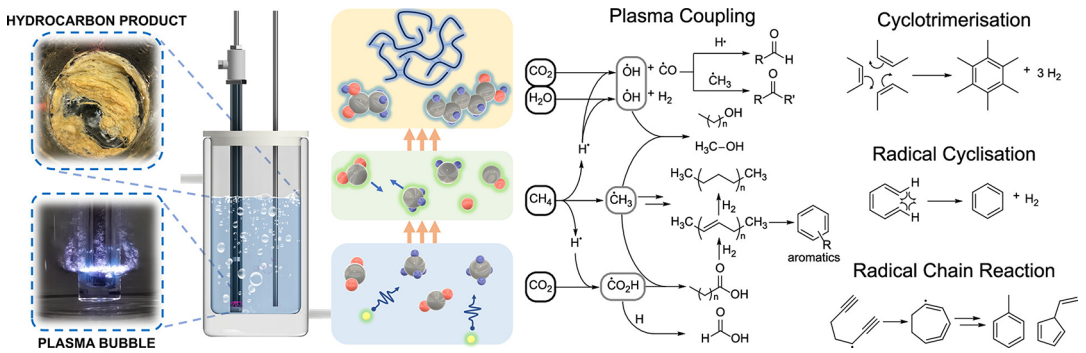

Figure 18. (Left) Schematic of the NTP reactor configuration, plasma bubbles, and solid long-chain hydrocarbon products. (Right) Proposed CO_2/CH_4 plasma coupling and aromatic formation pathways. Adapted from ref 288. Copyright 2024 American Chemical Society.

Similarly, reactions of CO_2 with C_{2+} alkanes can yield an expanded product slate,[283] and the addition of O_2 has been shown to shift the products from syngas toward oxygenates due to the higher concentration of oxygen containing radicals such as O, OH, and HO_2, from electron impact dissociation followed by reaction with H atoms.[284]

Much of the NTP-catalytic CO_2 hydrogenation literature, highlighted above, has focused the production of C_1 molecules like CO, CH_4, and CH_3OH. Strategies to promote carbon coupling are of significant interest, though, especially given the target of higher value products for less energy efficient NTP systems. Successful thermocatalytic approaches to promote C−C coupling reactions such as adding water to the CO_2 feedstock,[285] have also been demonstrated in DBD-catalytic CO_2 hydrogenation to form ethanol over a Cu_2O/CeO_2 catalyst with the assistance of water.[286] Meng, et al. combined isotope-tracing experiments and DFT calculations to determine that H_2O is dissociated in the NTP to produce adsorbed OH* and gas-phase OH radicals, both of which promote C−C coupling through CO-H_2CO bonding and facilitate hydrogenation through proton transfer. Adsorbed H_2O and OH enhances the desorption of ethanol, further increasing alcohol selectivity. While higher water concentrations favors selectivity to ethanol, lower concentrations (H_2O/CO_2 molar ratio below 0.5) facilitate methanol formation and higher CO_2 conversion, consistent with previous work by this group and others,[266,287] also highlighting the ability of H_2O addition to act as a switch controlling alcohol selectivity.

Until this point, the NTP systems reviewed have operated in the gas and vapor phase, with water as a notable reactant. Liquid based conversion approaches, which, while not new, are being applied for a variety of CO_2 conversion strategies to form valuable products. In gas−liquid systems, which are described in detail elsewhere,[130] gas-phase generated plasmas can interact with the liquid, most commonly water, to create reactive species such as OH radicals, that can contribute to the formation of liquid products like methanol. In contrast to the commonly observed smaller hydrocarbon and oxygenate products, a recent contribution from Knezevic, et al., has demonstrated hydrocarbon chain growth up to C_{40} (including oxygenated products) from biogas constituents using non-thermal plasma in a bubbling gas−water system.[288] This approach facilitates continuous removal of the long-chain products by phase separation of the solid products from water as shown in Figure 18 which likely also limits back reaction by the plasma. These solid products were only formed under conditions below 40% CO_2 and not when 100% CH_4 was delivered as the reactant, highlighting the role of CO_2 chemistry in the process with the selectivity being highly dependent on the CO_2/CH_4 reactant ratio. Reaction pathways primarily mediated by radical intermediates were proposed for the (oxygenated) hydrocarbon and aromatic product formation (Figure 18). Although this work did not include a catalyst or other scavenging strategies, these approaches could be readily integrated to tune the selectivity of the products.

The majority of catalysts investigated for NTP CO_2 conversion have been inspired by thermocatalytic systems. While these catalysts have provided notable insight into NTP catalytic chemistry, there exists a significant opportunity to tailor catalyst materials to the NTP environment.[135−137,289] There are a variety of well-studied packing and/or catalyst systems such as ferroelectric materials that have been shown to impact the plasma properties and therefore the plasma chemistry (or chemical species in the plasma), and these and other catalyst features have been extensively discussed.[137,290] To take advantage of the resulting plasma chemistry, several catalyst design criteria have been explored or proposed including (i) multivalent oxide catalysts that can accommodate oxygen vacancies for CO_2 activation and/or to scavenge oxygen radicals, (ii) catalysts that can effectively react rather than quench radicals or vibrationally excited species, and (iii) photocatalysts to capture otherwise wasted energy from electronic transitions, although it is still challenging to deconvolute changes that the catalyst has on the plasma properties from the resulting chemistry. For a thorough discussion of these concepts, see a recent perspective from Bogaerts, et al. on plasma-catalyst synergy.[134] Strategies have been explored both to promote targeted interactions between NTP generated species and catalysts or adsorbates on catalysts through E-R reactions and to selectively enhance the population of NTP activated species that contribute productively to catalytic reactions. As noted above, in DBD, the population of vibrationally excited CO_2 is low, thereby limiting these types of reactions. Recently, Kim, et al., identified a 10 wt% Pd_2Ga/SiO_2 alloy catalyst that enhanced the proportion of vibrationally excited species in a fluidized bed DBD reactor, leading to CO_2 conversion in the RWGS reaction exceeding the thermodynamic equilibrium.[291]

From a catalyst design perspective, photocatalysts have been found to improve the conversion efficiency in DBD and GA plasma by utilizing the ultraviolet−visible photon energy in the plasma emission spectrum, although there is still debate in the literature as to the impact the utilization of wasted photons can have on the efficiency of the plasma processes, especially for

https://doi.org/10.1021/acs.chemrev.5c00361
Chem. Rev. 2026, 126, 5028−5082

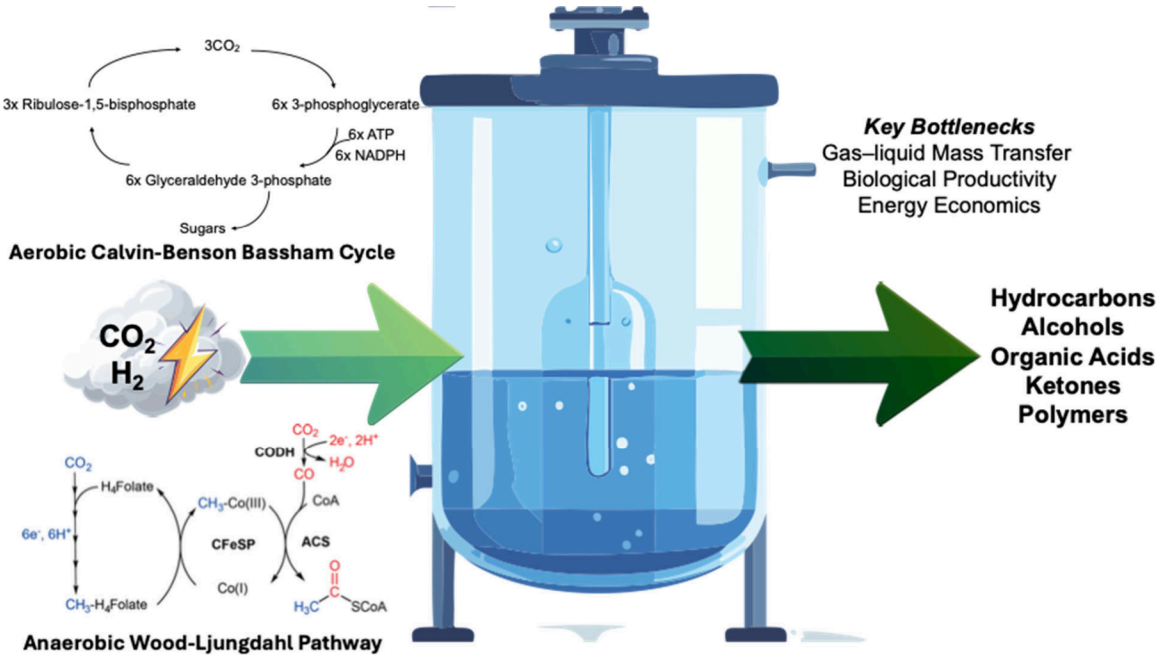

Figure 19. Overview of CO_2 fermentation platforms for biological carbon conversion. CO_2 is biologically converted to value-added chemicals and fuel precursors through microbial fermentation processes that couple carbon fixation with externally supplied reducing power. CO_2 is provided as a gaseous substrate, while reductants such as H_2, electricity, or light supply the electrons and energy required to drive endergonic reduction reactions. (Inset Left) Microbial carbon fixation is enabled by distinct metabolic pathways, including aerobic Calvin-Benson Bassham (CBB) cycle in phototrophic and chemoautotrophic organisms and the Wood Ljungdahl (WL) pathway in acetogenic bacteria, which channel CO2 in central metabolites such as acetyl-CoA and sugar phosphates. The WL methyl branch is colored blue and the carbonyl branch is colored red. CFeSP − corrinoid iron−sulfur protein, CODH − carbon monoxide dehydrogenase, ACS − acetyl-CoA synthase. WL pathway schematic reprinted from ref 300 (Right). Copyright 2022 American Chemical Society. These intermediates are subsequently converted into a broad product suite encompassing organic acids, alcohols, hydrocarbons, and specialty chemicals. Despite significant progress, key challenges remain, including low CO_2 mass transfer, dependence on external energy inputs, limited product titers and rates, pathway and host constraints, and scale-up and process-integration barriers.

photocatalytic materials commonly integrated into plasma catalytic systems such as TiO_2 with limited visible light absorption.[292] Halide perovskites have more recently emerged as photocatalysts for CO_2 reduction,[293] due to high absorption coefficients, wide visible light absorption range, and tunable bandgap, spurring interest in this materials system for plasma catalytic applications. There are multiple examples of ABO_3-type perovskite catalysts in the literature demonstrating enhanced NTP conversion of CO_2, including heterojunction structures based on $CsPbBr_3$ designed to promote separation and limit recombination of photoexcited carriers.[294,295] Recently, machine learning was applied by Shen, et al., to develop an accurate predictive model for the DBD CO_2 conversion efficiency for a Cs_2TeCl_6 photocatalyst based on experimentally tuned process parameters of catalyst mass, gas flow rate, and discharge power.[296]

Still, research is needed to deconvolute improvements in CO_2 reactivity related to photoconversion (as well as plasma catalytic conversion in general) from changes to the plasma environment such as increased microdischarge time and density and improved charge uniformity, resulting from differences in the properties of the catalysts. In addition to NTP-photocatalytic systems, plasma technologies are finding their way into multiple hybrid technologies for conversion including electrocatalysis and biocatalysis, research areas that are also discussed in this contribution. These types of plasma hybrid technologies have been recently discussed for different catalytic conversion processes.[130,257,297] Plasma technologies, particularly those combining multiple reactants/products, as a whole though, are hampered by low selectivity to higher value products beyond syngas for warm plasma systems and low energy efficiencies and selectivities for DBD plasmas. A greater understanding of reaction mechanisms is needed to help guide reactor and catalyst design to promote targeted reactions with high energy efficiency as well as to enable the effective utilization of abundant secondary reactants such as water and nitrogen that can expand the possible product slates.[298,299]

3.3. CO_2 Fermentation

CO_2 fermentation is a biotechnological process that converts carbon dioxide into value-added products using microorganisms or engineered enzymes (Figure 19). CO_2 presents an abundant and relative cheap point source substrate. However, unlike sugar fermentation, in which the substrate carries the reducing power needed for product formation, CO_2 bioconversion routes typically require external energy (e.g., H_2, electricity, or light) to power product formation. As discussed above, falling renewable power costs and maturing green H_2 supply chains have led to intensified interest in CO_2 fermentation pathways. Indeed, recent advances in CO_2 fermentation have enabled direct bioconversion to produce broad product suites, ranging from biopolymers to diverse fuel precursor molecules. This approach leverages the unique CO_2-assimilating metabolisms of autotrophic microbes, such as acetogens, methanogens, and phototrophs, or synthetically engineered strains harboring new-to-nature CO_2 fixation pathways, that utilize CO_2 as a carbon source. The process is conventionally facilitated through canonical CO_2 assimilatory

https://doi.org/10.1021/acs.chemrev.5c00361
Chem. Rev. 2026, 126, 5028−5082

pathways, including the Wood-Ljungdahl pathway, Calvin Benson Bassham (CBB) cycle, and the reductive tricarboxylic acid (rTCA) cycle (discussed in detail in Section 4.2).

As of 2020, CO_2 fermentation had reached pilot and early commercial stages, with ongoing research focused on improving CO_2 assimilation and biosynthetic metabolic pathways, optimizing reactors for enhanced gas mass transfer, and reducing costs via enhanced process efficiencies to enable large-scale industrial deployment. Indeed, companies like LanzaTech, NovoNutrients, and Solar Foods have begun commercializing CO_2-based fermentation for biofuels, single-cell proteins, and specialty chemicals. Additionally, integration with carbon capture and utilization (CCU) initiatives was gaining traction, positioning CO_2 fermentation as a viable solution for reducing industrial emissions. However, despite the technological potential of CO_2 fermentation, viable deployment continues to face several technical, economic, and biological challenges. CO_2 is notably a highly oxidized and thermodynamically stable molecule, with relatively low energy content, thus requiring significant energy input to be converted into reduced carbon compounds. This, in turn, necessitates efficient energy sources, such as hydrogen, electricity, or light to help drive assimilation, which can be costly or technically challenging to integrate. Indeed, autotrophic microorganisms often require external reducing agents (e.g., H_2, formate, or CO) to drive CO_2 conversion. Ensuring a sustainable and cost-effective supply of these electron donors is crucial for scalability (discussed further in Section 6).

Related, many CO_2-fixing microorganisms have slow growth rates (e.g., > 3hr doubling time for model acetogens versus ∼ 20−30min for *E. coli*) and 2−3× lower volumetric productivities compared to sugar-utilizing heterotrophic systems. This is due, in part, to mass transfer induced limitations to substrate availability and decreased flux to reduced products relative to conventional sugar bioconversion platforms. Further, while metabolic engineering and synthetic biology approaches have enabled the development of improved CO_2-fixing strains (Section 4.2), many autotrophic microbes have complex regulatory networks and are less amenable to genetic modifications than model organisms like *E. coli* or *Saccharomyces cerevisiae*. Finally, from a deployment perspective, CO_2 has low solubility in aqueous media (poor gas−liquid mass transfer), which restricts its bioavailability for microbial uptake. Reactor design improvements, such as gas fermentation systems with enhanced gas solubilization and mass transfer capacity, are needed to overcome this limitation. Addressing these challenges requires interdisciplinary efforts in metabolic engineering, reactor design, process optimization, and policy support to make CO_2 fermentation a viable strategy for sustainable bioproduction.

A key advance in recent CO_2 fermentation efforts is the utilization of hydrogen as an energy and/or reductant source and is the basis for several emerging "power-to-x" technologies. Hydrogenotrophic microorganisms have been engineered to convert CO_2 and H_2 into fuel molecules, such as ethanol or butanol.[301] Indeed, *Clostridium autoethanogenum* is an exemplary Clostridia that has recently been metabolically rewired to produce diols, ethylene glycol, and ethyl acetate via targeted metabolic engineering and incorporation of heterologous biosynthetic components, among other high-value metabolic intermediates.[302−305] By tuning the ratio of CO_2:hydrogen in these microorganisms' feed regimes, metabolism can be shifted toward higher yields of desired target products.[304,306] Metabolic engineering efforts in *Rhodobacter* spp. have enabled photofermentative production of hydrogen, polyhydroxybutyrate, and terpenes from CO_2.[307−310] Researchers have also engineered variants of the facultative chemolithotroph, *Cupriavidus necator*, to produce myriad product suites, including methyl ketones, polyhydroxyalkanoates, and isoprenoids (for extensive review, please refer to Panich, 2021[311]). Additionally, this organism has been proposed as a chassis for the production of microbial protein from CO_2 and diverse waste substrates.[312] There have also been substantial advances in CO_2/H_2 fermentation using methanogenic archaea for the production of methane (CH_4), wherein CO_2:H_2 tuning has been shown to impact both archael community structure as well as production of CH_4.[313,314]

Given the poor solubility of CO_2 and H_2 in water, a key hurdle in efficient CO_2 fermentation strategies is the optimization of gas−liquid mass transfer. Alternative reactor configurations, such as bubble columns and rotating packed bed (RPB) reactors, present opportunities for enhanced mass transfer.[315,316] Biocatalyst immobilization offer additional opportunities to reduce mass transfer barriers while achieving improved process intensification.[317,318] Recent studies have employed inverse modeling to define bubble size dynamics, leading to improved predictions of gas holdup and mass transfer rates, and in turn, more efficient reactor designs.[319] Optimization of design and operating conditions of RPB-based CO_2 capture systems have also been evaluated, demonstrating cost savings and reduced packing volumes compared to traditional methods, and highlight the potential of RPBs in scaling up CO_2 fermentation processes.[320] Experiments using dielectric barrier discharge (DBD) reactors in burst mode have notably shown increased CO_2 conversion rates and energy efficiency in preliminary studies.[321] Finally, recent analyses have evaluated gas mass transfer enhancements in external loop reactors, reflective of proprietary configurations deployment in industry (e.g., Lanzatech's syngas conversion technologies).[322] Computational fluid dynamics defined the impact of bubble size and product formation (ethanol) upon volumetric mass transfer coefficient and mass transfer capacity, suggesting mass transfer limitations can be alleviated for some gas bioconversion processes. Collectively, recent advances in reactor design portend substantial advances to the field of gas fermentation at large, including specific benefits to poor solubility gaseous substrates, such as CO_2.

4. EMERGING TRENDS IN CO_2 CONVERSION

4.1. Reacting Bound States of CO_2 via Reactive Carbon Capture (RCC)

An integrated CO_2 capture and utilization approach known as reactive carbon capture (RCC) has recently emerged as a process to access reduced, value-added products through a process intensification approach that first adsorbs CO_2 and then reacts the bound species, typically by switching the feed to H_2, in a single reactor. This process is especially attractive for dilute CO_2 streams, such as flue gas streams having 5−15% CO_2 where the capture costs are comparatively higher than concentrated CO_2 streams (e.g., ethanol fermentation off-gas at 99%).[323−325] The advantages arise from the ability to circumvent multiple process steps and associated capital expenditures of the typical approach, capture − release − purification − compression − transport − storage, prior to the

https://doi.org/10.1021/acs.chemrev.5c00361
Chem. Rev. 2026, 126, 5028−5082

desired utilization. Considering advantages from the chemistry perspective, adsorption of the CO_2 molecule at a capture site breaks the linearity and thereby activates the bound carbonate or bicarbonate species for reduction at lower temperatures and pressures. By keeping the bound CO_2 in the reactor for the reductive desorption step, the RCC approach opens new routes to control selectivity through catalyst design compared to traditional cofed CO_2 hydrogenation reactions. From the process perspective, the ability to work with dilute CO_2 streams, including direct air capture, enables modularity in process design to match the scale of CO_2 source, H_2 source and product volumes required at the site, going against traditional wisdom to take advantage of economies of scale by always seeking large-scale equipment that may not match all three considerations noted here. Considering the case of methanol production via this approach, Freyman and co-workers demonstrated that there is potential to reduce cost and energy requirements by nearly 50% each compared to a conventional capture and conversion approach, clearly motivating research to realize these savings.[326]

Early reports of RCC focused on methanation in an isothermal reactor, where CO_2 capture was followed by H_2 reduction at a single temperature (320 °C) and atmospheric pressure.[327,328] This group published a series of papers outlining the necessary components of dual function materials (DFMs, also called bifunctional materials, BFM), where adsorbent species, such as CaO and Na_2O, are coupled with traditional methanation catalysts based on Ru and Ni.[329−333] Initial reports highlighted the applicability to flue gas streams, and later, the materials were shown to perform well under conditions relevant to direct air capture and conversion (i.e., 420 ppm CO_2).[334] These early reports have been recently reviewed,[335] including a review of the industrial applicability of DFMs.[336] It is important to note that many fundamental catalysis science aspects remain unexplored for these DFMs, especially the interplay and interface between capture sites (alkali metal oxides) and hydrogenation sites (transition metals). The role of moisture and impurities on CO_2 binding and reaction mechanisms is an ongoing area of research by this group,[337] and additional spectroscopic and mechanistic studies would be a welcome addition to this literature. Notably, these early reports utilized alkali and alkaline earth metals as capture agents that can operate at the temperatures needed for methanation (>300 °C). Conceptually, researchers have targeted tethered amines as capture agents due to their utility for CO_2 capture from air and industrial sources. However, a recent paper presents two case studies that identify the mismatch between capture temperature (<80 °C) and reactive desorption temperature (>200 °C) as a limiting factor for amine-based DFMs, in addition to potential catalyst site poisoning by the amine.[338] Thermal degradation of amine capture agents at the elevated temperatures required for catalysis further constrains the practical application of amine-based reactive capture systems. Building on the demonstration of an amine-based photoswing direct air capture system,[339] which established light-driven regeneration as a viable alternative to thermal desorption, Halingstad et al. recently reported a photoreactive capture system that directly couples CO_2 capture with catalytic conversion.[340] The design employed broadband-absorbing titanium nitride (TiN) nanoparticles dispersed within a polymeric amine matrix to enable CO_2 hydrogenation under comparatively mild conditions, achieving conversion of ∼ 70% of captured CO_2 to CH_4 across multiple cycles without measurable amine degradation.

Crawford et al. extended the DFM concept to be built upon microporous zeolites, using faujasite (FAU) as the support for Na-based CO_2 capture sites, termed zeolite dual-function materials, ZFMs.[341] The construction of Ru-Na/FAU directed the captured CO_2 to methane and Pt-Na/FAU generated CO, demonstrating selectivity control through the addition of the appropriate catalytic metal. This report utilized a temperature swing for the reactive desorption step, rather than the isothermal approach pioneered by Farrauto, and high yields of 80−100% of the captured CO_2 were observed. Rather than using different DFM compositions to direct selectivity, reports from the past 5 years have presented the concept of "switchable" catalysis, where the same DFM composition could target methane or CO by the choice of reaction conditions. The concept was first reported in traditional, fixed-bed CO_2 hydrogenation feeding a 4:1 mixture of H_2:CO_2 over a series of Fe- and Ru-promoted $Ni/Ce_{0.5}Zr_{0.5}O_2$ catalysts. The Ru-Ni catalyst demonstrated high selectivity (>80%) for methane at 350 °C and CO at 700 °C, and could be cycled back-and-forth between these two temperatures day-by-day.[342] Merkouri et al. extended the concept to cyclic RCC operation with either H_2 or CH_4 fed in the reactive desorption step to generate CH_4 via methanation with H_2, or CO via RWGS or dry reforming of methane (DRM). Here, the more traditional DFM composition employing an alkali CO_2 capture agent (Na, K, Ca oxides) with a Ni-Ru bimetallic catalyst were supported on a CeO_2-Al_2O_3 support.[343] The authors identified the NiRuCa formulation as the overall best DFM, providing per-cycle yields of 104 $\mu mol_{CH4}/g_{DFM}$ in methanation, 58 $\mu mol_{CO}/g_{DFM}$ in RWGS and 338 $\mu mol_{CO}/g_{DFM}$ in DRM, which are comparable to the molar yields from methanation reported by Farrauto. Merkouri et al. also performed TEA for a conceptual switchable catalysis process.[344] The authors reported that methanation was more profitable than targeting methanol synthesis via CO, and a low payback period of just 4 years was determined. As with many CO_2 hydrogenation approaches, whether traditional fixed-bed cofed hydrogenation or RCC, the cost of electricity and H_2 are key economic drivers.

More recently, methanol has been targeted as a value-added product directly from CO_2 via RCC approaches, that is, not through CO generation via RCC with subsequent methanol synthesis. The opportunity was well-motivated through an analysis of a conceptual RCC process, where significant savings in capital expenditures, operating expenses, and total energy input were identified for RCC versus the multistep CO_2 capture and utilization approaches.[326] A critical assumption was catalytic performance from the DFM that resembled typical methanol synthesis, presenting the experimental targets that needed to be achieved to realize the benefits. Experimentally, two notable recent papers have made progress toward these cost and energy savings. Using a stacked-bed approach, rather than a DFM, Wirner et al., demonstrated 150 $\mu mol/g$ capture on a Na/Al_2O_3 sorbent sitting above traditional CZA methanol synthesis catalyst, but only 12 $\mu mol_{MeOH}/g$ yield due to low conversion of the captured CO_2 (20%) with low selectivity to methanol (22%). Jeong-Potter et al. used similar components, but added the alkali capture sites (K, Ca) directly to the CZA catalyst, giving DFM compositions termed Alk/CZA.[345] K/CZA provided the best performance of this series in RCC cycles, giving 59.0 $\mu mol_{MeOH}/g_{DFM}$ (46% selectivity from captured CO_2) in a

https://doi.org/10.1021/acs.chemrev.5c00361
Chem. Rev. 2026, 126, 5028−5082

Table 2. Comparison of Natural and Representative Synthetic* CO_2 Fixation Pathways[a]

Pathway		No. of Reactions	Product	ATP/CO2 (mol/mol)	NAD(P)H/CO2 (mol/mol)
Calvin cycle	aerobic	11	GA-3P	3	2
3-hydroxypropionate bicycle	aerobic	16	pyruvate	1.67	1.67
Wood−Ljungdahl pathway	anaerobic	8	acetyl-CoA	0.5	2
reductive TCA cycle	anaerobic	9	acetyl-CoA	1	2
dicarboxylate-4−hydroxybutyrate cycle	anaerobic	14	acetyl-CoA	1.5	2
3-hydroxypropionate−4-hydroxybutyrate cycle	aerobic	16	acetyl-CoA	2	2
CETCH cycle	*aerobic*	*12*	*glyoxylate*	*1*	*1*
ASAP	*aerobic*	*11*	*starch*	*0.5*	*2*
POAP cycle	*anaerobic*	*4*	*oxalate*	*1*	*0.5*

[a]Synthetic pathways are denoted in italic. Reprinted from ref 359. Copyright 2022 American Chemical Society.

temperature−pressure swing cycle. Importantly, the methane selectivity was just 4.4%. The authors presented important catalysis science concepts to consider for temperature and/or pressure swing operation, such as how the changing ratio of H_2/CO_2 and surface populations must be considered to develop accurate mechanistic explanations that can lead to new DFM design. This group also explored the TEA and LCA around the Alk/CZA catalyzed RCC-to-MeOH approach, bringing the experimental data into a similar contextual framework outlined by Freyman.[346] Using the moderate performance from the CZA parent material reported by Jeong-Potter et al., not the best-performing K/CZA, the TEA identified a path toward cost-competitive MeOH production compared to the multistep CCU approach. As noted above, green H_2 cost was a key driver. Interestingly, the LCA identified a 21% water consumption savings using the RCC approach over traditional CCU. This was attributed to significantly less water required in RCC for the CO_2 capture step, which requires steam regeneration in the baseline CCU process used as a comparison.

The above thermal approaches have demonstrated success to a variety of products. Nonetheless, limited throughput caused by deadtime associated with startup, shutdown, and heating/cooling between cycle steps, as well as low efficiency due to desorption of unreacted CO_2 during heating in some cases is a significant challenge for the advancement of RCC processes. Utilization of NTP to activate bound as well as desorbed CO_2 has the potential to ease the transition between the capture and conversion steps leading to improvements to overall process efficiency.[151] Similar NTP-based approaches to activate and convert CO_2 discussed in Section 2.3 can be applied for NTP RCC with inclusion of a solid sorbent material that is first saturated with CO_2 from various feedstock streams.[347−349] Liquid sorbents including ionic liquids (ILs), have been extensively studied for CO_2 capture and it has recently been demonstrated that the captured CO_2 can be converted to CO using plasma.[350] The differences in solubility between CO_2 and CO in the IL solution may also provide an avenue for product recovery.[351]

As with noncapture processes, other gases, specifically hydrogen sources, can be introduced during the desorption/reaction step.[352] Li, et al., investigated dry reforming of methane (DRM) in a DBD plasma reactor over the sorbent zeolite 5A. Methane addition during plasma-induced desorption of preadsorbed CO_2 yielded products including H_2, CO, hydrocarbons, and the byproduct H_2O. Although the majority of the observed products with the exception of CO can arise from CH_4 nonoxidative coupling, the presence of H_2O in the product stream indicated possible DRM reactions.[353] All the examples described thus far focus on a sorbent only configuration rather than integration with a DFM, which can provide catalytic reactivity. While many DFMs are suitable only for adsorption of CO_2, metal organic frameworks (MOFs) such as the Zn-based MOF-177, investigated by Gorky, et al., for RCC in a DBD reactor, can adsorb both CO_2 and CH_4, a challenging prospect due to the nonpolarity of CH_4 that only weakly interacts with most materials.[354]

Outstanding questions in the utilization of NTPs to activate bound CO_2 following capture from feed streams include mechanistic insights regarding surface versus gas phase reactivity, the role of DFMs in these processes, the impact of heating on desorption/reaction, and the influence of contaminants (e.g., H_2O, O_2 from DAC of CO_2) representative of realistic application of NTP RCC technologies. In summary, RCC is an emerging approach for CO_2 hydrogenation to fuels and chemicals that offers potential advantages over traditional, large-scale, multistep capture and conversion approaches. A variety of C_1 products can be accessed, and future work should focus on catalysis science to develop structure-performance relationships that can inform next-generation materials that can breakthrough low per-cycle yields to C_1 products and potentially enable selectivity to C_{2+} products.

4.2. Synthetic CO_2 Assimilation Pathways

As discussed in Section 3.3., biological upgrading of CO_2 presents a promising platform for direct conversion of CO_2 sources but is limited, in part, by energy-intensive and relatively slow kinetic CO_2 assimilation pathways. Indeed, an array of autotrophic microbes − possessing native metabolic machinery for capture and conversion of CO_2 − have been developed as biological conversion platforms to produce myriad bioproducts.[303,304,307,311,355−357] The primary CO_2 fixation pathways include the CBB cycle, the Wood-Ljungdahl (WL) pathway, the reductive tricarboxylic acid (rTCA) cycle, the 3-hydroxypropionate (3-HP) bicycle, and the archael hydroxypropionate-hydroxybutylate (HP-HB) cycle. Each pathway is characterized by distinct enzymatic mechanisms and energy requirements, with some relying on ATP-driven carboxylation reactions with varying energy requirements and reductant generation potential (Table 2). Such native biological CO_2 fixation pathways are inherently inefficient, and present large energy demand in the form of ATP, often limiting their deployment potential (for comprehensive review of CO_2 fixation pathway thermodynamics, please refer to (Zhao, 2021)[358]). Indeed, native CO_2 fixation pathways face both energy and reducing power constraints, requiring substantial ATP input or reduced cofactors (e.g., NAD(P)H, ferredoxin), limiting their efficiency in non-native hosts (Table 2).

https://doi.org/10.1021/acs.chemrev.5c00361
Chem. Rev. 2026, 126, 5028−5082

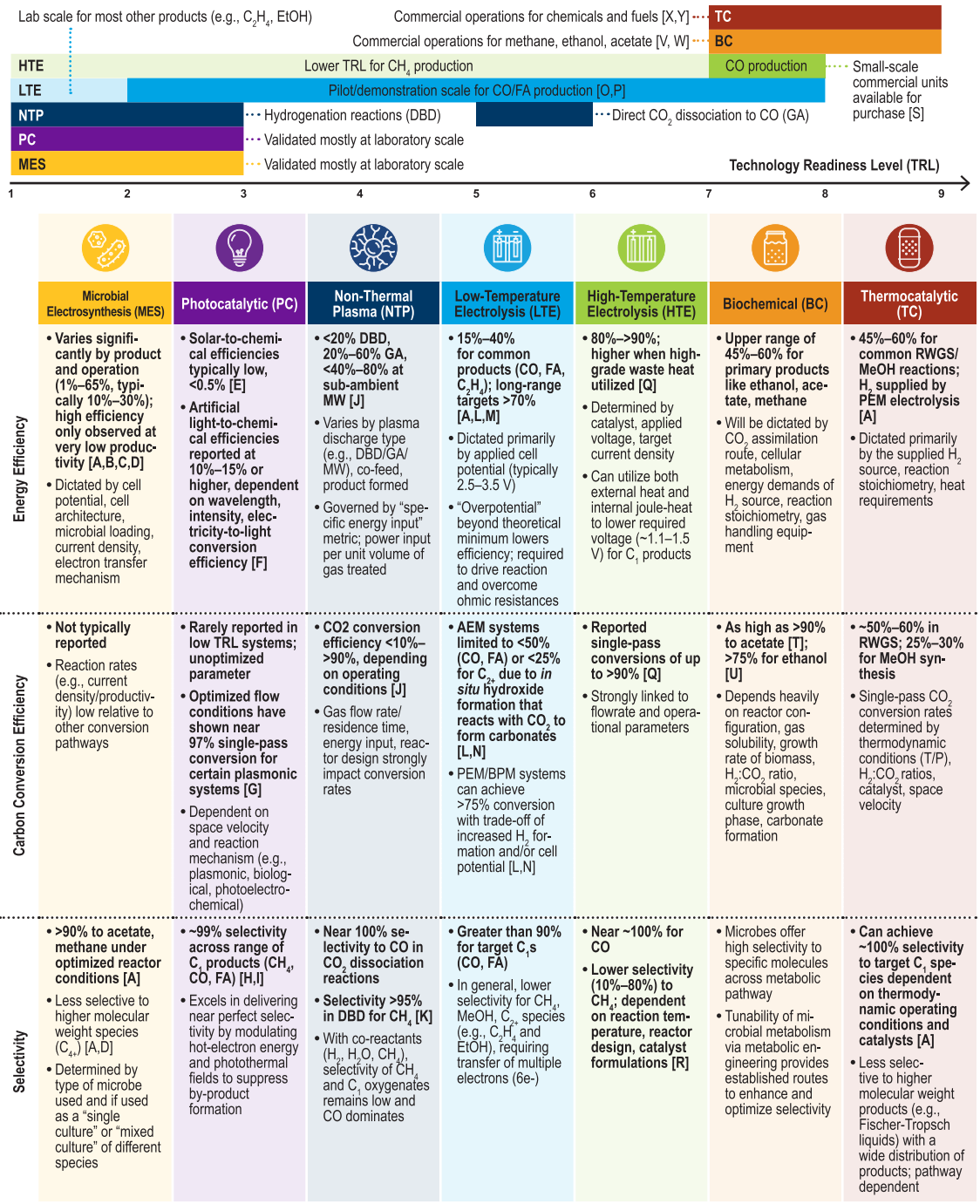

Figure 20. Comparative overview of cross-cutting technical performance metrics. references: [A],[4] [B],[202] [C],[370] [D],[371] [E],[372] [F],[177] [G],[373] [H],[374] [I],[375] [J],[123] [K],[124] [L],[376] [M],[377] [N],[7] [O],[378] [P],[379] [Q],[380] [R],[381] [S],[382] [T],[383] [U],[384] [V],[385] [W],[386] [X],[387] [Y][388]

Additionally, enzymatic and carbon conversion efficiency as well as oxygen sensitivity hinder key assimilation enzymes. For example, the key assimilatory enzymes ribulose-1,5-bisphosphate carboxylase/oxygenase (RuBisCO) in the CBB cycle and carbon monoxide dehydrogenase (CODH) in the WL pathway, respectively, often suffer from low catalytic efficiency and/or oxygen sensitivity, reducing overall carbon fixation rates.[360,361] Notably, some CO_2 fixation pathways, such as the rTCA cycle, require precise regulation to balance intermediate metabolite levels, as excessive accumulation can lead to toxicity.[362] Indeed, introduction of autotrophic CO_2 fixation pathways into heterotrophic microorganisms often requires the optimization of cofactor regeneration, redox balance, and central metabolism to support autotrophic growth.[363] Finally, while CO_2 fixation pathways have been extensively studied in laboratory conditions, their large-scale implementation in biotechnological applications requires further optimization of enzyme kinetics, thermodynamics, and metabolic flux.

Recently emerging synthetic biology efforts have targeted the development of new-to-nature CO_2 fixation pathways with enhanced energetics and efficiency to overcome the hurdles associated with conventional CO_2 assimilation pathways. The first reported synthetic CO_2 fixation pathway entailed the retrosynthetic development of the crotonyl−coenzyme A

https://doi.org/10.1021/acs.chemrev.5c00361
Chem. Rev. 2026, 126, 5028−5082

(CoA)/ethylmalonyl-CoA/hydroxybutyryl-CoA (CETCH) cycle (REF).[364] The CETCH cycle is comprised of 17 enzymes derived from nine different organisms spanning all domains of life. Following extensive optimization, the cycle was successfully deployed in vitro, demonstrating nearly 5X higher efficiency and requiring substantially fewer photons per CO_2 molecule fixed than conventional photoautotrophic pathways. To catalyze the reductive carboxylation of enoyl-CoA esters, the cycle leverages enoyl-CoA reductases (ECR), which are notably absent from all native CO_2 fixation pathways reported to date. ECR enzymes present promising catalysts as components of synthetic CO_2 fixation due, in part, to their broad substrate spectrum, oxygen insensitivity, and requirement of NADPH as a sole cofactor. Additionally, as recently noted by Tommasi,[365] ECR catalytic efficiency is approximately 2× greater than that of RuBisCO.

In the past five years, additional synthetic fixation pathways have been reported, achieving even higher conversion rates and efficiencies, underscoring the promise of synbio-mediated reactive capture strategies. For example, Cai and colleagues developed a hybrid chemo-biochemical pathway for starch synthesis from CO_2 and hydrogen in a cell-free enzyme-based system. The artificial starch anabolic pathway (ASAP), consisting of 11 reactions, demonstrates nearly order-of-magnitude higher CO_2-to-starch biosynthetic rate than that observed in maize and 5-fold higher rate than the CETCH cycle.[366] Another promising example is the tartronyl-CoA (TaCo) pathway, which facilitates direct assimilation of glycolate into central carbon metabolism.[367] Notably, this pathway enables carbon-positive photorespiration via the development of a new-to-nature enzyme, glycolyl-CoA carboxylase (GCC). The pathway notably facilitates carbon fixation that is independent of RuBisCO oxygen sensitivity limitations, bypassing a key bottleneck in conventional photosynthetic CO_2 fixation. Finally, in 2025, Santanowski and colleagues introduced the CORE cycle, a synthetic metabolic pathway that converts CO_2 to formate at aerobic conditions and ambient CO_2 levels, using NADPH as a sole reductant source, representing yet another advance in the field.[368] Synthetic CO_2 fixation pathways continue to emerge with continually improving energetics and efficiency; development of such new-to-nature CO_2 fixation pathways underscores the power of synthetic biology, wherein heterologous and native metabolic machinery can be paired to establish new-to-nature functionalities. Effective incorporation and optimization into production hosts will be needed to bring to bear the full potential of these pathways.

5. CROSS-COMPARISON OF CO_2 CONVERSION PATHWAYS

With CO_2 conversion R&D experiencing exponential growth over the past decade, a wide assortment of potential conversion technologies have received attention, spanning technology readiness levels (TRL) from laboratory to commercial scale as discussed in Sections 2 − 4. A natural question that arises from such a diverse set of potential conversion pathways is "under what conditions might a future user seek out one pathway over another?" or "what are the purported advantages or unique aspects of one pathway versus another?". In Section 5 we offer perspectives around these questions and provide a high-level comparative summary of the seven noted conversion pathways to highlight key cross-cutting technical metrics and their relative advantages and limitations. The intention of this assessment is not to endorse any one technology but rather emphasize key defining attributes of each of the noted conversion pathways along with the potential opportunity space.

The pathway summaries shown below are split across two comprising tables. The first table examines the technical cross-cutting metrics of pathways while the second table highlights qualitative characteristics of each pathway and summarizes commonly cited strengths, challenges, and tradeoffs. In both tables the pathways are loosely ordered by technical maturity with the lowest TRL appearing on the left and progressively moving right to higher TRL.

The cross-cutting technical metrics reported in Figure 20, while offering a snapshot of current performance ranges reflective of recent literature, should not be considered without an understanding of their key caveats and shortcomings which are summarized here. One notable limitation in this approach involves pathway product distribution. Specifically, no one single product is consistently produced across all seven pathways, making an apples-to-apples comparison of technical performance impractical. In response to this limitation, our approach has been to, where appropriate, report a range of published values for each metric across the most commonly cited C_1-C_2 products over the last 5 years. For example, the NTP, LTE, and HTE pathways may reflect the performance of synthesizing carbon monoxide whereas the MES and BC data may be more reflective of acetate and methane formation, owing to their specialized biological assimilation chemistry. Our aim is that this approach provides an "order of magnitude" idea of what to expect for a given pathway, which, in reality, varies based on process complexity, targeted end product, and the specific operating conditions of the process.

Further, as performance metrics may be aggregated across multiple studies, care should be always taken when correlating all of these performance metrics together. For example, systems operating at state-of-the-art efficiency may not be able to achieve the reported state-of-the-art durability which can create challenges with appropriately understanding the state of these technologies and representing them in technoeconomic analyses or other high-level representations. Many of the metrics and technologies summarized in Figure 20 are specific to laboratory scale systems yet mature technologies will be manufactured and deployed at scales significantly larger than current R&D scale systems. This need for manufacturing scale up, while qualitative, does serve as an important control on the optimal performance metrics for each conversion technology. The potential need for large-scale deployments of these technologies and the importance of manufacturing economies of scale for capital cost reductions means that R&D must target advances that can be manufactured at scale.[369] For example, R&D low-temperature electrolyzer membrane electrode assemblies (MEAs) are generally manufactured using a hands-on ultrasonic spray coating process while commercial MEAs are typically manufactured via continuous throughput roll-to-roll processes. New materials and MEA designs for low-temperature electrolyzers must ensure that these advances are relevant to at-scale manufacturing processes.

5.1. Energy Efficiency

As stated throughout the review, energy efficiency is one of the key defining metrics of CO_2 conversion. Starting from a point of no intrinsic energy content (i.e., heating value) and

https://doi.org/10.1021/acs.chemrev.5c00361
Chem. Rev. 2026, 126, 5028−5082

predominately comprised of oxygen, a substantial amount of input energy—in the form of electricity, heat, and/or hydrogen—is required to conduct the necessary reaction steps to produce most CO_2-derived products at scale. Consequently, the economic viability and competitiveness with incumbent methods is inextricably linked to future assumptions around the cost and availability of the supplied energy and, correspondingly, the efficiency at which it is consumed.

Across the seven considered pathways, energy is generally consumed in one of three ways: directly via electrons (LTE, HTE, NTP, MES), indirectly through low-carbon hydrogen (TC, BC), or via light (PC). For electrolysis and microbial electrosynthesis pathways, energy input is primarily based on the applied cell potential and the subsequent charge delivered to the surface of the electrocatalyst. Shown in Figure 20, for LTE and MES, the applied voltage in these systems typically ranges from 2.0 − 4.0 V, depending on the operating conditions, target product, and desired productivity (i.e., current density). When compared against the theoretical minimum voltages based on thermodynamic principles, these reported voltages are notably higher, needing additional driving force to overcome internal resistances and drive the kinetics at meaningful rates. These inefficiencies lead to reported energy efficiencies in the range of ∼ 10−40%. As these systems mature over time, it is expected that voltages will fall and efficiencies will improve; however, with more mature H_2O electrolysis systems showing long-term targets of ∼ 70%, it is reasonable to expect that CO_2-focused electrolysis may find a ceiling around similar, or lower, levels depending on product. A notable standout to the upside is high temperature electrolysis. By operating at high temperature regimes (typically 800 − 850 °C) and through leveraging internally generated joule heat, HTE electrolyzers can operate with a much lower overall voltage demand in the range of ∼ 1.2 − 1.5V, leading to observed energy efficiencies in some cases exceeding 95%.[105] Like electrolysis, nonthermal plasma pathways similarly experience a wide range of observed energy efficiencies from as low as < 20% to approaching 80% depending on tradeoffs around reactor configuration, specific energy input, residence time of the reactants, and other technical parameters.

In the case of H_2-mediated CO_2 conversion, pathway energy efficiency is primarily controlled by two parameters: (1) the efficiency of producing the H_2 feedstock and (2) the efficiency in which the H_2 is utilized for CO_2 conversion. While there are many routes to producing H_2 (see: Table 4) and their review is outside the scope of this work, commonly cited low-carbon H_2 sources include PEM and alkaline systems with typical operating energy efficiencies in the range of ∼ 55−65%. From this starting point, it places an inherent cap on energy efficiency from H_2-mediated CO_2 conversion processes. Further, in the conversion (e.g., methanol synthesis, ethanol fermentation, methanation, etc.) there are also unavoidable stoichiometric inefficiencies in how H_2 is ultimately consumed within the reaction pathways. To effectively deoxygenate the CO_2 feedstock and balance the overall reaction, water is typically formed as a byproduct as shown in Equations 7 − 9, where for some products (e.g., methane, ethanol) up to 50% of the incoming H_2 goes toward the formation of H_2O that provides little to no value. Therefore, often only a fraction of the incoming H_2—produced with a typical efficiency of 55−65%—may end up in the final product, further limiting the maximum possible CO_2 to product energy efficiency. Shown in Figure 20, while also product dependent, estimates across thermo and biocatalysis typically fall in the 45−60% net energy efficiency range.

$$CO_2 + 3H_2 \rightarrow CH_3OH + \boldsymbol{H_2O} \quad (7)$$

$$CO_2 + 4H_2 \rightarrow CH_4 + 2\boldsymbol{H_2O} \quad (8)$$

$$2CO_2 + 6H_2 \rightarrow C_2H_5OH + 3\boldsymbol{H_2O} \quad (9)$$

Lastly, the remaining major mechanism for energy transfer considered herein is light, either in the form of direct solar-to-chemical conversion (i.e., natural light) or artificial illumination. Current state of the art data reflected in Figure 20 reveal solar-driven photocatalytic systems typically exhibit overall efficiencies below 1%, whereas artificially illuminated systems can achieve 10−15% light-to-chemical efficiencies, though these values remain highly sensitive to spectral distribution, photon flux, and catalyst architecture. Looking ahead, improvements in light-source efficiency and photonic utilization offer a path toward higher-performing photodriven CO_2 conversion. Continued advances in highwall-plug efficiency LEDs and better spectral matching between emitters and catalyst absorption bands will reduce optical and electrical losses, while emerging plasmonic, photonic, and nanostructured catalyst designs promise greater light assimilation and more efficient carrier generation.

5.2. Carbon Conversion Efficiency

Another vector for consideration in CO_2 conversion is carbon conversion efficiency. With many of the commonly proposed sources of CO_2 feedstock being dilute by nature (e.g., < 15% CO_2), such as direct air and point source industrial capture, the costs to sufficiently concentrate and utilize CO_2 can be high (see: Figure 26). Achieving high rates of carbon conversion is therefore key to efficiently utilizing the feedstock and minimizing process operating costs associated with purification, recapture, or recycling of unconverted CO_2. Further, from the perspective of emissions reductions, mitigating the rerelease of unreacted carbon can also carry significant life-cycle implications.

Highlighted in Figure 20, reported single pass conversion efficiency varies widely by pathway, from less than 5% to exceeding 97%. In the lowest TRL pathways (e.g., MES, PC) conversion is often not reported, with current research instead favoring other core "proof-of-concept" metrics such as productivity or energy efficiency. At the other end of the TRL spectrum, technically mature and optimized pathways such as thermocatalysis or biocatalysis commonly report a wide range for carbon conversion, often dictated by intrinsic thermodynamic or biological limitations. For example, in the case of industrially practiced equilibrium reactions such as water-gas shift and methanol synthesis, thermodynamics constrain single-pass conversion rates of these reversible reactions to typically ∼ 50−60% for CO and ∼ 25−30% for MeOH, depending on the specific operating conditions. In the case of biological conversion, the conversion of CO_2 to products is similarly intrinsically limited, but rather by the metabolism of the microbe itself and the amount carbon diverted away from products to maintain cellular growth and reproduction. Typical conversion values for common biological products range from 75% to 90% for ethanol and acetate, respectively. For other moderate TRL pathways (e.g., LTE, HTE, NTP), carbon conversion is largely a tunable parameter

https://doi.org/10.1021/acs.chemrev.5c00361
Chem. Rev. 2026, 126, 5028−5082

without rigid thermodynamic limits. Rather, single-pass carbon conversion is flexible based on the reactor design, electrolyte chemistry, and other operating conditions of a process. Ultimately, for these pathways the ideal target carbon conversion efficiency is likely to be case dependent, requiring consideration of the interplay between a combination of core operating parameters such as CO_2 cost, space velocity, equipment sizing, selectivity, and input energy.

5.3. Product Selectivity

In general, the most commonly targeted products or intermediates via CO_2 conversion include C_1 species such as methane, carbon monoxide, methanol, or formic acid. Not only do these products represent core building blocks across the chemicals and fuels industry, but C_1 products—especially those containing oxygen—are mechanistically easier to produce compared to multicarbon species. Indeed, each of the seven pathways considered have promising routes to producing C_1 molecules with selectivity exceeding 90%.

As product carbon number increases, the reaction mechanism(s) required to sequentially combine and link multiple carbon atoms in series becomes increasingly more complex and pathway-specific differences become more readily apparent. Some pathways, such as the high temperature electrolysis pathway, are considered unsuitable to form C_{2+} species altogether due to thermodynamic instabilities arising from high operating temperatures in O-SOECs. For most other pathways, C_{2+} species are possible, albeit at reduced selectivity relative to C_1 production. A notable example is low temperature electrolysis over Cu electrocatalysts where one study showed mixtures of up to 16 different products can be produced simultaneously, with 11 out of 16 being C_{2+}. However, with the selectivity toward most of the observed C_{2+} species being < 1%, economic separation and recovery becomes challenged.[46] Biochemical conversion pathways, however, are a standout exception to this rule of thumb on selectivity. Leveraging specialized metabolic pathways (e.g., Calvin-Benson Bassham, Wood Ljungdahl, Reductive TCA, etc.), biological routes can assimilate CO_2 to larger multicarbon products ($C_2 - C_{18+}$) often with near 100% selectivity. This is a key advantage for biochemical pathways and creates opportunities for process intensification where high molecular weight biopolymer or fuel-range molecules can be produced directly with fewer processing steps.

5.4. Pathway Strengths, Active Research Areas, and Scalability

5.4.1. Microbial Electrosynthesis. The field of microbial electrosynthesis sits at the intersection of electro- and biochemistry. This marriage of technologies offers the potential for several advantages including the ability to rapidly cycle on/off to follow electrical loads at periods of low-cost energy, the ability to leverage biological CO_2 fixation chemistry to directly produce higher molecular weight species with high selectivity, and high(er) contaminant tolerance and ability to interface with a more diverse set of lower purity substrates than electrolysis alone. Indeed, many of the prevailing proposed use cases of MES (e.g., wastewater upgrading) offer a unique opportunity space for MES relative to other feedstock-sensitive abiotic pathways.

However, owing to its low technical maturity, the MES pathway faces a myriad of both fundamental and technical challenges. The linking of both electrochemical and biochemical reactions makes for a complex network of possible electron transfer mechanisms (e.g., direct and extracellular) where the fundamental underlying mechanism is not yet fully understood and remains an active area of research. Further, MES pathways have so far demonstrated only very low productivity relative to more mature electrolysis processes. Specifically, the best-in-class reported current densities are typically on the scale of only ~ 10−20 mA/cm^2 or less whereas commercial electrolysis systems are 2 orders of magnitude higher (>2,000 mA/cm^2). Thus, without significant technological advancements, the surface area, and consequently capital costs, could be prohibitively high to operate MES at commercially relevant scales and rates. These challenges in productivity stem both from reactor engineering issues (e.g., higher internal resistances of biofilms) and inherent biological limitations around the rate at which microbes can utilize electrons.

5.4.2. Photocatalysis. Photocatalysis represents a unique but low TRL pathway for CO_2 conversion, offering many similar strengths to that of LTE, MES, and NTP with rapid cycle times, scalable and modular reactor architectures, and near-ambient operating conditions. A key differentiator, however, lies in the ability to utilize light—natural or artificial—as the reducing mechanism. In this manner, photocatalytic pathways are uniquely equipped to transform CO_2 into products without the typical external electrical input (or H_2 cofeeds), providing novel opportunities in siting and the ability to utilize the limitless resources of our sun. Further, using next-generation catalysts known as plasmonics, high-intensity light at specifically tailored wavelengths can be utilized to selectively excite photoreactive catalysts to drive chemical reactions versus classical reactions which rely on heating and/or pressurizing the entire reactor volumes.

Significant R&D, however, is still needed to bridge the gap between lab-scale novelties to commercially viable systems. One of the most significant barriers is the typical low single-digit energy efficiency at which light is converted into products, creating headwinds in terms of equipment sizing to reach comparable and relevant production scales. As such, more fundamental research is needed to better understand the complex reaction mechanisms underpinning the light-to-chemical conversion step(s). Long-term durability studies are another critically needed area of research to address known issues related to photocorrosion of nanoparticle catalysts and light-induced phase change of materials that currently present barriers to achieving long-term stability.

5.4.3. Non-Thermal Plasma. Situated between laboratory and pilot scale, NTP is a moderate TRL pathway that leverages the ability to selectively excite electrons to a state of high-energy nonlocal thermodynamic equilibrium, creating ionized gases and short-lived radical species conducive for C = O bond cleavage and CO_2 conversion. Unlike conventional pathways which employ heat and pressure to drive chemical reactions, NTP can operate at near-ambient conditions using exclusively electrical inputs or can generate heat without an external heat source, as is the case for warm discharges. Certain NTP reactor designs, such as DBD, can also be combined with heterogeneous catalysts in hybrid systems to take advantage of the reactive species inside the plasma plume to drive targeted chemistries with secondary reactants (e.g., H_2, CH_4, C_{2+} hydrocarbons, H_2O, etc.), although research is needed to steer the selectivity toward desired products beyond CO and H_2.

https://doi.org/10.1021/acs.chemrev.5c00361
Chem. Rev. 2026, 126, 5028−5082

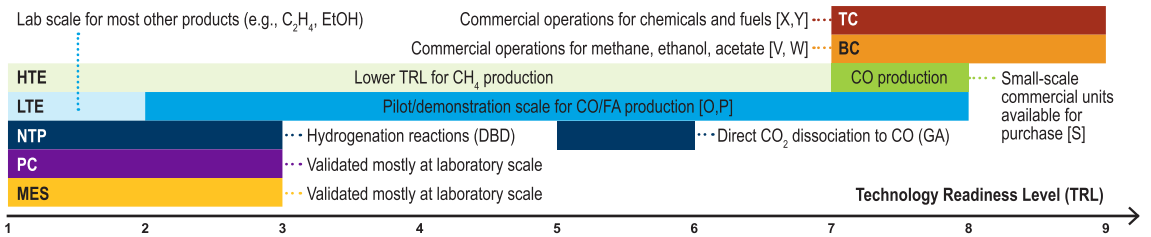

	Microbial Electrosynthesis (MES)	Photocatalytic (PC)	Non-Thermal Plasma (NTP)	Low-Temperature Electrolysis (LTE)	High-Temperature Electrolysis (HTE)	Biochemical (BC)	Thermocatalytic (TC)
Pathway Strengths	• Integration of biology with electrochemistry expands accessible products to include C_4–C_5 species at high selectivity • Bioelectrodes potentially less sensitive to contaminants; can interface with more diverse substrates (e.g., wastewater)	• Sunlight-to-molecule conversion can enable direct transformation CO_2 into fuels and chemicals without external electrical input • Near room-temperature operation with near-unity selectivity • Rapid startup and shutdown capacity	• Unique opportunities for hybrid systems with catalyst integration inside plasma zone (interaction with short lived radicals) • Rapid cycle times capable of matching intermittent electricity availability • Potential for near ambient conditions	• Wide and tunable production distribution based on electrocatalyst type • Rapid cycle times capable of matching intermittent electricity availability • Near ambient operation conditions	• High energy efficiency, especially when integrated with high-temperature waste heat (e.g., nuclear) • Potential for relative economic outperformance in areas where cost of energy is high due to low operating voltages	• Commercially vetted technology compatible with wide range of feedstocks and delivers high selectivity to products • Relatively low sensitivity to most contaminants; can interface with "dirtier" industrial feed streams than other pathways	• Commercially vetted technology; provides products with large market sizes • Potential to integrate with or near existing fuel/chemical facilities to lower overall costs
Pathway Challenges & Active Research Areas	• Low productivity relative to other conversion pathways • High internal ohmic resistances limit energy efficiency • Complex bio-electrochemical reactions not fully understood • Challenging to obtain both high efficiency and productivity simultaneously	• Low efficiencies due to charge carrier recombination • Mechanistic ambiguity difficult to disentangle • Photo-corrosion, nanoparticle sintering, and phase changes can reduce long-term catalyst stability	• Limited energy efficiency due to recombination of reactive species (DBD), low selectivity requiring separation steps • Some reactor configurations difficult to scale • Performance varied and dependent on type of reactor due to different dissociation mechanisms	• Low selectivity for >2e- products due to complex reaction mechanisms • High CO_2 losses to parasitic carbonate formation; carbonate crossover in AEMs • Poor long-term catalyst stability • Limited long-term durability of electrolyzers • High unit capital cost limits ability to economically operate at low-capacity factor	• Limited product distribution; high operating temperatures restrict products to C_1s only (CO, CH_4) • Poor long-term stability and durability of materials; ceramic electrolytes • Slower cycle times relative to other electrolyzers; may not be conducive to intermittent operation	• High energy barrier for CO_2 assimilation; synthetic CO_2 assimilation pathways present potentially superior energetics • Biogenic CO_2 evolution associated with carbon metabolism limits yield • Enhancing gas solubility and transport for increased productivity	• Low per-pass yields can pose separations challenges • Not as compatible with small-scale distributed applications as other conversion pathways
Scalability Considerations	• Reported current densities (~10-20 mA/cm^2) are two orders of magnitude lower than more mature electrolyzers; MES systems would require extremely large surface areas to attain commercially relevant production volumes [B]	• Modular, scalable design for flexible deployment • Scaling efforts confirm engineering feasibility, but stability, cost, reproducibility remain barriers • Scalable architectures that maintain optical uniformity and thermal management are lacking	• Proven modular and scalable designs must be considered for scaling (GA/MV) plasma types • Process scaling may be limited by low product selectivity and addition of separation steps	• Inherently modular stack designs conducive to match market demands; may not benefit strongly from economies of scale • Thermal management and gas separation critical areas to efficient scale-up	• Limited manufacturing and supply chain capacity; under development	• Conventional limitations associated with aeration of O_2-intensive bioprocesses may pose challenges at large scales	• Must establish stability and performance in the presence of impurities, such as water, NOx, SOx, H_2S, soot, O_2 • Pilot-scale operation is needed to identify and de-risk commercialization challenges

Figure 21. Comparative overview of pathway challenges and opportunities. References: [B][202] [O],[378] [P],[379] [S],[382] [V],[385] [W],[386] [X],[387] [Y][388]

Due to the short-lived nature of radicals and highly reactive nature of species produced inside of the plasma zone, one of the major challenges often cited for NTP is rapid recombination of reactants leading to low overall energy efficiency. For this reason, the production of C_{2+} species is similarly challenged due to the number of necessary steps required to sequentially link carbon atoms relative to the lifetime inside the plasma zone. R&D around novel reactor architectures to maximize the lifetime and utility of these reactive species and improve energy efficiency is underway; however, many of the reactor designs tested to date (e.g., gliding arc, microwave) have attributes that make scaling for large-scale deployment challenging (e.g., subambient pressure operation for hitting energy efficiency targets). New developments in reactor designs (e.g., ambient operation of MW systems) shows promise in efficiency improvements that also lend themselves toward scalability.[389] Further efforts to better understand the tradeoffs between reactor configuration and how best to optimize performance for potential scale up are an area of need. Finally, while NTP scale through a modular configuration in similar methods to LTE or PC (as exemplified by commercially available ozone generators), challenges with low selectivity when producing C_{2+} species can cause costly separations steps that may limit deployment.

5.4.4. Low-Temperature Electrolysis. Low temperature electrolysis represents a moderate TRL pathway for CO_2

https://doi.org/10.1021/acs.chemrev.5c00361
Chem. Rev. 2026, 126, 5028−5082

conversion with recent emerging pilot and precommercial activity in the space of C_1 chemistry. Some of the defining strengths of LTE include the (1) near-ambient operating conditions, (2) the potential for rapid on/off cycling, (3) modular "stack" designs where the size of electrolyzers can easily be scaled up or down to meet product demands, and (4) a wide and tunable product distribution. Indeed, potential product diversity is a key feature of LTE where, through careful manipulation of the applied voltage and metallic electrocatalyst environment, literature reports find that over 20+ unique species are possible across multiple carbon numbers (C_1-C_4) and chemical functionalities (alkanes, olefins, alcohols, glycols, acids, ketones, and aldehydes), making it the most diverse product slate of all the direct electron consuming pathways (i.e., LTE, HTE, MES, NTP).

Before these strengths can be fully realized at commercial scale, further R&D and engineering is needed to address several critical needs in LTE. First, although the known list of possible products is large, the selectivity at which C_{2+} species are produced is often low due to complex reaction and coupling mechanisms, contributing to prohibitively expensive purification and recovery costs. Further, to minimize selectivity challenges related to parasitic hydrogen generation side reactions, many studies opt for highly alkaline electrolytes. While successful at suppressing hydrogen formation, the alkaline conditions can result in up to 50−75% of the incoming CO_2 being consumed in the formation of carbonates, leading to low per-pass carbon conversion and membrane crossover issues. Finally, platinum group metal use and corresponding high capital costs of LTE stacks combined with poor long-term durability of the catalyst and stack componentry creates headwinds that challenge economic viability and act to limit the ability of electrolyzers to operate at low capacity factors otherwise needed to utilize low-cost electricity.

5.4.5. High-Temperature Electrolysis. Of the electrolysis-based pathways, high-temperature solid oxide electrolysis currently represents the most technically mature and commercially accessible option. Indeed, modular SOEC units have been deployed commercially for applications in space exploration and chemical synthesis.[30] Highlighted in Figure 20 and Figure 21, one of the main advantages cited for HTE pathways is the potential for energy efficiencies approaching 90%—or higher when high-grade waste heat is available (e.g., nuclear waste heat). In the current economic climate where energy demand is expected to grow meaningfully and therefore put upward pressure on energy costs into the foreseeable future, HTE presents a compelling option for minimizing energy costs with a technology that has been largely derisked.

While the uniquely high operating temperatures translates to benefits in operating efficiency, it is not without tradeoffs. One of the most significant drawbacks to high operating temperature is the impact on product formation. Whereas pathways operating at near-ambient conditions have access to a wide and often tunable set of possible products spanning multiple carbon numbers, the high temperature nature of SOECs is thermodynamically unfavorable for C-C bond formation, causing intermediates to rapidly decompose into exclusively C_1 products, specifically methane and carbon monoxide. Another consequence of high operating temperatures is less flexibility in potential on/off cycling or electrical load following. Whereas lower temperature systems may be more easily cycled to potentially follow daily or hourly fluctuations in the electric grid, high temperature electrolyzers intentionally avoid large or frequent temperature swings to minimize thermal stresses and durability issues with the comprising ceramic and metal componentry. Instead of completely cycling on/off, HTE systems often favor a "hot standby" mode where the electrolyzer is held at elevated temperature without producing a product; however, prolonged duration in this state has a negative impact on energy efficiency.

5.4.6. Biochemical Conversion. Biochemical fermentation represents the highest TRL and commercially vetted biotic CO_2 conversion pathway. Leveraging similar natural and man-made CO_2 assimilation pathways as in the case of MES, biocatalysis offers routes to unique and diverse sets of products—in particular acids and alcohols—with high selectivity. Further, being a purely biological route without reliance on metal catalysts/electrocatalysts, biocatalytic systems show the highest resistance to contaminants in feed streams, making it an excellent pathway for pairing with a wide variety of CO_2 point sources, requiring minimal preprocessing or clean up.

Most of the significant remaining challenges surrounding biological conversion involve hydrogen. Specifically, to convert CO_2 biologically in the absence of other carbon oxide or energy carrying species (e.g., CO, formic acid, sugar), external H_2 is typically a required cofeed to supply reducing energy. Thus, the competitiveness of biocatalytic systems is linked to the source of H_2 and the associated cost, carbon intensity, and efficiency at which it is sourced. Furthermore, ongoing research continues to explore novel ways of increasing gas−liquid mass transfer to ensure effective uptake and utilization of the CO_2 and H_2 gases by the microorganisms, a key to enhancing overall productivity.

5.4.7. Thermocatalysis. Across the seven considered pathways for CO_2 conversion, thermocatalysis represents the most mature and commercially accessible option for near-term adoption. Benefitting from decades of R&D and infrastructure investments by the petroleum industry, a broad suite of thermocatalytic reactions and processes relevant to CO_2 conversion (e.g., CO_2 hydrogenation) have been derisked and commercially vetted at scale. Through these pathways, thermocatalysis offers the potential for industry to leverage off-the-shelf ready technologies and access a range of high-volume products spanning alcohols, olefins, and fuels.

Despite the underlying chemical reaction mechanisms involved with CO_2 thermocatalysis being well understood and largely optimized, TC processes can still face unavoidable thermodynamic barriers. As noted earlier, low per-pass conversion of equilibrium reactions can increase operational complexity and raise costs related to product separation and recycle. Further, with capital equipment costs being strongly correlated to economies of scale, TC processes are most often operated at very large, centralized facilities. Relative to other, more modular CO_2 conversion designs, this intrinsic scaling behavior makes TC pathways potentially not as competitive in small-scale distributed CO_2 conversion applications. Finally, unlike the biological systems which can excel at handling raw, or minimally processed waste gas streams, the metallic catalysts used in TC can be more sensitive or easily poisoned by some common contaminants (e.g., sulfur containing compounds) found in CO_2 point sources. Thus, TC pathways require careful consideration on the source of CO_2 and strategies to mitigate the impacts of common impurities (e.g., NO_x, SO_x, H_2S, Soot, O_2, etc.).

https://doi.org/10.1021/acs.chemrev.5c00361
Chem. Rev. 2026, 126, 5028−5082

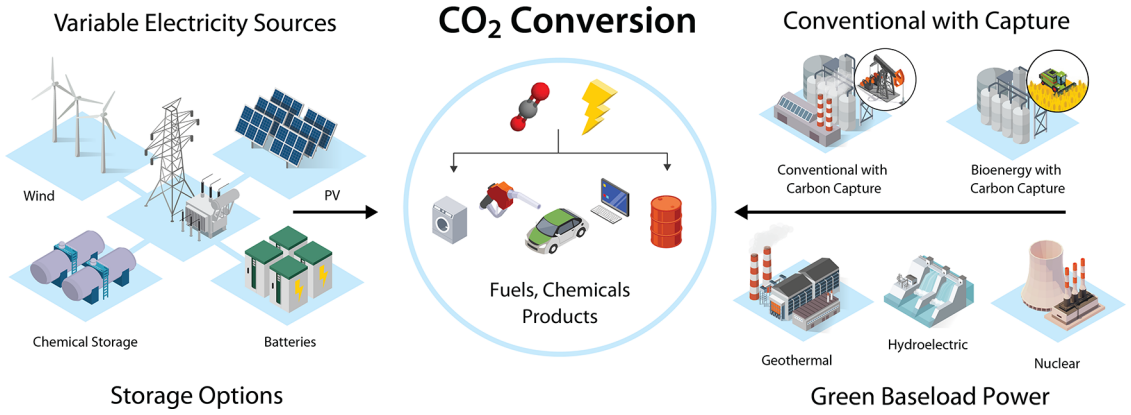

Figure 22. Many modes of supplying electricity for CO_2 conversion

6. LOGISTICS FOR CO_2 CONVERSION CHEMISTRY AND BARRIERS TO SCALE UP

Sections 2−5 have focused on emerging and developing chemistries for the conversion of CO_2 into value-added products. While significant R&D opportunities exist in the realm of performance, scale-up, and long-term durability of these pathways, it is important to also acknowledge the feedstocks these processes require and how the governing costs and logistics of sourcing said feedstocks impact the viability, optimal design, and integration of conversion pathways. These considerations are the focus of Section 6, where we review major feedstocks used in CO_2 conversion pathways, summarize market and production scale considerations for these technologies, review the current state of commercial adoption of CO_2 conversion technologies, and conclude with major takeaways and challenges associated with these early stage demonstrations.

6.1. Sourcing Electricity

Whether seeking to minimize the cost of production or life cycle impacts of a CO_2-based product, the source and availability of electricity is nearly always the principal consideration.[18,25,390] As such, strategies to drive down levelized cost of production through integration of low-cost and low-carbon sources of energy often act as controls on how, when, and where CO_2 conversion technologies can be deployed. At the level of this review, we find two major considerations for electricity sourcing for CO_2 conversion: 1) spatial and temporal dynamics of renewable generation and how downstream loads might optimally integrate, and 2) bulk availability of low-cost, low-carbon intensity electricity and competing uses and emerging large loads. This section discusses considerations for electricity sourcing regardless of if the CO_2 is consumed directly (e.g., in electrochemical/NTP CO_2 reduction) or indirectly using an energy-dense feedstock (e.g., CO_2 hydrogenation/fermentation mediated with H_2 produced via electrochemical water splitting).

Several potential approaches exist for supplying renewable electricity to CO_2 conversion. Wind and solar photovoltaic (PV) generation are the lowest-cost source of new renewable generation in many locations in the United States, but their generation is variable based on wind speeds and solar irradiance, respectively, factors that shift on a diurnal and seasonal basis for a given location. Balancing direct input energy from renewable generation requires some form of storage either in the form of battery energy storage or physical intermediate storage (e.g., hydrogen storage). Regardless of the approach, these needs increase the overall project capital costs, invoking a tradeoff between capital costs of equipment and operating costs associated with electricity consumption that will be discussed further in Section 6.4. CO_2 conversion might also be integrated into the electric grid to balance generation and load, but grid integration requires consideration of the carbon intensity of the grid generation mix at a given time and location and subsequent impacts to the carbon intensity of CO_2 based products. The possible combination of electricity generation and storage technologies is long − there is likely not a one size fits all solution for all locations and conversion pathways as shown in Figure 22, but electricity supply is a critical factor for the feasibility of CO_2 conversion pathways. In the remainder of this section we discuss broad trends in electricity generation and storage and in grid infrastructure and future large loads in the context of the technologies reviewed in Sections 2-5.

In the past five years, the cost per unit energy ($/MWh) for new wind and PV has continued to fall[391] and rates of deployment for these technologies continues to increase and become a larger share of installed generation capacity in many countries.[392] Deployment of variable renewable energy (VRE) resources is supported by recent decreases in the cost of short-duration battery energy storage that can help balance daily mismatches between generation and load, especially in the case of PV for shifting generated energy later in the day to meet evening peak demands.[393] These technologies for generation and storage are being deployed at a time when grid operators are anticipating increased loads across sectors, including data centers,[394] cryptocurrency mining, light-duty transportation electrification,[395] and production of hydrogen. Understanding these dynamics is critical for CO_2 conversion pathways that are likely to be large consumers of VRE either directly behind the meter or indirectly through integration with evolving grid infrastructure.

Being potential large consumers of electricity, it is paramount for CO_2 conversion pathways to understand the macro trends influencing the evolution of grid infrastructure and energy markets because these trends drive how conversion pathways might chose to interact with the evolving electricity system. For example, deployment strategies for in front of the meter (connected with the electric grid) or behind the meter (direct connection with generation technology and isolated from the broader grid) energy supply for CO_2 conversion will drastically impact how one might choose to operate the system

https://doi.org/10.1021/acs.chemrev.5c00361
Chem. Rev. 2026, 126, 5028−5082

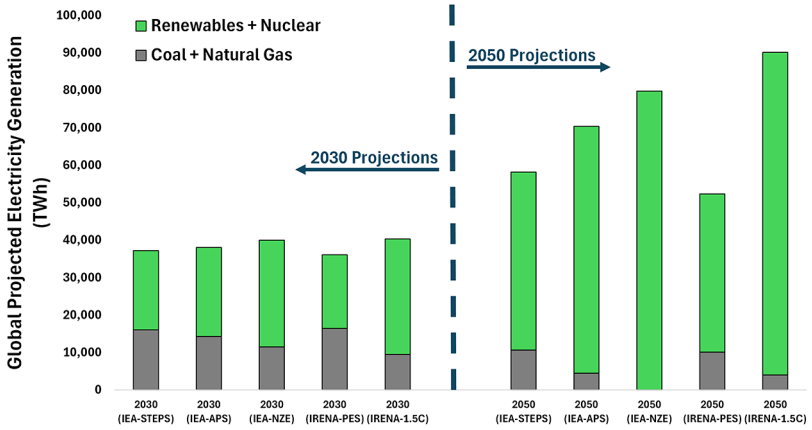

Figure 23. Projected electricity generation by source in 2030 and 2050 as reported by IEA and IRENA. STEPS = Stated Policies Scenario, APS = Annouced Pledges Scenario, NZE = Net Zero Emissions by 2050 Scenario, PES = Planned Energy Scenario, 1.5 = 1.5 Degree Celsius Scenario. Data from refs 398 and 399.

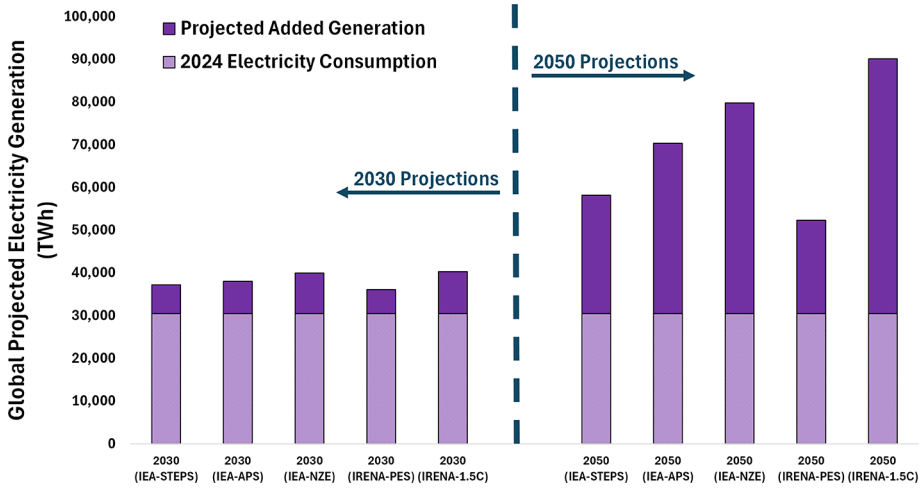

Figure 24. Projected additional electricity generation in 2030 and 2050 relative to 2024 levels. STEPS = Stated Policies Scenario, APS = Annouced Pledges Scenario, NZE = Net Zero Emissions by 2050 Scenario, PES = Planned Energy Scenario, 1.5 = 1.5 Degree Celsius Scenario. Data from refs 398 and 399.

as well as the capital investment required for intermediate storage of energy or products and reactants. Given the multitude of options available and region-specific sensitivities, this review does not set out to prescribe a best-case approach for electricity sourcing. At any rate, the best-case will very likely vary from technology to technology, location to location, and what changes the grid has undergone that impact future large loads.

To provide several illustrative examples of regional and technologically dependent CO_2 conversion pathways, we summarize selected recent work in this area, but readers should note that this is a rapidly evolving field. Recent U.S. focused work has evaluated different regions as potential hubs for CO_2 conversion based on the availability of CO_2 feedstocks and low-cost grid electricity.[396] Key considerations and takeaways from this work include the importance of regional grid mixes and power markets, variable costs of power purchase agreements (PPAs), dynamic wholesale power markets, and generation assets and changing demand mixes in each region influence the cost of accessing electricity at MW to GW scales. As such, for grid-tied (in front of the meter) CO_2 conversion technologies, an understanding of regional grid assets, transmission infrastructure, and applicable utility rate structure dictate design components and operational dynamics of the conversion pathway is critical. Considering recent work analyzing behind-the-meter systems producing hydrogen, major implications include the importance of complementary wind and solar PV mixes, increasing generation and therefore electrolyzer capacity factors and capital utilization.[397] Most large scale CO_2 conversion technologies powered with behind the meter VRE are likely to require some form or storage to smooth output, either in the form of electrical energy storage or physical product and feedstock storage. The favorability of using either or both storage technologies is determined by local VRE resources, capital costs of system equipment, and flexibility in product offtake.

Regardless of variance in system design and integration strategies, one certainty is that as CO_2 conversion chemistries continue to mature and are derisked, their scalability and impact in the marketplace will ultimately be tied to the amount of available low-carbon electricity. In Figure 23 future projections for the total global electricity generation in 2030 and 2050 as reported by IEA and IRENA are shown. The data

https://doi.org/10.1021/acs.chemrev.5c00361
Chem. Rev. 2026, 126, 5028−5082

encompasses scenarios (e.g., STEPS/PES) reflective of the stated policies and plans by governments, as well as scenarios (e.g., NZE, 1.5C) corresponding to a deeper electrification of the global economy with the incorporation of constraints on system-wide emissions. Based on these projections, estimates suggest that globally in 2030 the total amount of renewable electricity (incl. nuclear) may range from 20,000 TWh in the conversative scenarios to 31,000 TWh in the aggressive electrification scenarios. The figure for renewables increases in 2050, reaching 47,000 TWh to 86,000 TWh in the conservative and aggressive scenarios, respectively.

Being still only a fledgling industry, as of 2024 CO_2 conversion and other "Power-to-X" pathways do not yet significantly contribute to the approximately 30,500 TWh consumed annually (2024) to sustain global business-as-usual activities. Thus, it is important to put in perspective how much of the projected renewable electricity generation would be needed to sustain the current economic status-quo versus the myriads of new use cases, such as CO_2 conversion chemistry. Shown in Figure 24, when the total generation projections for 2030 and 2050 are compared against current 2024 consumption levels, the data reveal that depending on scenario, between 5,600 and 9,800 TWh may be added by 2030, reaching an additional projected 21,800 to 59,600 TWh by 2050.

A key question arising from these data is, given the strong demand for electricity across a multitude of different end markets, what fraction of the added electricity generation could feasibly be utilized for CO_2 conversion, and what impact could that have on the existing chemicals and fuels market? Estimates show that global demand for electricity has accelerated in 2024 and is now expected to grow by an average of 3.4% per year through 2026, driven by strong growth in emerging economies as well as strong growth across data centers, AI, and cryptocurrencies.[400] In fact, according to the IEA, it is estimated that over roughly the next decade approximately 67 − 81% of new capacity growth will be driven by light duty vehicle electrification, heat pumps, office and residential cooling, and other energy intensive industries (e.g., data centers, crypto mining, industrial heat) depending on the region and electricity scenario.[398] Across the various electricity scenarios considered by IEA as shown in Figure 25, hydrogen production, an important input feedstock for many "Power-to-X" or "e-fuels" pathways, represents between 3.4% and 23.9% of the global added capacity, depending on scenario and region.

Collectively, if it were assumed that all of the electricity allocated to "hydrogen production" were utilized for e-products, it is possible offer an order-of-magnitude estimate for the possible impacts on chemicals and fuels markets. In Table 3 we show the hypothetical electricity required to meet

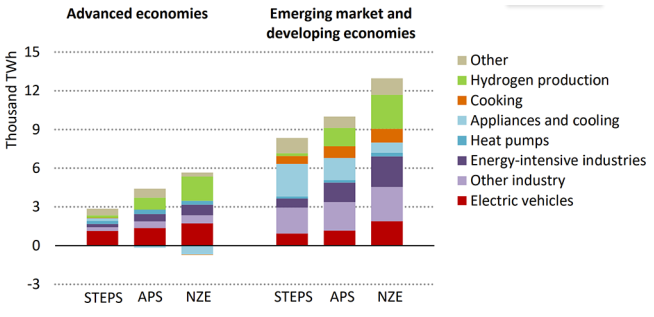

Figure 25. Electricity demand growth by application and IEA scenario from 2023 to 2035. Figure courtesy of IEA. Reproduced from ref 398.

Table 3. Estimated Electricity Demand for Four Common CO_2-Based Products

Product	Energy Intensity (GJ/tonne)[a]	2030 Market Consumption (MMT/y)[b]	2030 Electricity Demand (TWh)[c]	Fraction of 2030 Renewable Electricity for e-products (%, STEPS/APS /NZE)[d]
Ethylene	94.0	400	10,440	4510/860/460
Methanol	43.9	120	1,450	630/120/65
CH_4 (RNG)	102.1	3,000	85,120	36760/7020/3740
PTL−SAF	101.0	350	9,820	4240/810/430

[a]Assumes a net energy efficiency of 50%. Values based on thermodynamic calculations.[4] [b]Based on 2024 values and CAGR of 3%. [c]Calculated from multiplying energy intensity and estimated 2030 market consumption. [d]Represents what fraction of the available electricity generation attributed to "hydrogen production and e-products" in the IEA STEPS, APS, and NZE scenarios it would take to produce 100% of the 2030 market consumption of each product. For example, in the case of ethylene in the STEPS scenario, it would take 4510% of the planned electricity growth in e-products to produce 100% of the ethylene market in 2030.

100% of the projected 2030 market demand of four commonly cited CO_2-based products, assuming an overall net 50% energy efficiency process. Note, as shown in Figure 20, actual energy efficiency varies widely between pathway and product. Herein, the 50% estimate is provided as a simplifying and illustrative benchmark only, representative of a hypothetical moderate TRL conversion pathway. Further, while we recognize that displacing 100% of any single chemical market by 2030 is unrealistic, this calculation nevertheless illustrates the potential impact CO_2 conversion could have. Using this back-of-the-envelope approach reveals that meeting the global demand for any one of these common products in the stated plans and policies scenario (STEPS) would require from 630% to > 36,760% of the total electricity generation projected for "hydrogen generation" from 2024 to 2030. In the announced pledges scenario (APS), the requirements are reduced to 120% and 7,020%. In the most optimiztic NZE scenario, the requirements are 65% to 3,740%. Although only meant to serve as approximations, these data bring to light several important takeaways as it relates to sourcing electricity and the scale up of CO_2 conversion:

(1) For many of the commonly cited possible products (Table 3), a CO_2 conversion alternative would represent one of the most energy demanding processes ever recorded for making gaseous and liquid chemicals at the commercial scale. For perspective, at 50% energy efficiency the estimated energy intensity values of CO_2 conversion products are in some cases > 3× that of modern "energy intensive" processes such as NH_3 synthesis via Haber Bosch (~30 GJ/tonne).

(2) Energy intensity can vary widely per product and is influenced by both the conversion specific factors such as applied voltages and selectivity but also the intrinsic chemistry (e.g., number of mols electrons/H_2 utilized per molecule of product, final oxidation state, amount of retained oxygen, etc.).

https://doi.org/10.1021/acs.chemrev.5c00361
Chem. Rev. 2026, 126, 5028−5082

(3) Based on current electricity forecasts for growth and utilization, CO_2-based "e-products" are likely to comprise only a small fraction of fuels and chemicals production by 2030 if relying on existing installed generation capacity. Building dedicated new generation to meet these emerging demands is technically possible, but requires consideration of existing grid and energy infrastructure, and total available renewable resources.

(4) For e-products and CO_2 conversion to make a significant impact on chemicals and fuels markets in the future, renewable electricity generation capacity and the associated transmission, storage, and other supporting infrastructure will likely need to be expanded meaningfully beyond even the most optimiztic scenarios currently proposed (e.g., deep electrification NZE, 1.5C).[401]

6.2. Sourcing H_2

Hydrogen is a critical chemical building block for many of the CO_2 conversion processes reviewed here. Trends in hydrogen production, transmission and storage infrastructure build out, and end-uses are important considerations for any downstream users of hydrogen. The economics and life-cycle impact of processes that consume hydrogen often is driven by how, where, and when that hydrogen is produced, where aggregate statistics that capture these aspects are \$/kg H_2 levelized production cost (LCOH) and kg CO_2eq/kg H_2 produced, respectively. Along with these two metrics, the availability of hydrogen (i.e., steady state vs dynamic supply) and location of production is a key consideration for processes consuming hydrogen that will be discussed in this section.

There are a variety of possible technologies available for producing hydrogen, with some highlighted in Table 4. While an exhaustive evaluation of these production options is beyond the scope of this review and other literature has thoroughly reviewed production technologies,[402] factors such as facility siting, operation, and economics do influence downstream users of the hydrogen, including CO_2 conversion and are discussed here. Namely, the location, operational dynamics, and supporting infrastructure for these hydrogen production technologies are critical considerations for downstream users. For example, hydrogen production from water electrolysis that is powered by renewable electricity could be located on-site with the renewable generation but would need a colocated offtake for hydrogen or storage and transportation to enable moving hydrogen to the offtake. Depending on the offtake requirements, electrolyzer technology, and utility rate structure, hydrogen could also be produced at a steady state or dynamically as determined by renewable output or grid price signals in systems that are grid-tied.

CO_2 conversion technologies are not the only consumers of hydrogen today or in the future. Major consumers of hydrogen today include oil refineries and ammonia synthesis plants,[403] although many other potential end-uses are under consideration such as medium- and heavy-duty transportation, steelmaking, and hydrogen for long duration energy storage in the electric power sector.[404] As these end-uses evolve and develop, it is likely that not all of them will have the same willingness-to-pay for hydrogen.[403] Therefore, the emergence of various markets for hydrogen will potentially depend on the delivered cost of hydrogen, its availability, and cost parity with any existing fuels that may already be used in a process or application. How hydrogen demand and markets evolve to

Table 4. Summary of Existing and Emerging Hydrogen Production Technologies and High-Level Considerations.

Pathway [-]	Major resource requirement(s) during operational stage[-]	LCOH driver(s) [-]	Variable output notes	Demonstrated production scale [kg H_2/day]
Low-temperature water electrolysis	Water, electricity	Cost of electricity and electrolyzer capital cost and durability	Variable operation for electrolyzers sourcing energy from behind-the-meter renewables or in dynamic grid pricing schemes	About 8,000 kg H_2/day[a]
High-temperature water electrolysis	Water, electricity, heat	Cost of electricity, electrolyzer durability and efficiency	Current systems likely operate at steady state, although R&D is focused on electrolyzer stacks that enable dynamic operation	About 2,400 kg H_2/day[b]
Steam methane reforming	Natural gas, dairy gas, landfill gas	Natural gas price	Generally operates at steady state with high capital utilization	About 50,000 kg H_2/day
Geologic hydrogen	None	Unknown	Unknown	n/a
Biomass carbon removal and storage (BiCRS)	Woody biomass, municipal solid waste, agricultural residues	Feedstock cost, feedstock preprocessing, gasification performance	Generally operates at steady state with high capital utilization	Not yet commercially active

[a]Ref 410. [b]Ref 411.

https://doi.org/10.1021/acs.chemrev.5c00361
Chem. Rev. 2026, 126, 5028−5082

meet increasing demand, and competition among competing end-uses are important considerations for CO_2 conversion pathways that could be large-scale end-users of this molecule.

The evolution of LCOH from different hydrogen production technologies is a critical factor of consideration for CO_2 conversion pathways that use hydrogen as a feedstock. Accurate estimates for LCOH in the near term and long-term future are important for informing development of CO_2 conversion technologies. Quantification of these ranges is beyond the scope of this review, and instead we focus on qualitative cost drivers for major hydrogen production pathways (Table 4). The cost drivers of LCOH depend on the pathway, but for many the largest cost driver is the input feedstock, such as electricity for water electrolyzers, biomass for gasification, and natural gas for steam methane reforming. To provide readers with examples of high level considerations and cost drivers, the following paragraphs discuss considerations for low-temperature water electrolysis and steam methane reforming of natural gas, two of the most prevalent existing and emerging hydrogen pathways.

Technologies such as low- and high-temperature water electrolysis have significant R&D targets set across performance and cost metrics that, if achieved, would likely reduce the LCOH from these technologies.[405] All of the considerations for electricity sourcing discussed in Section 6.1 apply to electrolyzers, with significant R&D focused on enabling these systems to reduce the cost of electricity and lower total LCOH.[406] These efforts generally seek to optimize materials, performance, and cost to enable electrolyzers to operate dynamically based on direct VRE power input or dispatch the electrolyzer based on hourly grid pricing signals in wholesale power markets.[407] Future deployments for water electrolyzers could be either located near low-cost electricity to minimize LCOH for production, or near offtake to minimize hydrogen transport and/or storage costs.

For natural gas based hydrogen production, the cost of natural gas feedstock generally is the largest component of LCOH. Given the large capital investment associated with SMR based hydrogen production and offtake requirements for hydrogen, these facilities tend to be operated at high capital utilization factors, are constructed at large scales, and are located near low-cost natural gas and hydrogen offtakes. For example, existing hydrogen production via steam methane reforming of natural gas for refinery applications is predominantly located in the Gulf Coast of the United States, using large scale facilities close to hydrogen offtakes. For SMR systems that are deployed with carbon capture and sequestration (CCS), the LCOH and total CI for the process will vary and are primarily subject to the cost of natural gas and upstream methane leakage rates and sourcing assumptions (e.g., domestic, imported LNG, etc.), respectively.[408,409]

An understanding of production integration opportunities, competition between end-uses, and evolution of hydrogen transportation and storage could serve consumers of the hydrogen such as CO_2 conversion. As an example, while we noted that hydrogen produced from steam methane reforming of natural gas has conventionally been colocated with the hydrogen offtake, new infrastructure investments in pipelines and storage and LCOH reductions from water electrolysis could drive changes in future siting and hydrogen availability. It is possible that water electrolyzers could be installed where low-cost electricity is abundant, leveraging hydrogen pipelines to buffer dynamic hydrogen production while moving this molecule to various offtakes. How and where this infrastructure evolves is subject to notable uncertainty but this evolution and any resulting market development is an important consideration for CO_2 conversion pathways.

6.3. Sourcing CO_2

Beyond critical electricity and energy-carrying feedstocks like hydrogen and in some technology pathways methane, the final ingredient in CO_2 conversion chemistry is CO_2 itself, serving as the primary carbon building block for more complex products. Unlike typical commoditized chemical feedstocks that have robust and dedicated supply chains, CO_2 is differentiated in that historically it has been viewed primarily as a waste byproduct to be released to the atmosphere with little to no market interest outside of smaller specialized cases such as the food and beverage industry or enhanced oil recovery.[412]

One of the current challenges contributing to the significant underutilization of CO_2 is the cost of capture and concentrating dilute resources, whether they are from point source emissions or the atmosphere. Shown in Table 5, the concentration of available CO_2 sources ranges from as low as ~425 ppm in the atmosphere to near 100% in the case of select industries such as bioethanol fermentation. More often, however, point source concentrations fall in the 3−15% range. The corresponding cost to capture the CO_2, shown in Figure 26, correlates with concentration with the high purity sources showing relatively low costs of capture of in range of $20-$30/ton and the more common dilute sources such as waste streams from coal and natural gas power generation at ~$50 to more than $150/ton CO_2. In the most extreme case of dilute direct air capture, reported cost estimates can range from $230 to > $800/tonne depending on scale, technology, and assumed gains in technical performance.[413]

Table 5. CO_2 Concentrations by Source, Modified from Ref 414

Process	CO_2 Concentration (vol%)
Power: Coal	12−15
Power: Natural Gas	3−10
Power: Fuel Oil	3−8
Cement Production	20
Refinery Operations	3−13
Integrated Steel Mills	15
Ethylene Production	12
Ammonia: Process	100
Ammonia: Fuel Combustion	8
Ethylene Oxide Production	100
Bioenergy	3−8
Fermentation	100
Atmospheric	0.000425

Balancing the availability, purity, and capture dynamics surrounding sourcing of CO_2 will be key considerations for the CO_2 conversion community. Over the near-term, first-of-a-kind CO_2 conversion processes are naturally most likely to favor point sources exhibiting the lowest capture costs, especially those also providing low carbon intensity biogenic CO_2 such as fermentation plants. However, as shown in Figure 26, the availability of these high purity sources is limited, representing only a minor fraction of the total CO_2 supply. As CO_2 conversion processes mature and begin to scale, they are likely to be forced to leverage progressively more dilute sources

https://doi.org/10.1021/acs.chemrev.5c00361
Chem. Rev. 2026, 126, 5028−5082

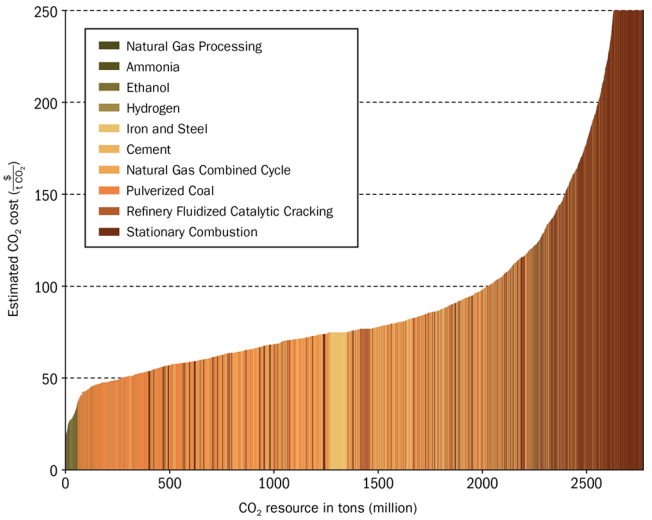

Figure 26. United States supply curve for point source capture of CO_2 feedstocks. Reproduced from ref 415.

of CO_2 at higher expense which could impact economic viability.

6.4. Economics and Scale Up of CO_2 Conversion

Over the past decade interest in CO_2 conversion has surged, not only in the academic world (see: Figure 1) but also commercially where follow-through from the laboratory to the private sector has seen the deployment of pilot and small commercial scale projects. A *noncomprehensive* list of recent major commissioned, announced, and canceled CO_2 conversion projects is provided in Table 6.

Acknowledging that this is a nonexhaustive list, the projects shown in Table 6 nevertheless reveal several trends in the scale up and deployment of CO_2 conversion. The listed projects highlight that although there is a notable concentration in thermocatalysis, there is currently no single "winning" strategy. Rather, investments into CO_2 conversion are being made across a breadth of technologies including electrochemistry, thermocatalysis, biological upgrading, and other hybrid approaches. The near-term targeted products, however, do show initial consolidation specifically around e-methanol and e-fuels (e.g., methanol to gasoline, RWGS to CO followed by Fischer−Tropsch). This near-term focus may be attributed to several factors. First, from a technical standpoint, the synthesis of methanol and/or FT-based fuels from C_1 (typically CO via RWGS) + H_2 has a rich history and has been largely derisked. Numerous providers (see: Johnson Matthey eMERALD, Topsoe G2L eFuels), now offer off-the-shelf licensable packages for CO_2 conversion, providing immediate solutions for first of a kind plants with limited downside technical risk.[388,430] Further, within the past five years there has been a strong market pull for decarbonization specifically in the marine and aviation sectors which are viewed as "difficult to decarbonize" through electrification alone and expected to remain reliant on liquid energy dense fuels far into the future.[15] CO_2-conversion pathways to e-fuels are considered to be well situated to deliver such products at a significantly reduced carbon intensity versus conventional options. Further, e-methanol doubles both as a potential fuel but also as a major platform molecule across the chemicals industry, notably as a precursor to the high-volume olefins markets.

Yet, despite the encouraging developments toward commercialization over the past several years, CO_2 conversion technologies are expected to face long-term headwinds around breaking into the established chemicals and fuels markets. Conventional markets are dominated by economy-of-scale, large volume industries that have been optimized over multiple decades, presenting high barriers to entry with high initial capital costs and low profit margins.[431] Consequently, meaningful scale up of CO_2 conversion has moved at a more modest pace and some of the largest proposed capital projects have recently been terminated, citing a challenging economic environment, uncertainty in policy, and slowing demand.[417] Encouragingly, recent techno-economic analysis (TEA) studies on CO_2 conversion find plentiful opportunities to continue to improve on cost and overall economic competitiveness into the future. In Figure 27 and Figure 28 we show published TEA results over the past 5 years (2020−2024) specifically for producing CO and MeOH across the notable conversion pathways. It should be stressed that calculated product costs across TEA studies can vary widely in that each study may utilize different methodologies or assumptions in determining technical performance, input costs, incentives, future scenarios, etc. Our goal herein is to broadly segregate studies by product, conversion technology, and whether or not the assumptions were reflective of the current "state of technology" (SOT) or more optimiztic "future" (FUT) leaning. This approach is intended to provide an order of magnitude estimate for cost projections as well as insights into general trends.

In Figure 27, a review of TEA studies on CO production costs points toward a wide range of calculated production costs from ∼ $0.23/kg CO to > $2.00/kg CO. Direct comparison to incumbent CO market cost is muddied both by its different markets (e.g., as bulk synthesis gas constituent versus high purity bottled CO) at different price points, as well as sensitivity to underlying natural gas costs. Nevertheless, Figure 27 reveals that across the various pathways, all studies find that under current SOT conditions, CO_2-based CO is not yet competitive with the lower end target US market price (c.a., 2019$0.15/kg) representative of a bulk, "over the fence" syngas cost.[432] However, when considering the top end price range (i.e., $0.60/kg) more closely associated with high-purity gas markets combined with future case technical performance where studies account for elements such as: reducing capital costs of the core conversion technologies (e.g., electrolyzers, plasma reactors, etc.), increasing catalytic performance (e.g., CO_2 conversion, selectivity, yield, energy efficiency), increasing productivity (e.g., current density, turnover frequency), several studies show the possibility for an economically competitive process.[7] The studies for CO_2-based MeOH in Figure 28 highlight a similar trend where the current state of the art exceeds the current market price, in some cases significantly so, such as for the low-temperature electrolysis pathway. These TEA results also support the observations provided in Table 6 highlighting thermocatalysis as a more near-term preferred pathway for MeOH synthesis of the two prominent options. However, unlike the CO data (a two electron process), the future looking data for MeOH (a six electron process) suggest that none of the studies found a pathway to entirely close the gap with the current market price of 2019$0.26/kg, pointing toward a potentially challenging economic perspective.

When all possible vectors for reducing e-product costs are ranked, lowering the input feedstock cost is most consistently cited the number one barrier to CO_2 conversion economic

https://doi.org/10.1021/acs.chemrev.5c00361
Chem. Rev. 2026, 126, 5028−5082

Table 6. Prominent Commissioned, Announced, and Canceled Projects from 2020−2025

Commissioned	Announced	Canceled
Provider: HIF Global	**Provider**: Twelve	**Provider**: Orsted
CO2 Source: Biogenic from fermentation	**CO2 Source**: Biogenic CO_2	**Project**: FlagshipONE
Pathway: Thermocatalysis	**Pathway**: Electrolysis	**Pathway**: Thermocatalysis
Product: e-Methanol/Gasoline	**Product**: Carbon Monoxide/e-SAF	**Product**: e-Methanol
Capacity: 130k L/yr	**Capacity**: >40,000 gal/yr	**Capacity**: 55k tonne/yr
Location: Punta Arenas, Chile	**Location**: Washington, USA	**Location**: Ornskodsvik, Sweden
Year: 2022	**Target Year**: 2025	**Year**: 2024
ref: 416	**ref**: 378	**Reason**: slower than expected demand for long-term offtakers
		ref: 417
Provider: CRI	**Provider**: CRI	**Provider**: Haldor Topsoe
CO2 Source: Coke production	**CO2 Source**: Biomass combustion	**Project**: e-CO
Pathway: Thermocatalysis	**Pathway**: Thermocatalysis	**Pathway**: SOEC
Product: e-Methanol	**Product**: e-Methanol	**Product**: e-CO
Capacity: 110k tonnes/yr	**Capacity**: 170k tonnes/yr	**Capacity**: 96 Nm^3 CO/hr
Location: Anyang, China	**Location**: Liaoyuan, China	**Location**: Ohio, USA
Year: 2022	**Year**: 2025	**Year**: 2021
ref: 387	**ref**: 418	**Reason**: Undisclosed
Provider: CRI	**Provider**: Liquid Wind	
CO2 Source: Waste gases from EO production	**CO2 Source**: Biogenic CO_2	
Pathway: Thermocatalysis	**Pathway**: Thermocatalysis	
Product: e-Methanol	**Product**: e-Methanol	
Capacity: 100k tonnes/yr	**Capacity**: 130k tonnes/yr	
Location: Lianyuangang, China	**Location**: Sundsvall, Sweden	
Year: 2023	**Year**: 2027	
ref: 419	**ref**: 420	
Provider: European Energy	**Provider**: Liquid Wind	
CO2 Source: Biogas	**CO2 Source**: Biogenic CO_2	
Pathway: Thermocatalysis	**Pathway**: Thermocatalysis	
Product: e-Methanol	**Product**: e-Methanol	
Capacity: 42k tonnes/yr	**Capacity**: 130k tonnes/yr	
Location: Kasso, Denmark	**Location**: Umea, Sweden	
Year: 2025	**Year**: 2028	
ref: 421	**ref**: 422	
Provider: Total/Sunfire	**Provider**: Avantium	
CO2 Source: Refinery CO_2	**CO2 Source**: -	
Pathway: Thermocatalysis	**Pathway**: Electrocatalysis	
Product: e-Methanol	**Product**: PLGA Polymer	
Capacity: Demo	**Capacity**: 10 tonnes/yr	
Location: Leuna, Germany	**Location**:	
Year: 2021	**Year**: 2026+	
ref: 423	**ref**: 424	
Provider: Electrochaea	**Provider**: Reolum	
CO2 Source: Biogas	**CO2 Source**: Biogenic from Biomass	
Pathway: Biomethanation	**Pathway**: Thermocatalysis	
Product: Methane	**Product**: e-Methanol	
Capacity: 2.8m Nm^3 Methane/yr	**Capacity**: 140 kt/yr	
Location: Roslev, Denmark	**Location**: Castilla y Leon, Spain	
Year: 2024	**Year**: 2027	
ref: 386	**ref**: 425	
Provider: Infinium	**Provider**: HIF Global	
CO2 Source: Refinery CO_2	**CO2 Source**: Bioethanol CO_2	
Pathway: Fischer−Tropsch derivative	**Pathway**: Thermocatalysis	
Product: e-Fuels	**Product**: e-Methanol	
Capacity: 2,220 gal/day	**Capacity**: 700 kt/yr	
Location: Texas, USA	**Location**: Paysandu, Uruguay	
Year: 2023	**Year**: 2025+	
ref: 426, 427	**ref**: 428	
Provider: Synhelion		
CO2 Source: Biogas		
Pathway: Thermal Redox + FT		
Product: e-Fuels		
Capacity: 1,000s of liters/yr		
Location: Julich, Germany		
Year: 2024		
ref: 429		

viability, specifically in the form of sourcing low-cost electricity (or other energy feedstocks).[390,436,443,444] With energy pricing factoring so significantly into forecasts for CO_2 economic viability, an often-discussed cost minimization strategy is dynamic operation and load following of the electric grid and renewables generation. This approach relies on cycling key process equipment (e.g., electrolyzers, plasma reactors, etc.) on/off, letting operators take advantage of dislocations in daily electricity pricing and periods of curtailment or overgeneration either to drive the CO_2 conversion chemistry and/or to produce H_2 via electrolysis.[432] While dynamic operation could be a key differentiator between conventional and power-to-X pathways, and the ability to operate selectively during times with the lowest cost of energy may offer opportunities to potentially increase economic competitiveness, the tradeoff with durability, process capacity factor, and capital utilization are critical considerations that should not be neglected.

By intentionally operating a process at low capacity factor, for example, cycling on and off on a daily basis to load follow renewables generation, in effect that plant is producing less

https://doi.org/10.1021/acs.chemrev.5c00361
Chem. Rev. 2026, 126, 5028−5082

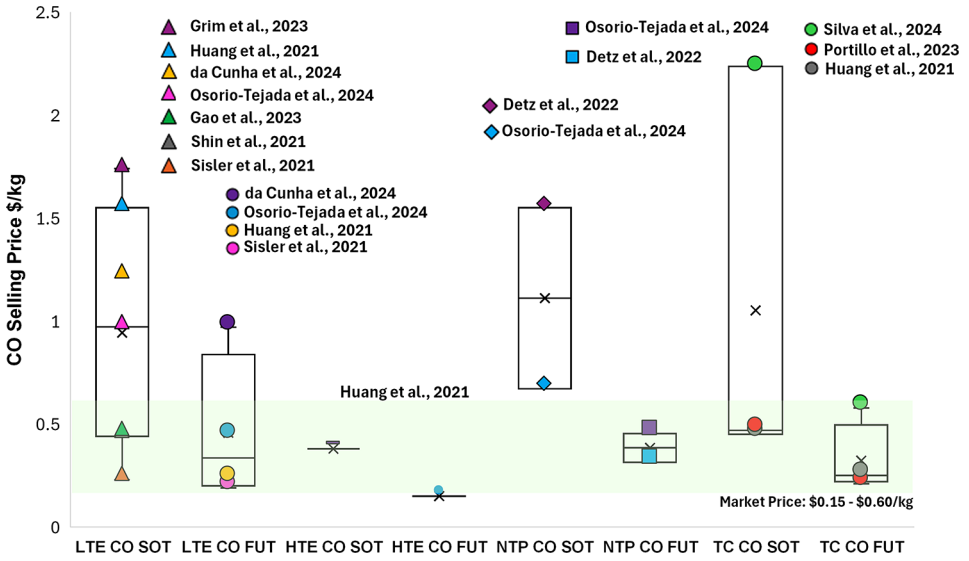

Figure 27. TEA studies on the conversion of CO_2 to CO (2020−2024). LTE SOT refs: 18, 24, 25, 433−436. LTE Fut refs: 18, 433, 435, 436. HTE ref: 18. NTP refs: 435, 437. TC refs: 18, 438, 439.

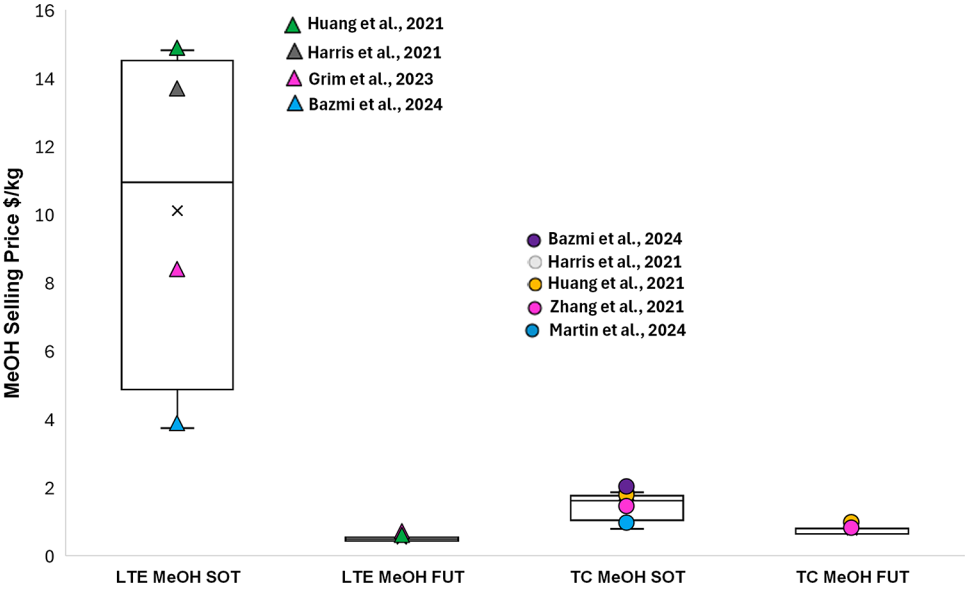

Figure 28. TEA studies on the conversion of CO_2 to MeOH (2020−2024). LTE refs: 18, 24, 440, 441. TC refs: 18, 346, 440−442

goods for the same capital investment and correspondingly the relative impact of the CAPEX, and often product levelized cost, goes up. This effect is illustrated in Figure 29 for e-CO where C. da Cunha and Resasco show that "even when using cheap wholesale solar electricity, high capacity factors are required to make [CO_2 conversion] economical".[436] They further suggest that at current electrolyzer capital costs, analysts should consider neglecting wind or solar utilization altogether, finding that the low capacity factors of direct use (without storage) make economical operation "impossible" even at discounted electricity pricing.[436] These findings, combined with concerns around the durability impacts of cycling and the associated stresses to the equipment, highlight the critical need for lowering total system capital costs and improving overall durability, both to enable dynamic operation and improving the economic competitiveness of CO_2 conversion.[18,445]

Clearly, how a CO_2 conversion pathway is deployed and integrated into the broader energy and chemicals sectors has implications for the importance and relevance of various R&D metrics. Some emerging system designs incorporate a dynamic process step, such as dynamic supply of electricity or production of hydrogen via water electrolysis. Whether downstream steps also operate dynamically or whether storage is used as a buffer has implications for key economic and therefore R&D priorities for the process as a whole. Adding buffer storage either in the form of physical hydrogen storage or electrical battery energy storage increases overall capital costs. In dynamic systems, the total capital cost determines the optimal operating capacity factor, or capital utilization. A lower overall capital cost allows the system to operate at a lower capacity factor, increasing flexibility.[406] For this hypothetical system R&D that reduces capital costs in other components and durability during dynamic operation would be critical priorities. For a system operated at steady state, overall efficiency may be more relevant than lowering overall capital costs. In other words, the integration and operation strategies

https://doi.org/10.1021/acs.chemrev.5c00361
Chem. Rev. 2026, 126, 5028−5082

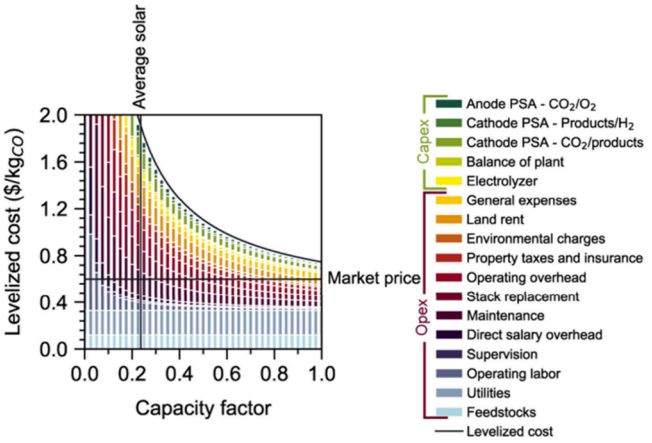

Figure 29. Impact of capacity factor and electricity price on the levelized cost of e-CO. Reproduced from ref 436. Copyright 2024 American Chemical Society.

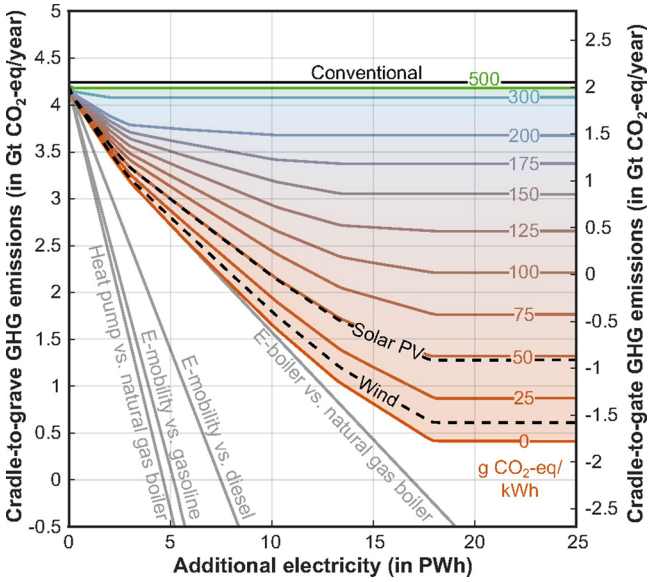

Figure 30. Cradle-to-grave and cradle-to-gate CO_2e emissions for the chemical industry producing 20 large volume chemicals in 2030 as a function of the amount of additional electricity available and its carbon footprint in grams of CO_2 equivalent/kilowatt hour. The black solid line represents CO_2e emissions in the conventional electricity scenario with the colored lines representing various low(er) carbon electricity scenarios. The light gray lines represent CO_2e emissions reductions using electricity for e-mobility to substitute gasoline or diesel cars, or for heat generation in a heat pump or an e-boiler to substitute heat from natural gas boilers. Reproduced with permission from ref 401. Copyright 2019, National Academy of Sciences.

for CO_2 conversion pathways determine optimal capital and operating cost tradeoffs and have significant implications for R&D priorities.

Ultimately, the most successful first-of-a-kind CO_2 conversion projects to date have generally taken advantage of some combination of policy support, niche markets where consumers are willing to pay a "green premium", and/or financial certainty through dedicated offtake agreements. Many of the first movers listed in Table 6 have also further derisked these initial investments through utilization of existing brownfield infrastructure thereby minimizing costly upfront capital investments. Other new projects have sought colocation and integration with existing low-cost waste resources such as refining off gases or waste biogas that already contain mixtures of $CO/CO_2/H_2$. Utilizing these waste resources directly as opposed to deliberate on-purpose production of the feedstocks (e.g., H_2O electrolysis + direct air capture) minimizes feedstock cost and further derisks the investment. Moving forward and over the longer term as companies pursue larger greenfield deployments, the importance of research and development to advance the performance and cost of CO_2 conversion at scale will become even more critical to demonstrate economic viability for large capital projects with multidecade planned lifetimes.

6.5. Environmental Impacts of CO_2 Conversion at Scale

Life-cycle and other environmental assessments of CO_2 conversion pathways typically converge on a central theme: independent of the selected pathway and core conversion technology, CO_2-based products can be produced with a significantly lower carbon intensity than conventional routes, but typically only when powered by energy sources comprising a near zero carbon footprint.[444,446−449] Acknowledging that CO_2 conversion is inherently energy intensive (Table 3) and renewable electricity availability is expected to be a hotly contested resource least the next several decades (cf., Figure 23 and Figure 24), two key questions currently being asked by researchers are: (1) can we provide the amount of low-cost, low-carbon electricity needed to drive CO_2 conversion at large scales, and, if yes, (2) should we use it for the chemicals and fuels industries over other competing use cases?[401]

Life-cycle analyses by Katelhon et al. tackle these critical questions as shown in Figure 30. They report that from an CO_2e emissions minimization perspective, utilizing renewable electricity resources for heat pumps, electrification of light and medium duty vehicles, and use for direct electric heating (e-boilers) all show a higher climate mitigation potential than producing CO_2-based e-products, even under the assumption of electricity emissions factor of 0 g CO_2e/kWh.[401] In other words, although e-products may offer substantial climate benefits relative to conventional pathways to chemicals and fuels, the calculated net CO_2e benefit would be lower than in utilizing renewables across other use cases. Thus, from the perspective of maximizing climate benefits, they argue e-products should only be pursued once the other aforementioned options are exhausted. Katelhon et al. also note that these findings apply to grid-connected applications and that for off-grid or "behind the meter" applications of CO_2 conversion, the results may be different. Specifically, in locations where renewable electricity resources are favorable but grid infrastructure or demand is not nearby, CO_2 conversion represents an attractive option to utilize these stranded resources and potentially transform regionally bound electricity into more easily transportable products (e.g., energy dense liquids).[401]

A second analysis by de Kleijne et al. in 2022 further supports these conclusions. Their life-cycle analysis converges around the idea that from a climate perspective, making "e-products"—in their case electrolytic H_2 instead of CO_2 conversion to products—to have a lower overall benefit than similar commonly cited use cases. Specifically, shown in Figure 31, de Kleijne concludes that utilizing renewable electricity to produce "green" H_2 avoids fewer CO_2e emissions than utilizing electricity for transportation, heat pumps, or simply displacing conventional power generation (e.g., coal, natural gas).[450] This finding and concept of environmental opportunity cost was

https://doi.org/10.1021/acs.chemrev.5c00361
Chem. Rev. 2026, 126, 5028−5082

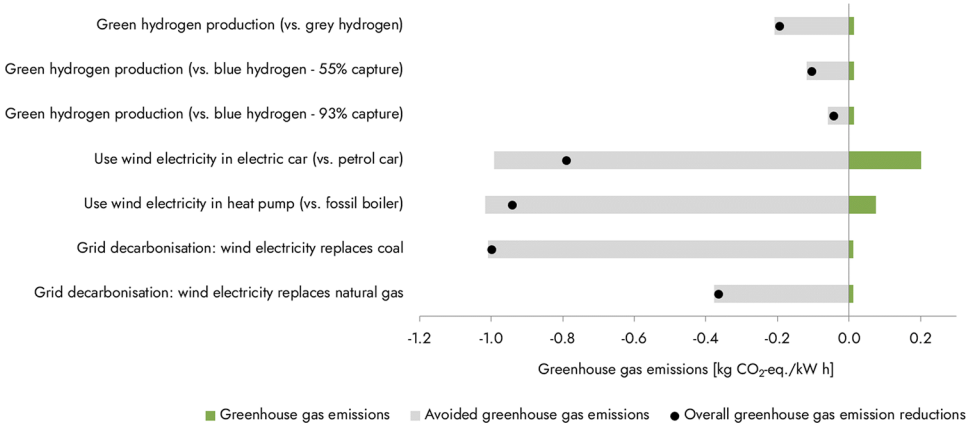

Figure 31. CO_2 emissions and avoided emissions for different ways of using 1 kWh of offshore wind generation. Reproduced with permission from ref 450. Copyright 2022, Royal Society of Chemistry.

further corroborated by Ravikumar et al. who studied CO_2-based methanol production finding, that until the carbon intensity of the electricity grid drops below 82 g CO_2e/kWh, is it more environmentally beneficial to supply renewable energy to the grid rather that use it to convert CO_2 into methanol.[451]

Indeed, from governmental mandates to tax incentives to offering consumers environmentally friendly alternatives in the marketplace, there are many potential reasons why companies have and will continue to pursue CO_2 conversion. However, these analyses show that owing to their intrinsic energy intensive properties, CO_2-based e-products carry a significant energy "opportunity cost" and that at least over the near-term, may not always represent the best way to maximize climate benefits, depending on how other industries evolve and decarbonize over time. Nevertheless, over the long-term, the massive quantities of available CO_2 combined with the insatiable demand for chemicals and fuels points to a future where CO_2-based products can play a significant role in fostering a circular economy. Consequently, research and development efforts supporting CO_2 conversion should continue such that once economic, policy, and environmental conditions are favorable for these technologies to take significant market share, the community is ready.

7. CONCLUSIONS AND OUTLOOK

Born out of a desire to stem rising levels of atmospheric CO_2, the field of CO_2 conversion and utilization has experienced a period of rapid growth over the past two decades. Offering the ability to repurpose "waste" carbon resources into chemicals and fuels by way of low-carbon electricity, CO_2 conversion is heralded as a means to bring the benefits of deep electrification to many of the otherwise "difficult to decarbonize" industrial sectors. Further, with the ability to tap into the approximately 3,330 gigatonnes of CO_2 (i.e., ~ 900 gigatonnes of carbon) in the atmosphere from any point in the world via direct air capture, CO_2 conversion technologies can be decoupled from existing infrastructure and other geographical constraints, thereby improving supply chain resiliency, promoting carbon circularity, and offering new opportunities for the chemical storage of stranded energy assets.

In this manuscript we have reviewed the most recent advancements (2020−2025) across prominent pathways for CO_2 conversion spanning the fields of electrochemistry, photochemistry, biochemistry, plasma, and thermocatalysis. Specifically, we have highlighted how the collective fundamental understanding of chemical mechanisms and challenges for electron-mediated and H_2-mediated CO_2 conversion have evolved over the past six years and how these new insights have contributed toward improved technical metrics and scale up of CO_2 conversion. This review also discussed the outlook on the availability of critical feedstocks for CO_2 conversion including electricity, H_2, and CO_2 itself, finding the availability of low-cost and low-carbon electricity to be the principle limiting factor in widespread adoption of CO_2 conversion for likely the next several decades. We further discussed the current commercial and economic status of CO_2 conversion, finding recent commercial activity to be largely dominated by e-methanol and e-fuel production efforts. TEA studies performed during this time predict the cost of these, and other CO_2-based products, to exceed that of conventional methods over the nearest-term, with some studies finding that if sharp reductions in CAPEX, feedstock costs, and energy use can be realized over time there may be pathways to reaching price points at or below those of conventional pathways used today. Finally, we conclude the review with a discussion on the environmental outlook for CO_2 conversion, highlighting that the critical ingredient for ultimately lowering emissions will be the carbon footprint of the energy source (e.g., electricity or H_2). We also highlight the concept of "opportunity cost" recently discussed across life-cycle analyses, noting that due to the significant energy cost associated with CO_2 conversion, the community must weigh the benefits of diverting low-carbon electricity toward CO_2 conversion versus the myriads of other potential use cases and the relative benefits of each.

■ ASSOCIATED CONTENT

Supporting Information

The Supporting Information is available free of charge at https://pubs.acs.org/doi/10.1021/acs.chemrev.5c00361.

Half-cell reactions for CO_2RR; Anatomy of a CO_2 conversion electrolyzer; metrics used in CO_2RR; advantages, challenges, and failure modes of LTE CO_2RR electrolyzers; comparative review of the chemical advantages, challenges, and reported performance of dominant low-temperature CO_2 electrolyzer architectures from the 2020−2025 literature; and review of key chemical degradation mechanisms in low-temperature CO_2 electrolyzers, their performance impacts, and mitigation strategies (PDF)

https://doi.org/10.1021/acs.chemrev.5c00361
Chem. Rev. 2026, 126, 5028−5082

AUTHOR INFORMATION

Corresponding Author

R. Gary Grim − *National Laboratory of the Rockies, Golden, Colorado 80401, United States;* orcid.org/0000-0002-1154-7795; Email: gary.grim@nlr.gov

Authors

Alex Badgett − *National Laboratory of the Rockies, Golden, Colorado 80401, United States*

Wade A. Braunecker − *National Laboratory of the Rockies, Golden, Colorado 80401, United States;* orcid.org/0000-0003-0773-9580

Michael T. Guarnieri − *National Laboratory of the Rockies, Golden, Colorado 80401, United States*

Susan E. Habas − *National Laboratory of the Rockies, Golden, Colorado 80401, United States;* orcid.org/0000-0002-3893-8454

Christopher Hahn − *Lawrence Livermore National Laboratory, Livermore, California 94550, United States;* orcid.org/0000-0002-2772-6341

Kenneth Neyerlin − *National Laboratory of the Rockies, Golden, Colorado 80401, United States;* orcid.org/0000-0002-6753-9698

Aditya Prajapati − *Lawrence Livermore National Laboratory, Livermore, California 94550, United States*

Daniel A. Ruddy − *National Laboratory of the Rockies, Golden, Colorado 80401, United States;* orcid.org/0000-0003-2654-3778

Roxanne Z. Walker − *National Laboratory of the Rockies, Golden, Colorado 80401, United States*

Complete contact information is available at: https://pubs.acs.org/10.1021/acs.chemrev.5c00361

Author Contributions

CRediT: R. Gary Grim conceptualization, writing-original draft, writing review and editing, project administration; Alex Badgett conceptualization, writing-original draft (electricity and H_2); Wade A. Braunecker conceptualization, writing-original draft (photochemistry); Michael T. Guarnieri conceptualization, writing-original draft (MES, fermentation, direct CO2 utilization); Susan E. Habas conceptualization, writing-original draft (plasma); Christopher Hahn conceptualization, writing-original draft (LTE); Kenneth Neyerlin conceptualization, writing-original draft (LTE); Aditya Prajapati conceptualization, writing-original draft (LTE); Daniel A. Ruddy conceptualization, writing-original draft (thermocatalysis); Roxanne Walker conceptualization, writing-original draft (plasma).

Notes

The authors declare no competing financial interest.

Biographies

Gary Grim is a staff scientist at the National Laboratory of the Rockies, Center for Catalytic Carbon Transformation and Scale-up (Colorado, USA). He received his Ph.D. in Chemical Engineering from the Colorado School of Mines (Golden, Colorado, USA) in 2014. His research interests include the sustainable production fuels and chemicals.

Alex Badgett works as a researcher in the Industrial Systems and Fuels group in NLR's Strategic Energy Analysis Center. His work analyzes interfaces and opportunities between hydrogen production from water electrolyzers and an evolving power sector. Alex also performs bottom up cost estimation and critical materials and supply chain analysis for various electrolyzer technologies to understand barriers and opportunities to manufacturing, deploying, and recycling these systems at scale. Alex holds a B.S. in Geological Engineering and M.S. in Advanced Energy Systems from the Colorado School of Mines.

Wade A. Braunecker is a senior scientist and group manager in the Chemistry and Nanoscience Center at the National Laboratory of the Rockies (Colorado, USA). He received his Ph.D. in Chemistry from Carnegie Mellon University in 2008. His current research integrates materials chemistry and polymer science with various optical techniques to advance gas storage, separation, and catalytic systems.

Mike T. Guarnieri is a Distinguished Member of the Research Staff at the National Laboratory of the Rockies and the Biological Conversion Platform Leader within the Biosciences Center at the National Laboratory of the Rockies (Colorado, USA). He received his Ph.D. in Biochemistry and Molecular Genetics from the University of Colorado School of Medicine (Aurora, CO) in 2009. Dr. Guarnieri's research targets diverse biotechnological applications, spanning bioenergy, bioremediation, and biosecurity, via the development and deployment of molecular systems biology approaches.

Susan E. Habas is a Senior Scientist and Distinguished Member of Research Staff in the Catalytic Carbon Transformation & Scale-up Center at the National Laboratory of the Rockies (Colorado, USA). She received her Ph.D. in Chemistry from the University of California, Berkeley in 2008. Her current research focuses on the development of innovative catalysts for selective transformations of renewable and waste carbon sources into fuels and chemicals.

Christopher Hahn is a Deputy Group Leader of the Materials Energy and Carbon Security Group and Deputy Director of the Laboratory for Energy Applications for the Future at Lawrence Livermore National Laboratory. He received his Ph.D. in Chemistry from the University of California Berkeley and conducted his postdoctoral research at Stanford University in the Department of Chemical Engineering. Dr. Hahn has more than a decade of experience developing electrochemical conversion technologies and is currently leading projects on CO_2 electrolyzer scale-up, reactive capture of CO2, and biomass conversion.

Kenneth Neyerlin is a Distinguished Member of the Research Staff at the National Laboratory of the Rockies, where he is the principal investigator for numerous fuel cell and electrochemical conversion projects. He received his Ph.D. in Chemical Engineering from the University of Rochester (NY) in 2007. Dr. Neyerlin's research is focused on the application of advanced electrochemical diagnostics to deconvolute voltage losses in electrochemical systems, enabling mitigation strategies that target the optimization of materials and component interfaces, along with electrode and device design, providing implementable solutions for electrochemical reactors at scale.

Aditya Prajapati is a Principal Investigator and Research Scientist in the Materials Science Division at Lawrence Livermore National Laboratory (LLNL). He received his Ph.D. in Chemical Engineering from the University of Illinois at Chicago in 2022. With a multidisciplinary approach encompassing electrochemistry, catalysis, advanced manufacturing, Multiphysics modeling, and machine learning, Dr Prajapati's research aims to design energy-efficient systems for electrochemical CO_2 reduction, N_2 oxidation, and specialty chemical electro-synthesis to improve performance, durability, and scalability.

https://doi.org/10.1021/acs.chemrev.5c00361
Chem. Rev. 2026, 126, 5028−5082

Daniel A. Ruddy is a senior scientist at the National Laboratory of the Rockies, Center for Catalytic Carbon Transformation and Scale-up (Colorado, USA). He received his Ph.D. in chemistry from the Univ. of California-Berkeley (Berkeley, California, USA) in 2008. His research seeks to integrate the synthesis, characterization, and performance testing of functional molecules and materials to enable renewable fuels and chemicals production and advance related energy technologies.

Roxanne Walker is a Director's Fellow Postdoctoral Researcher in the Catalytic Carbon Transformation and & Scale-up Center at the National Laboratory of the Rockies (Colorado, USA). She received her Ph.D. in Nuclear Engineering and Radiological Sciences from the University of Michigan in 2024. Her current research focuses on developing nonthermal plasma-liquid catalytic systems for upgrading feedstocks into fuels and chemicals.

■ ACKNOWLEDGMENTS

The work authored by R.G.G., A.B., W.A.B., M.T.G., S.E.H., K.N., D.A.R., and R.Z.W. was performed at the National Laboratory of the Rockies for the U.S. Department of Energy (DOE) under Contract No. DE-AC36-08GO28308. Funding provided by U.S. Department of Energy Office of Energy Efficiency and Renewable Energy Bioenergy Technologies Office. Work by A.P. and C.H. was performed under the auspices of the U.S. Department of Energy by Lawrence Livermore National Laboratory under Contract DE-AC52-07NA27344 and was supported by U.S. Department of Energy Office of Energy Efficiency and Renewable Energy Bioenergy Technologies Office with IM release number LLNL-JRNL-2014485. The views expressed in the article do not necessarily represent the views of the DOE or the U.S. Government. The U.S. Government retains and the publisher, by accepting the article for publication, acknowledges that the U.S. Government retains a nonexclusive, paid-up, irrevocable, worldwide license to publish or reproduce the published form of this work, or allow others to do so, for U.S. Government purposes. Authors would also like to acknowledge Wilson Smith for his contributions to the conceptualization of the electrolysis sections.

■ REFERENCES

(1) Liu, Z.; Deng, Z.; Davis, S. J.; Ciais, P. Global Carbon Emissions in 2023. *Nat. Rev. Earth Environ.* **2024**, *5* (4), 253−254.
(2) Ritchie, H.; Roser, M. CO_2 Emissions Dataset: Our Sources and Methods. *Our World Data* 2024.
(3) United Nations Environment Programme. *The Emissions Gap Report 2017: A UN Environment Synthesis Report*; The Emissions Gap Report; UN, 2017.
(4) Grim, R. G.; Huang, Z.; Guarnieri, M. T.; Ferrell, J. R.; Tao, L.; Schaidle, J. A. Transforming the Carbon Economy: Challenges and Opportunities in the Convergence of Low-Cost Electricity and Reductive CO_2 Utilization. *Energy Environ. Sci.* **2020**, *13* (2), 472−494.
(5) Bushuyev, O. S.; De Luna, P.; Dinh, C. T.; Tao, L.; Saur, G.; Van De Lagemaat, J.; Kelley, S. O.; Sargent, E. H. What Should We Make with CO2 and How Can We Make It? *Joule* **2018**, *2* (5), 825−832.
(6) Smith, W. A.; Burdyny, T.; Vermaas, D. A.; Geerlings, H. Pathways to Industrial-Scale Fuel Out of Thin Air from CO2 Electrolysis. *Joule* **2019**, *3* (8), 1822−1834.
(7) Overa, S.; Ko, B. H.; Zhao, Y.; Jiao, F. Electrochemical Approaches for CO2 Conversion to Chemicals: A Journey toward Practical Applications. *Acc. Chem. Res.* **2022**, *55* (5), 638−648.
(8) Dell'Aversano, S.; Villante, C.; Gallucci, K.; Vanga, G.; Di Giuliano, A. E-Fuels: A Comprehensive Review of the Most Promising Technological Alternatives towards an Energy Transition. *Energies* **2024**, *17* (16), 3995.
(9) Kuhl, K. P.; Cave, E. R.; Abram, D. N.; Jaramillo, T. F. New Insights into the Electrochemical Reduction of Carbon Dioxide on Metallic Copper Surfaces. *Energy Environ. Sci.* **2012**, *5* (5), 7050.
(10) Snoeckx, R.; Bogaerts, A. Plasma Technology - a Novel Solution for CO_2 Conversion? *Chem. Soc. Rev.* **2017**, *46* (19), 5805−5863.
(11) Dessì, P.; Rovira-Alsina, L.; Sánchez, C.; Dinesh, G. K.; Tong, W.; Chatterjee, P.; Tedesco, M.; Farràs, P.; Hamelers, H. M. V.; Puig, S. Microbial Electrosynthesis: Towards Sustainable Biorefineries for Production of Green Chemicals from CO2 Emissions. *Biotechnol. Adv.* **2021**, *46*, 107675.
(12) Van Bavel, S.; Verma, S.; Negro, E.; Bracht, M. Integrating CO_2 Electrolysis into the Gas-to-Liquids-Power-to-Liquids Process. *ACS Energy Lett.* **2020**, *5* (8), 2597−2601.
(13) *Clean Fuel Production Credit | Internal Revenue Service*. https://www.irs.gov/credits-deductions/clean-fuel-production-credit (accessed 2025-04-30).
(14) *ReFuelEU Aviation - European Commission*. https://transport.ec.europa.eu/transport-modes/air/environment/refueleu-aviation_en (accessed 2024-12-30).
(15) Grim, R. G.; Ravikumar, D.; Tan, E. C. D.; Huang, Z.; Ferrell, J. R.; Resch, M.; Li, Z.; Mevawala, C.; Phillips, S. D.; Snowden-Swan, L.; Tao, L.; Schaidle, J. A. Electrifying the Production of Sustainable Aviation Fuel: The Risks, Economics, and Environmental Benefits of Emerging Pathways Including CO_2. *Energy Environ. Sci.* **2022**, *15* (11), 4798−4812.
(16) Artz, J.; Müller, T. E.; Thenert, K.; Kleinekorte, J.; Meys, R.; Sternberg, A.; Bardow, A.; Leitner, W. Sustainable Conversion of Carbon Dioxide: An Integrated Review of Catalysis and Life Cycle Assessment. *Chem. Rev.* **2018**, *118* (2), 434−504.
(17) Sternberg, A.; Jens, C. M.; Bardow, A. Life Cycle Assessment of CO_2 -Based C1-Chemicals. *Green Chem.* **2017**, *19* (9), 2244−2259.
(18) Huang, Z.; Grim, R. G.; Schaidle, J. A.; Tao, L. The Economic Outlook for Converting CO_2 and Electrons to Molecules. *Energy Environ. Sci.* **2021**, *14* (7), 3664−3678.
(19) *Argonne GREET R&D Model*. https://greet.anl.gov/ (accessed 2024-12-30).
(20) Wang, L.; Shahbazi, A.; Hanna, M. A. Characterization of Corn Stover, Distiller Grains and Cattle Manure for Thermochemical Conversion. *Biomass Bioenergy* **2011**, *35* (1), 171−178.
(21) Rocha, G. J. D. M.; Nascimento, V. M.; Gonçalves, A. R.; Silva, V. F. N.; Martín, C. Influence of Mixed Sugarcane Bagasse Samples Evaluated by Elemental and Physical-Chemical Composition. *Ind. Crops Prod.* **2015**, *64*, 52−58.
(22) Vassilev, S. V.; Baxter, D.; Andersen, L. K.; Vassileva, C. G. An Overview of the Chemical Composition of Biomass. *Fuel* **2010**, *89* (5), 913−933.
(23) International Renewable Energy Agency. *Renewable Power Generation Costs in 2023*. https://www.irena.org/Publications/2024/Sep/Renewable-Power-Generation-Costs-in-2023 (accessed 2024-12-30).
(24) Grim, R. G.; Ferrell, J. R., Iii; Huang, Z.; Tao, L.; Resch, M. G. The Feasibility of Direct CO2 Conversion Technologies on Impacting Mid-Century Climate Goals. *Joule* **2023**, *7* (8), 1684−1699.
(25) Shin, H.; Hansen, K. U.; Jiao, F. Techno-Economic Assessment of Low-Temperature Carbon Dioxide Electrolysis. *Nat. Sustain.* **2021**, *4* (10), 911−919.
(26) Adnan, M. A.; Kibria, M. G. Comparative Techno-Economic and Life-Cycle Assessment of Power-to-Methanol Synthesis Pathways. *Appl. Energy* **2020**, *278*, 115614.
(27) Strange, R. The 2020 Covid-19 Pandemic and Global Value Chains. *J. Ind. Bus. Econ.* **2020**, *47* (3), 455−465.
(28) Cui, L.; Yue, S.; Nghiem, X.-H.; Duan, M. Exploring the Risk and Economic Vulnerability of Global Energy Supply Chain Interruption in the Context of Russo-Ukrainian War. *Resour. Policy* **2023**, *81*, 103373.

https://doi.org/10.1021/acs.chemrev.5c00361
Chem. Rev. 2026, 126, 5028−5082

(29) IRENA. Renewable Capacity Statistics 2024, 2024. https://www.irena.org/Publications/2024/Mar/Renewable-capacity-statistics-2024 (accessed 2024-12-12).
(30) Küngas, R. Review—Electrochemical CO_2 Reduction for CO Production: Comparison of Low- and High-Temperature Electrolysis Technologies. *J. Electrochem. Soc.* **2020**, *167* (4), 044508.
(31) Lee, H.; Kwon, S.; Park, N.; Cha, S. G.; Lee, E.; Kong, T.-H.; Cha, J.; Kwon, Y. Scalable Low-Temperature CO2 Electrolysis: Current Status and Outlook. *JACS Au* **2024**, *4* (9), 3383−3399.
(32) Mac Dowell, N.; Fennell, P. S.; Shah, N.; Maitland, G. C. The Role of CO2 Capture and Utilization in Mitigating Climate Change. *Nat. Clim. Change* **2017**, *7* (4), 243−249.
(33) Grim, R. G.; To, A. T.; Farberow, C. A.; Hensley, J. E.; Ruddy, D. A.; Schaidle, J. A. Growing the Bioeconomy through Catalysis: A Review of Recent Advancements in the Production of Fuels and Chemicals from Syngas-Derived Oxygenates. *ACS Catal.* **2019**, *9* (5), 4145−4172.
(34) Anekwe, I. M. S.; Isa, Y. M. Catalytic Conversion of Low Alcohol to Hydrocarbons: Challenges, Prospects, and Future Work Considerations. *Int. J. Energy Res.* **2023**, *2023*, 1−28.
(35) Stephens, I. E. L.; Chan, K.; Bagger, A.; Boettcher, S. W.; Bonin, J.; Boutin, E.; Buckley, A. K.; Buonsanti, R.; Cave, E. R.; Chang, X.; Chee, S. W.; da Silva, A. H. M.; de Luna, P.; Einsle, O.; Endrodi, B.; Escudero-Escribano, M.; Ferreira de Araujo, J. V.; Figueiredo, M. C.; Hahn, C.; Hansen, K. U.; Haussener, S.; Hunegnaw, S.; Huo, Z.; Hwang, Y. J.; Janáky, C.; Jayathilake, B. S.; Jiao, F.; Jovanov, Z. P.; Karimi, P.; Koper, M. T. M.; Kuhl, K. P.; Lee, W. H.; Liang, Z.; Liu, X.; Ma, S.; Ma, M.; Oh, H.-S.; Robert, M.; Cuenya, B. R.; Rossmeisl, J.; Roy, C.; Ryan, M. P.; Sargent, E. H.; Sebastián-Pascual, P.; Seger, B.; Steier, L.; Strasser, P.; Varela, A. S.; Vos, R. E.; Wang, X.; Xu, B.; Yadegari, H.; Zhou, Y. 2022 Roadmap on Low Temperature Electrochemical CO2 Reduction. *J. Phys. Energy* **2022**, *4* (4), 042003.
(36) Luo, Y.; Liu, T.; Wang, Y.; Ding, M. High-Temperature CO2 Electrolysis in Solid Oxide Electrolysis Cells Cathode: Advances and Perspective. *Chem Catal.* **2023**, *3* (12), 100815.
(37) Segets, D.; Andronescu, C.; Apfel, U.-P. Accelerating CO2 Electrochemical Conversion towards Industrial Implementation. *Nat. Commun.* **2023**, *14* (1), 7950.
(38) Nitopi, S.; Bertheussen, E.; Scott, S. B.; Liu, X.; Engstfeld, A. K.; Horch, S.; Seger, B.; Stephens, I. E. L.; Chan, K.; Hahn, C.; Nørskov, J. K.; Jaramillo, T. F.; Chorkendorff, I. Progress and Perspectives of Electrochemical CO_2 Reduction on Copper in Aqueous Electrolyte. *Chem. Rev.* **2019**, *119* (12), 7610−7672.
(39) Wakerley, D.; Lamaison, S.; Wicks, J.; Clemens, A.; Feaster, J.; Corral, D.; Jaffer, S. A.; Sarkar, A.; Fontecave, M.; Duoss, E. B.; Baker, S.; Sargent, E. H.; Jaramillo, T. F.; Hahn, C. Gas Diffusion Electrodes, Reactor Designs and Key Metrics of Low-Temperature CO2 Electrolysers. *Nat. Energy* **2022**, *7* (2), 130−143.
(40) Seger, B.; Kastlunger, G.; Bagger, A.; Scott, S. B. A Perspective on the Reaction Mechanisms of CO2 Electrolysis. *ACS Energy Lett.* **2025**, *10* (5), 2212−2227.
(41) Abdinejad, M.; Hossain, M. N.; Kraatz, H.-B. Homogeneous and Heterogeneous Molecular Catalysts for Electrochemical Reduction of Carbon Dioxide. *RSC Adv.* **2020**, *10* (62), 38013−38023.
(42) Zhang, S.; Fan, Q.; Xia, R.; Meyer, T. J. CO2 Reduction: From Homogeneous to Heterogeneous Electrocatalysis. *Acc. Chem. Res.* **2020**, *53* (1), 255−264.
(43) Hori, Y. Electrochemical CO2 Reduction on Metal Electrodes. In *Modern Aspects of Electrochemistry*; Vayenas, C. G., White, R. E., Gamboa-Aldeco, M. E., Eds.; Springer: New York, 2008; pp 89−189. .
(44) Liu, X.; Xiao, J.; Peng, H.; Hong, X.; Chan, K.; Nørskov, J. K. Understanding Trends in Electrochemical Carbon Dioxide Reduction Rates. *Nat. Commun.* **2017**, *8* (1), 15438.
(45) Han, N.; Wang, Y.; Yang, H.; Deng, J.; Wu, J.; Li, Y.; Li, Y. Ultrathin Bismuth Nanosheets from in Situ Topotactic Transformation for Selective Electrocatalytic CO2 Reduction to Formate. *Nat. Commun.* **2018**, *9* (1), 1320.
(46) Kuhl, K. P.; Cave, E. R.; Abram, D. N.; Jaramillo, T. F. New Insights into the Electrochemical Reduction of Carbon Dioxide on Metallic Copper Surfaces. *Energy Environ. Sci.* **2012**, *5* (5), 7050−7059.
(47) Peterson, A. A.; Abild-Pedersen, F.; Studt, F.; Rossmeisl, J.; Nørskov, J. K. How Copper Catalyzes the Electroreduction of Carbon Dioxide into Hydrocarbon Fuels. *Energy Environ. Sci.* **2010**, *3* (9), 1311−1315.
(48) Kortlever, R.; Shen, J.; Schouten, K. J. P.; Calle-Vallejo, F.; Koper, M. T. M. Catalysts and Reaction Pathways for the Electrochemical Reduction of Carbon Dioxide. *J. Phys. Chem. Lett.* **2015**, *6* (20), 4073−4082.
(49) Tyburski, R.; Liu, T.; Glover, S. D.; Hammarström, L. Proton-Coupled Electron Transfer Guidelines, Fair and Square. *J. Am. Chem. Soc.* **2021**, *143* (2), 560−576.
(50) García-Muelas, R.; Dattila, F.; Shinagawa, T.; Martín, A. J.; Pérez-Ramírez, J.; López, N. Origin of the Selective Electroreduction of Carbon Dioxide to Formate by Chalcogen Modified Copper. *J. Phys. Chem. Lett.* **2018**, *9* (24), 7153−7159.
(51) Gottle, A. J.; Koper, M. T. M. Proton-Coupled Electron Transfer in the Electrocatalysis of CO 2 Reduction: Prediction of Sequential vs. Concerted Pathways Using DFT. *Chem. Sci.* **2017**, *8* (1), 458−465.
(52) Kim, Y.; Park, S.; Shin, S.-J.; Choi, W.; Min, B. K.; Kim, H.; Kim, W.; Hwang, Y. J. Time-Resolved Observation of C-C Coupling Intermediates on Cu Electrodes for Selective Electrochemical CO2 Reduction. *Energy Environ. Sci.* **2020**, *13* (11), 4301−4311.
(53) Calle-Vallejo, F.; Koper, M. T. M. Theoretical Considerations on the Electroreduction of CO to C2 Species on Cu(100) Electrodes. *Angew. Chem., Int. Ed.* **2013**, *52* (28), 7282−7285.
(54) Montoya, J. H.; Shi, C.; Chan, K.; Nørskov, J. K. Theoretical Insights into a CO Dimerization Mechanism in CO2 Electroreduction. *J. Phys. Chem. Lett.* **2015**, *6* (11), 2032−2037.
(55) Verma, S.; Lu, S.; Kenis, P. J. A. Co-Electrolysis of CO2 and Glycerol as a Pathway to Carbon Chemicals with Improved Technoeconomics Due to Low Electricity Consumption. *Nat. Energy* **2019**, *4* (6), 466−474.
(56) Pang, Y.; Li, J.; Wang, Z.; Tan, C.-S.; Hsieh, P.-L.; Zhuang, T.-T.; Liang, Z.-Q.; Zou, C.; Wang, X.; De Luna, P.; Edwards, J. P.; Xu, Y.; Li, F.; Dinh, C.-T.; Zhong, M.; Lou, Y.; Wu, D.; Chen, L.-J.; Sargent, E. H.; Sinton, D. Efficient Electrocatalytic Conversion of Carbon Monoxide to Propanol Using Fragmented Copper. *Nat. Catal.* **2019**, *2* (3), 251−258.
(57) De Gregorio, G. L.; Burdyny, T.; Loiudice, A.; Iyengar, P.; Smith, W. A.; Buonsanti, R. Facet-Dependent Selectivity of Cu Catalysts in Electrochemical CO2 Reduction at Commercially Viable Current Densities. *ACS Catal.* **2020**, *10* (9), 4854−4862.
(58) Hahn, C.; Hatsukade, T.; Kim, Y.-G.; Vailionis, A.; Baricuatro, J. H.; Higgins, D. C.; Nitopi, S. A.; Soriaga, M. P.; Jaramillo, T. F. Engineering Cu Surfaces for the Electrocatalytic Conversion of CO2: Controlling Selectivity toward Oxygenates and Hydrocarbons. *Proc. Natl. Acad. Sci.* **2017**, *114* (23), 5918−5923.
(59) Dattila, F.; Garcıa-Muelas, R.; López, N. Active and Selective Ensembles in Oxide-Derived Copper Catalysts for CO2 Reduction. *ACS Energy Lett.* **2020**, *5* (10), 3176−3184.
(60) Wang, S.; Kou, T.; Baker, S. E.; Duoss, E. B.; Li, Y. Recent Progress in Electrochemical Reduction of CO2 by Oxide-Derived Copper Catalysts. *Mater. Today Nano* **2020**, *12*, 100096.
(61) Lum, Y.; Ager, J. W. Stability of Residual Oxides in Oxide-Derived Copper Catalysts for Electrochemical CO2 Reduction Investigated with 18O Labeling. *Angew. Chem., Int. Ed.* **2018**, *57* (2), 551−554.
(62) Lu, Q.; Rosen, J.; Zhou, Y.; Hutchings, G. S.; Kimmel, Y. C.; Chen, J. G.; Jiao, F. A Selective and Efficient Electrocatalyst for Carbon Dioxide Reduction. *Nat. Commun.* **2014**, *5* (1), 3242.
(63) Chen, Y.; Kanan, M. W. Tin Oxide Dependence of the CO2 Reduction Efficiency on Tin Electrodes and Enhanced Activity for Tin/Tin Oxide Thin-Film Catalysts. *J. Am. Chem. Soc.* **2012**, *134* (4), 1986−1989.

https://doi.org/10.1021/acs.chemrev.5c00361
Chem. Rev. 2026, 126, 5028−5082

(64) Singh, M. R.; Clark, E. L.; Bell, A. T. Effects of Electrolyte, Catalyst, and Membrane Composition and Operating Conditions on the Performance of Solar-Driven Electrochemical Reduction of Carbon Dioxide. *Phys. Chem. Chem. Phys.* **2015**, *17* (29), 18924−18936.
(65) Varela, A. S.; Kroschel, M.; Reier, T.; Strasser, P. Controlling the Selectivity of CO2 Electroreduction on Copper: The Effect of the Electrolyte Concentration and the Importance of the Local pH. *Catal. Today* **2016**, *260*, 8−13.
(66) Yang, K.; Kas, R.; Smith, W. A. In Situ Infrared Spectroscopy Reveals Persistent Alkalinity near Electrode Surfaces during CO2 Electroreduction. *J. Am. Chem. Soc.* **2019**, *141* (40), 15891−15900.
(67) Resasco, J.; Chen, L. D.; Clark, E.; Tsai, C.; Hahn, C.; Jaramillo, T. F.; Chan, K.; Bell, A. T. Promoter Effects of Alkali Metal Cations on the Electrochemical Reduction of Carbon Dioxide. *J. Am. Chem. Soc.* **2017**, *139* (32), 11277−11287.
(68) Gunathunge, C. M.; Ovalle, V. J.; Waegele, M. M. Probing Promoting Effects of Alkali Cations on the Reduction of CO at the Aqueous Electrolyte/Copper Interface. *Phys. Chem. Chem. Phys.* **2017**, *19* (44), 30166−30172.
(69) Ringe, S.; Clark, E. L.; Resasco, J.; Walton, A.; Seger, B.; Bell, A. T.; Chan, K. Understanding Cation Effects in Electrochemical CO_2 Reduction. *Energy Environ. Sci.* **2019**, *12* (10), 3001−3014.
(70) Rabinowitz, J. A.; Kanan, M. W. The Future of Low-Temperature Carbon Dioxide Electrolysis Depends on Solving One Basic Problem. *Nat. Commun.* **2020**, *11* (1), 5231.
(71) Ma, M.; Clark, E. L.; Therkildsen, K. T.; Dalsgaard, S.; Chorkendorff, I.; Seger, B. Insights into the Carbon Balance for CO2 Electroreduction on Cu Using Gas Diffusion Electrode Reactor Designs. *Energy Environ. Sci.* **2020**, *13* (3), 977−985.
(72) Verma, S.; Hamasaki, Y.; Kim, C.; Huang, W.; Lu, S.; Jhong, H.-R. M.; Gewirth, A. A.; Fujigaya, T.; Nakashima, N.; Kenis, P. J. A. Insights into the Low Overpotential Electroreduction of CO_2 to CO on a Supported Gold Catalyst in an Alkaline Flow Electrolyzer. *ACS Energy Lett.* **2018**, *3* (1), 193−198.
(73) Ozden, A.; García de Arquer, F. P.; Huang, J. E.; Wicks, J.; Sisler, J.; Miao, R. K.; O'Brien, C. P.; Lee, G.; Wang, X.; Ip, A. H.; Sargent, E. H.; Sinton, D. Carbon-Efficient Carbon Dioxide Electrolysers. *Nat. Sustain.* **2022**, *5* (7), 563−573.
(74) Xie, K.; Miao, R. K.; Ozden, A.; Liu, S.; Chen, Z.; Dinh, C.-T.; Huang, J. E.; Xu, Q.; Gabardo, C. M.; Lee, G.; Edwards, J. P.; O'Brien, C. P.; Boettcher, S. W.; Sinton, D.; Sargent, E. H. Bipolar Membrane Electrolyzers Enable High Single-Pass CO2 Electroreduction to Multicarbon Products. *Nat. Commun.* **2022**, *13* (1), 3609.
(75) Lee, H.; Kwon, S.; Park, N.; Cha, S. G.; Lee, E.; Kong, T.-H.; Cha, J.; Kwon, Y. Scalable Low-Temperature CO2 Electrolysis: Current Status and Outlook. *JACS Au* **2024**, *4* (9), 3383−3399.
(76) Wong, A. B. The Microenvironment Frontier for Electrochemical CO2 Conversion. *Acc. Mater. Res.* **2024**, *5* (12), 1453−1456.
(77) Chen, J.; Qiu, H.; Zhao, Y.; Yang, H.; Fan, L.; Liu, Z.; Xi, S.; Zheng, G.; Chen, J.; Chen, L.; Liu, Y.; Guo, L.; Wang, L. Selective and Stable CO2 Electroreduction at High Rates via Control of Local H2O/CO2 Ratio. *Nat. Commun.* **2024**, *15* (1), 5893.
(78) Sassenburg, M.; Kelly, M.; Subramanian, S.; Smith, W. A.; Burdyny, T. Zero-Gap Electrochemical CO2 Reduction Cells: Challenges and Operational Strategies for Prevention of Salt Precipitation. *ACS Energy Lett.* **2023**, *8* (1), 321−331.
(79) Habibzadeh, F.; Mardle, P.; Zhao, N.; Riley, H. D.; Salvatore, D. A.; Berlinguette, C. P.; Holdcroft, S.; Shi, Z. Ion Exchange Membranes in Electrochemical CO2 Reduction Processes. *Electrochem. Energy Rev.* **2023**, *6* (1), 26.
(80) Heßelmann, M.; Lee, J. K.; Chae, S.; Tricker, A.; Keller, R. G.; Wessling, M.; Su, J.; Kushner, D.; Weber, A. Z.; Peng, X. Pure-Water-Fed Forward-Bias Bipolar Membrane CO2 Electrolyzer. *ACS Appl. Mater. Interfaces* **2024**, *16* (19), 24649−24659.
(81) Hu, L.; Wrubel, J. A.; Baez-Cotto, C. M.; Intia, F.; Park, J. H.; Kropf, A. J.; Kariuki, N.; Huang, Z.; Farghaly, A.; Amichi, L.; Saha, P.; Tao, L.; Cullen, D. A.; Myers, D. J.; Ferrandon, M. S.; Neyerlin, K. C. A Scalable Membrane Electrode Assembly Architecture for Efficient Electrochemical Conversion of CO2 to Formic Acid. *Nat. Commun.* **2023**, *14* (1), 7605.
(82) Monteiro, M. C. O.; Dattila, F.; López, N.; Koper, M. T. M. The Role of Cation Acidity on the Competition between Hydrogen Evolution and CO2 Reduction on Gold Electrodes. *J. Am. Chem. Soc.* **2022**, *144* (4), 1589−1602.
(83) Huang, J. E.; Li, F.; Ozden, A.; Sedighian Rasouli, A.; García de Arquer, F. P.; Liu, S.; Zhang, S.; Luo, M.; Wang, X.; Lum, Y.; Xu, Y.; Bertens, K.; Miao, R. K.; Dinh, C.-T.; Sinton, D.; Sargent, E. H. CO_2 Electrolysis to Multicarbon Products in Strong Acid. *Science* **2021**, *372* (6546), 1074−1078.
(84) Kuang, M.; Zheng, G. Interfacial Microenvironments for Carbon Dioxide Electro-Upgrading to Multicarbon Products. *Chem Catal.* **2023**, *3* (4), 100565.
(85) Zhang, H.; Gao, J.; Raciti, D.; Hall, A. S. Promoting Cu-Catalysed CO2 Electroreduction to Multicarbon Products by Tuning the Activity of H2O. *Nat. Catal.* **2023**, *6* (9), 807−817.
(86) Nesbitt, N. T.; Smith, W. A. Water and Solute Activities Regulate CO2 Reduction in Gas-Diffusion Electrodes. *J. Phys. Chem. C* **2021**, *125* (24), 13085−13095.
(87) Vasilyev, D. V.; Dyson, P. J. The Role of Organic Promoters in the Electroreduction of Carbon Dioxide. *ACS Catal.* **2021**, *11* (3), 1392−1405.
(88) Nie, W.; Heim, G. P.; Watkins, N. B.; Agapie, T.; Peters, J. C. Organic Additive-Derived Films on Cu Electrodes Promote Electrochemical CO2 Reduction to C2+ Products Under Strongly Acidic Conditions. *Angew. Chem., Int. Ed.* **2023**, *62* (12), No. e202216102.
(89) Peng, Y.; Zhan, C.; Jeon, H. S.; Frandsen, W.; Cuenya, B. R.; Kley, C. S. Organic Thin Films Enable Retaining the Oxidation State of Copper Catalysts during CO2 Electroreduction. *ACS Appl. Mater. Interfaces* **2024**, *16* (5), 6562−6568.
(90) Deng, H.; Chen, Z.; Wang, Y. Ionomer and Membrane Designs for Low-Temperature CO2 and CO Electrolysis. *ChemSusChem* **2025**, *18* (4), No. e202401728.
(91) Goldman, M.; Prajapati, A.; Cross, N. R.; Clemens, A.; Chu, A. T.; Gutierrez, L.; Marufu, M.; Krall, E.; Ehlinger, V.; Moore, T.; Duoss, E. B.; Baker, S. E.; Hahn, C. Designing Ionomers to Control Water Content for Low-Voltage Ethylene Production from CO2 Electrolysis. *Chem Catal.* **2025**, *5*, 101497.
(92) Henckel, D. A.; Saha, P.; Rajana, S.; Baez-Cotto, C.; Taylor, A. K.; Liu, Z.; Resch, M. G.; Masel, R. I.; Neyerlin, K. C. Understanding Limitations in Electrochemical Conversion to CO at Low CO2 Concentrations. *ACS Energy Lett.* **2024**, *9* (7), 3433−3439.
(93) Chang, M.; Ren, W.; Ni, W.; Lee, S.; Hu, X. Ionomers Modify the Selectivity of Cu-Catalyzed Electrochemical CO2 Reduction. *ChemSusChem* **2023**, *16* (5), No. e202201687.
(94) Wang, J.; Huang, B.; Xiao, L.; Wang, G.; Zhuang, L. Operando Spectroscopic Insights into CO2 Reduction at Electrode/Polyelectrolyte Interfaces. *Angew. Chem., Int. Ed.* **2025**, *64* (32), No. e202509423.
(95) Abarca, J. A.; Warmuth, L.; Rieder, A.; Dutta, A.; Vesztergom, S.; Broekmann, P.; Irabien, A.; Díaz-Sainz, G. GDE Stability in CO2 Electroreduction to Formate: The Role of Ionomer Type and Loading. *ACS Catal.* **2025**, *15* (11), 8753−8767.
(96) Rossi, K.; Buonsanti, R. Shaping Copper Nanocatalysts to Steer Selectivity in the Electrochemical CO2 Reduction Reaction. *Acc. Chem. Res.* **2022**, *55* (5), 629−637.
(97) Yoon, A.; Poon, J.; Grosse, P.; Chee, S. W.; Cuenya, B. R. Iodide-Mediated Cu Catalyst Restructuring during CO2 Electroreduction. *J. Mater. Chem. A* **2022**, *10* (26), 14041−14050.
(98) Cheng, D.; Nguyen, K.-L. C.; Sumaria, V.; Wei, Z.; Zhang, Z.; Gee, W.; Li, Y.; Morales-Guio, C. G.; Heyde, M.; Roldan Cuenya, B.; Alexandrova, A. N.; Sautet, P. Structure Sensitivity and Catalyst Restructuring for CO2 Electro-Reduction on Copper. *Nat. Commun.* **2025**, *16* (1), 4064.
(99) Fang, W.; Guo, W.; Lu, R.; Yan, Y.; Liu, X.; Wu, D.; Li, F. M.; Zhou, Y.; He, C.; Xia, C.; Niu, H.; Wang, S.; Liu, Y.; Mao, Y.; Zhang, C.; You, B.; Pang, Y.; Duan, L.; Yang, X.; Song, F.; Zhai, T.; Wang, G.; Guo, X.; Tan, B.; Yao, T.; Wang, Z.; Xia, B. Y. Durable CO2

https://doi.org/10.1021/acs.chemrev.5c00361
Chem. Rev. 2026, 126, 5028−5082

Conversion in the Proton-Exchange Membrane System. *Nature* **2024**, *626* (7997), 86−91.
(100) Segev, G.; Kibsgaard, J.; Hahn, C.; Xu, Z. J.; Cheng, W.-H.; Deutsch, T. G.; Xiang, C.; Zhang, J. Z.; Hammarström, L.; Nocera, D. G.; Weber, A. Z.; Agbo, P.; Hisatomi, T.; Osterloh, F. E.; Domen, K.; Abdi, F. F.; Haussener, S.; Miller, D. J.; Ardo, S.; McIntyre, P. C.; Hannappel, T.; Hu, S.; Atwater, H.; Gregoire, J. M.; Ertem, M. Z.; Sharp, I. D.; Choi, K.-S.; Lee, J. S.; Ishitani, O.; Ager, J. W.; Prabhakar, R. R.; Bell, A. T.; Boettcher, S. W.; Vincent, K.; Takanabe, K.; Artero, V.; Napier, R.; Cuenya, B. R.; Koper, M. T. M.; Van De Krol, R.; Houle, F. The 2022 Solar Fuels Roadmap. *J. Phys. Appl. Phys.* **2022**, *55* (32), 323003.
(101) Hou, X.; Jiang, Y.; Wei, K.; Jiang, C.; Jen, T.-C.; Yao, Y.; Liu, X.; Ma, J.; Irvine, J. T. S. Syngas Production from CO2 and H2O via Solid-Oxide Electrolyzer Cells: Fundamentals, Materials, Degradation, Operating Conditions, and Applications. *Chem. Rev.* **2024**, *124* (8), 5119−5166.
(102) Du, Y.; Ling, H.; Zhao, L.; Jiang, H.; Kong, J.; Liu, P.; Zhou, T. The Development of Solid Oxide Electrolysis Cells: Critical Materials, Technologies and Prospects. *J. Power Sources* **2024**, *607*, 234608.
(103) Zheng, Y.; Wang, J.; Yu, B.; Zhang, W.; Chen, J.; Qiao, J.; Zhang, J. A Review of High Temperature Co-Electrolysis of H_2 O and CO_2 to Produce Sustainable Fuels Using Solid Oxide Electrolysis Cells (SOECs): Advanced Materials and Technology. *Chem. Soc. Rev.* **2017**, *46* (5), 1427−1463.
(104) Hauch, A.; Küngas, R.; Blennow, P.; Hansen, A. B.; Hansen, J. B.; Mathiesen, B. V.; Mogensen, M. B. Recent Advances in Solid Oxide Cell Technology for Electrolysis. *Science* **2020**, *370* (6513), No. eaba6118.
(105) Ebbesen, S. D.; Jensen, S. H.; Hauch, A.; Mogensen, M. B. High Temperature Electrolysis in Alkaline Cells, Solid Proton Conducting Cells, and Solid Oxide Cells. *Chem. Rev.* **2014**, *114* (21), 10697−10734.
(106) Song, Y.; Zhang, X.; Xie, K.; Wang, G.; Bao, X. High-Temperature CO_2 Electrolysis in Solid Oxide Electrolysis Cells: Developments, Challenges, and Prospects. *Adv. Mater.* **2019**, *31* (50), 1902033.
(107) Han, X.; Peng, C.; Mabaleha, S.; Zheng, Y.; Xu, X. Recent Development and Modification of Perovskite-Based CO_2 Electrolysis Solid Oxide Electrolysis Cell Cathode. *ChemSusChem* **2025**, *18* (23), No. e202501327.
(108) Panunzi, A. P.; Duranti, L.; Draz, U.; Licoccia, S.; D'Ottavi, C.; Di Bartolomeo, E. Improved Surface Activity of Lanthanum Ferrite Perovskite Oxide through Controlled Pt-Doping for Solid Oxide Cell (SOC) Electrodes. *Ceram. Int.* **2024**, *50* (17, Part B), 31442−31450.
(109) Chang, H.; Tian, W.; Chen, H.; Li, S.-D.; Shao, Z. Improved CO2 Electrolysis by a Fe Nanoparticle-Decorated (Ce, La, Sr)-(CrFe)O3-δ Perovskite Using a Combined Strategy of Lattice Defect-Building. *Electrochim. Acta* **2023**, *439*, 141699.
(110) Skafte, T. L.; Blennow, P.; Hjelm, J.; Graves, C. Carbon Deposition and Sulfur Poisoning during CO2 Electrolysis in Nickel-Based Solid Oxide Cell Electrodes. *J. Power Sources* **2018**, *373*, 54−60.
(111) Wang, S.; Qian, B.; Wang, Z.; Yin, B.; Zheng, Y.; Ge, L.; Chen, H.; Yang, H. High Catalytic Activity of Fe-Based Perovskite Fuel Electrode for Direct CO2 Electroreduction in SOECs. *J. Alloys Compd.* **2021**, *888*, 161573.
(112) Kröll, L.; De Haart, L. G. J.; Vinke, I.; Eichel, R.-A. Degradation Mechanisms in Solid-Oxide Fuel and Electrolyzer Cells: Analytical Description of Nickel Agglomeration in a Ni/Y S Z Electrode. *Phys. Rev. Appl.* **2017**, *7* (4), 044007.
(113) Li, Z.; Cui, L.; Luo, J.; Li, J.; Sun, Y. Perovskite Chromite With In-Situ Assembled Ni-Co Nano-Alloys: A Potential Bifunctional Electrode Catalyst for Solid Oxide Cells. *Front. Chem.* **2021**, *8*, 595608.
(114) Hu, F.; Ling, Y.; Fang, S.; Sui, L.; Xiao, H.; Huang, Y.; Wang, S.; He, B.; Zhao, L. Engineering Dual-Exsolution on Self-Assembled Cathode to Achieve Efficient Electrocatalytic CO2 Reduction. *Appl. Catal. B Environ.* **2023**, *337*, 122968.
(115) Sharma, V.; Kumar, S.; Shandilya, M.; Saha, A.; Tiwari, K. Perovskite-Powered Dopants for Electrodes in next-Generation Solid Oxide Fuel Cells. *J. Power Sources* **2026**, *665*, 239091.
(116) Wang, J.; Zhang, G.; Sun, N.; Xu, H.; Zheng, G.; Zhang, X.; Wu, Y.; Chen, T.; Xu, L.; Wang, S. A Robust High-Entropy Perovskite Fuel Electrode for Direct CO2 Electrolysis on Air Electrode-Supported Solid Oxide Electrolysis Cells. *Int. J. Hydrog. Energy* **2025**, *105*, 980−989.
(117) Wang, C.; Zhu, Y.; Zhao, L.; Wang, R.; Jin, J.; Gong, Y.; Wang, H.; He, B. Enhancing CO2 Electrolysis Efficiency via In-Situ Exsolution in High-Entropy Perovskite Electrodes. *Sep. Purif. Technol.* **2025**, *354*, 128950.
(118) Zhang, N.; Zhang, W.; Wu, M.; Wang, R.; Gong, Y.; Wang, H.; Jin, J.; Zhao, L.; He, B. Entropy-Engineered Perovskite Cathodes: A Novel Approach for Efficient and Durable CO2 Electrolysis. *J. Colloid Interface Sci.* **2025**, *682*, 70−79.
(119) Chen, Z.; Wang, J.; Li, M.; Dong, J.; Xu, R.; Cheng, J.; Xiong, K.; Rao, M.; Chen, C.; Shen, C.; Li, X.; Ling, Y. Boosting the CO2 Electrolysis Performance Using High Entropy Stable La0.2Pr0.2Sm0.2Sr0.2Ca0.2Fe0.9Ni0.1O3-δ Electrode for Symmetric Solid Oxide Electrolysis Cells. *Fuel* **2024**, *359*, 130464.
(120) Wang, T.; Sun, N.; Wang, R.; Dong, D.; Wei, T.; Wang, Z. In-Situ Dual-Exsolved Nanometal Anchoring on Heterogeneous Composite Nanofiber Using as SOEC Cathode for Direct and Highly Efficient CO2 Electrolysis. *J. Power Sources* **2025**, *626*, 235821.
(121) Goldston, R. J. *Introduction to Plasma Physics*; CRC Press: Boca Raton, 2020.
(122) Snoeckx, R.; Bogaerts, A. Plasma Technology - a Novel Solution for CO2 Conversion? *Chem. Soc. Rev.* **2017**, *46* (19), 5805−5863.
(123) Bogaerts, A.; Centi, G. Plasma Technology for CO2 Conversion: A Personal Perspective on Prospects and Gaps. *Front. Energy Res.* **2020**, *8*, 111.
(124) Ullah, S.; Gao, Y.; Dou, L.; Liu, Y.; Shao, T.; Yang, Y.; Murphy, A. B. Recent Trends in Plasma-Assisted CO2 Methanation: A Critical Review of Recent Studies. *Plasma Chem. Plasma Process.* **2023**, *43* (6), 1335−1383.
(125) Bogaerts, A.; Centi, G. Plasma Technology for CO2 Conversion: A Personal Perspective on Prospects and Gaps. *Front. Energy Res.* **2020**, *8*, DOI: 10.3389/fenrg.2020.00111.
(126) Wang, W.; Berthelot, A.; Kolev, S.; Tu, X.; Bogaerts, A. CO_2 Conversion in a Gliding Arc Plasma: 1D Cylindrical Discharge Model. *Plasma Sources Sci. Technol.* **2016**, *25* (6), 065012.
(127) Jie, Z.; Liu, C.; Huang, S.; Zhang, G. Mechanisms of Gas Temperature Variation of the Atmospheric Microwave Plasma Torch. *J. Appl. Phys.* **2021**, *129* (23), 233302.
(128) Li, R.; Liu, J.; Du, J.; Meng, C.; Bian, C.; Liu, C.; Han, F. Research Progress in DBD Plasma-Catalyzed CO2 Conversion. *Ind. Eng. Chem. Res.* **2025**, *64* (13), 6931−6955.
(129) George, A.; Shen, B.; Craven, M.; Wang, Y.; Kang, D.; Wu, C.; Tu, X. A Review of Non-Thermal Plasma Technology: A Novel Solution for CO2 Conversion and Utilization. *Renew. Sustain. Energy Rev.* **2021**, *135*, 109702.
(130) Sun, J.; Qu, Z.; Gao, Y.; Li, T.; Hong, J.; Zhang, T.; Zhou, R.; Liu, D.; Tu, X.; Chen, G.; Brüser, V.; Weltmann, K.-D.; Mei, D.; Fang, Z.; Borras, A.; Barranco, A.; Xu, S.; Ma, C.; Dou, L.; Zhang, S.; Shao, T.; Chen, G.; Liu, D.; Lu, X.; Bo, Z.; Chiang, W.-H.; Vasilev, K.; Keidar, M.; Nikiforov, A.; Jalili, A. R.; Cullen, P. J.; Dai, L.; Hessel, V.; Bogaerts, A.; Murphy, A. B.; Zhou, R.; Ostrikov, K. (Ken). Plasma Power-to-X (PP2X): Status and Opportunities for Non-Thermal Plasma Technologies. *J. Phys. Appl. Phys.* **2024**, *57* (50), 503002.
(131) Longo, V.; Centi, G.; Perathoner, S.; Genovese, C. CO2 Utilisation with Plasma Technologies. *Curr. Opin. Green Sustain. Chem.* **2024**, *46*, 100893.
(132) Ong, M. Y.; Nomanbhay, S.; Kusumo, F.; Show, P. L. Application of Microwave Plasma Technology to Convert Carbon

https://doi.org/10.1021/acs.chemrev.5c00361
Chem. Rev. 2026, 126, 5028−5082

Dioxide (CO2) into High Value Products: A Review. *J. Clean. Prod.* **2022**, *336*, 130447.
(133) Yin, Y.; Yang, T.; Li, Z.; Devid, E.; Auerbach, D.; Kleyn, A. W. CO2 Conversion by Plasma: How to Get Efficient CO2 Conversion and High Energy Efficiency. *Phys. Chem. Chem. Phys.* **2021**, *23* (13), 7974−7987.
(134) Van Turnhout, J.; Rouwenhorst, K.; Lefferts, L.; Bogaerts, A. Plasma Catalysis: What Is Needed to Create Synergy? *EES Catal.* **2025**, *3* (4), 669−693.
(135) Gao, X.; Liang, J.; Wu, L.; Wu, L.; Kawi, S. Dielectric Barrier Discharge Plasma-Assisted Catalytic CO2 Hydrogenation: Synergy of Catalyst and Plasma. *Catalysts* **2022**, *12* (1), 66.
(136) Xu, S.; Chen, H.; Fan, X. Rational Design of Catalysts for Non-Thermal Plasma (NTP) Catalysis: A Reflective Review. *Catal. Today* **2023**, *419*, 114144.
(137) Loenders, B.; Michiels, R.; Bogaerts, A. Is a Catalyst Always Beneficial in Plasma Catalysis? Insights from the Many Physical and Chemical Interactions. *J. Energy Chem.* **2023**, *85*, 501−533.
(138) Mohanan, A.; Snoeckx, R.; Cha, M. S. Temperature-Dependent Kinetics of Plasma-Based CO_2 Conversion: Interplay of Electron-Driven and Thermal-Driven Chemistry. *ChemSusChem* **2025**, *18* (6), No. e202401526.
(139) Hosseini Rad, R.; Brüser, V.; Schiorlin, M.; Schäfer, J.; Brandenburg, R. Enhancement of CO2 Splitting in a Coaxial Dielectric Barrier Discharge by Pressure Increase, Packed Bed and Catalyst Addition. *Chem. Eng. J.* **2023**, *456*, 141072.
(140) Khunda, D.; Li, S.; Cherkasov, N.; Rishard, M. Z. M.; Chaffee, A. L.; Rebrov, E. V. Effect of Temperature on the CO2 Splitting Rate in a DBD Microreactor. *React. Chem. Eng.* **2023**, *8* (9), 2223−2233.
(141) Aerts, R.; Somers, W.; Bogaerts, A. Carbon Dioxide Splitting in a Dielectric Barrier Discharge Plasma: A Combined Experimental and Computational Study. *ChemSusChem* **2015**, *8* (4), 702−716.
(142) Wang, L.; Du, X.; Yi, Y.; Wang, H.; Gul, M.; Zhu, Y.; Tu, X. Plasma-Enhanced Direct Conversion of CO2 to CO over Oxygen-Deficient Mo-Doped CeO2. *Chem. Commun.* **2020**, *56* (94), 14801−14804.
(143) Gao, Y.; Zhou, R.; Chen, B.; Xiao, L.; Zhao, X.; Sun, J.; Zhou, R.; Zhang, J.; Liu, Z. Plasma Catalysis-Driven Decomposition of CO2: Optimizing Energy Distribution with NiCo-CuO Catalyst. *ACS Sustain. Chem. Eng.* **2024**, *12* (29), 10993−11005.
(144) Hegemann, D. Plasma Activation Mechanisms Governed by Specific Energy Input: Potential and Perspectives. *Plasma Process. Polym.* **2023**, *20* (5), 2300010.
(145) Vertongen, R.; Bogaerts, A. How Important Is Reactor Design for CO2 Conversion in Warm Plasmas? *J. CO2 Util.* **2023**, *72*, 102510.
(146) Long, Y.; Wang, X.; Zhang, H.; Wang, K.; Ong, W.-L.; Bogaerts, A.; Li, K.; Lu, C.; Li, X.; Yan, J.; Tu, X.; Zhang, H. Plasma Chemical Looping: Unlocking High-Efficiency CO_2 Conversion to Clean CO at Mild Temperatures. *JACS Au* **2024**, *4* (7), 2462−2473.
(147) Girard-Sahun, F.; Biondo, O.; Trenchev, G.; Van Rooij, G.; Bogaerts, A. Carbon Bed Post-Plasma to Enhance the CO2 Conversion and Remove O2 from the Product Stream. *Chem. Eng. J.* **2022**, *442*, 136268.
(148) Hecimovic, A.; Kiefer, C. K.; Meindl, A.; Antunes, R.; Fantz, U. Fast Gas Quenching of Microwave Plasma Effluent for Enhanced CO2 Conversion. *J. CO2 Util.* **2023**, *71*, 102473.
(149) Mercer, E. R.; Van Alphen, S.; Van Deursen, C. F. A. M.; Righart, T. W. H.; Bongers, W. A.; Snyders, R.; Bogaerts, A.; Van De Sanden, M. C. M.; Peeters, F. J. J. Post-Plasma Quenching to Improve Conversion and Energy Efficiency in a CO2 Microwave Plasma. *Fuel* **2023**, *334*, 126734.
(150) Soldatov, S.; Link, G.; Silberer, L.; Schmedt, C. M.; Carbone, E.; D'Isa, F.; Jelonnek, J.; Dittmeyer, R.; Navarrete, A. Time-Resolved Optical Emission Spectroscopy Reveals Nonequilibrium Conditions for CO_2 Splitting in Atmospheric Plasma Sustained with Ultrafast Microwave Pulsation. *ACS Energy Lett.* **2021**, *6* (1), 124−130.
(151) Li, S.; Felice, G. D.; Eichkorn, S.; Shao, T.; Gallucci, F. A Review on Plasma-Based CO2 Utilization: Process Considerations in the Development of Sustainable Chemical Production. *Plasma Sci. Technol.* **2024**, *26* (9), 094001.
(152) Liu, Z.; Zhou, W.; Xie, Y.; Liu, F.; Fang, Z.; Zhang, G.; Jin, W. Highly Effective CO2 Splitting in a Plasma-Assisted Membrane Reactor. *J. Membr. Sci.* **2023**, *685*, 121981.
(153) Haycock, D. J.; Clarke, R. J.; Go, D. B.; Schneider, W. F.; Hicks, J. C. Fundamental Insights and Emerging Opportunities in Plasma Catalysis for Light Alkane Conversion. *Curr. Opin. Green Sustain. Chem.* **2025**, *51*, 100987.
(154) Beil, S. B.; Bonnet, S.; Casadevall, C.; Detz, R. J.; Eisenreich, F.; Glover, S. D.; Kerzig, C.; Næsborg, L.; Pullen, S.; Storch, G.; Wei, N.; Zeymer, C. Challenges and Future Perspectives in Photocatalysis: Conclusions from an Interdisciplinary Workshop. *JACS Au* **2024**, *4* (8), 2746−2766.
(155) Albero, J.; Peng, Y.; García, H. Photocatalytic CO2 Reduction to C2+ Products. *ACS Catal* **2020**, *10* (10), 5734−5749.
(156) Huang, N.-Y.; Chen, D.; Zheng, Y.-T.; Xu, Q. Photocatalytic CO2 Reduction to Multi-Carbon Products. *Chem.-Eur. J.* **2025**, *31* (53), No. e02207.
(157) He, Y.; Yin, L.; Yuan, N.; Zhang, G. Adsorption and Activation, Active Site and Reaction Pathway of Photocatalytic CO2 Reduction: A Review. *Chem Eng J* **2024**, *481*, 148754.
(158) Chung, H. Y.; Wong, R. J.; Wu, H.; Gunawan, D.; Amal, R.; Ng, Y. H. Scalable and Integrated Photocatalytic Reactor Systems for Solar-to-Fuel Production: Photoredox and Photoreforming Processes. *Adv Energy Mater* **2025**, *15* (28), 2404956.
(159) Liu, B.; Wu, H.; Parkin, I. P. New Insights into the Fundamental Principle of Semiconductor Photocatalysis. *ACS Omega* **2020**, *5* (24), 14847−14856.
(160) Franchi, D.; Amara, Z. Applications of Sensitized Semiconductors as Heterogeneous Visible-Light Photocatalysts in Organic Synthesis. *ACS Sustain. Chem Eng* **2020**, *8* (41), 15405−15429.
(161) Xue, Y.; Chao, D. Organic and Non-Precious Metal Photosensitizers for Photocatalytic CO2 Reduction. *ChemPhotoChem* **2024**, *8* (12), No. e202400246.
(162) Luo, Y.-H.; Dong, L.-Z.; Liu, J.; Li, S.-L.; Lan, Y.-Q. From Molecular Metal Complex to Metal-Organic Framework: The CO2 Reduction Photocatalysts with Clear and Tunable Structure. *Coord. Chem. Rev.* **2019**, *390*, 86−126.
(163) Verma, R.; Sharma, G.; Polshettiwar, V. The Paradox of Thermal vs. Non-Thermal Effects in Plasmonic Photocatalysis. *Nat Commun* **2024**, *15* (1), 7974.
(164) Dhiman, M. Plasmonic Nanocatalysis for Solar Energy Harvesting and Sustainable Chemistry. *J Mater Chem A* **2020**, *8* (20), 10074−10095.
(165) Cheng, Q.; Wang, L.; Huang, J. Solar-Driven Nanocatalysts for CO2 Upcycling: The Structure-Performance Correlation. *Carbon Neutral Syst* **2025**, *1* (1), 5.
(166) Jiang, W.; Loh, H.; Low, B. Q. L.; Zhu, H.; Low, J.; Heng, J. Z. X.; Tang, K. Y.; Li, Z.; Loh, X. J.; Ye, E.; Xiong, Y. Role of Oxygen Vacancy in Metal Oxides for Photocatalytic CO2 Reduction. *Appl Catal B Env.* **2023**, *321*, 122079.
(167) Zhang, T.; Low, J.; Yu, J.; Tyryshkin, A. M.; Mikmeková, E.; Asefa, T. A Blinking Mesoporous TiO2-x Composed of Nanosized Anatase with Unusually Long-Lived Trapped Charge Carriers. *Angew Chem Int Ed* **2020**, *59* (35), 15000−15007.
(168) Wu, M.; Zhu, J.; Wu, Y.; Liu, S.; Zheng, K.; Wang, S.; Li, B.; Li, J.; Liu, C.; Hu, J.; Zhu, J.; Pan, Y.; Sun, Y.; Xie, Y. Photocatalytic Oxidative Coupling of Methane to Ethane Using CO2 as a Soft Oxidant over the Au/TiO2-Vo Nanosheets. *Angew Chem Int Ed* **2025**, *64* (5), No. e202414814.
(169) Yang, J.; Chen, Z.; Zhang, L.; Zhang, Q. Covalent Organic Frameworks for Photocatalytic Reduction of Carbon Dioxide: A Review. *ACS Nano* **2024**, *18* (33), 21804−21835.
(170) Khan, M.; Akmal, Z.; Tayyab, M.; Mansoor, S.; Zeb, A.; Ye, Z.; Zhang, J.; Wu, S.; Wang, L. MOFs Materials as Photocatalysts for CO2 Reduction: Progress, Challenges and Perspectives. *Carbon Capture Sci Tech* **2024**, *11*, 100191.

https://doi.org/10.1021/acs.chemrev.5c00361
Chem. Rev. 2026, 126, 5028−5082

(171) Zhang, Q.; Gao, S.; Guo, Y.; Wang, H.; Wei, J.; Su, X.; Zhang, H.; Liu, Z.; Wang, J. Designing Covalent Organic Frameworks with Co-O4 Atomic Sites for Efficient CO2 Photoreduction. *Nat. Commun* **2023**, *14* (1), 1147.
(172) Zhou, M.; Wang, Z.; Mei, A.; Yang, Z.; Chen, W.; Ou, S.; Wang, S.; Chen, K.; Reiss, P.; Qi, K.; Ma, J.; Liu, Y. Photocatalytic CO2 Reduction Using La-Ni Bimetallic Sites within a Covalent Organic Framework. *Nat. Commun* **2023**, *14* (1), 2473.
(173) Haider, S. N.-U.-Z.; Qureshi, W. A.; Ali, R. N.; Shaosheng, R.; Naveed, A.; Ali, A.; Yaseen, M.; Liu, Q.; Yang, J. Contemporary Advances in Photocatalytic CO2 Reduction Using Single-Atom Catalysts Supported on Carbon-Based Materials. *Adv. Colloid Interface Sci.* **2024**, *323*, 103068.
(174) Zhu, Z.; Tang, R.; Li, C.; An, X.; He, L. Promises of Plasmonic Antenna-Reactor Systems in Gas-Phase CO2 Photocatalysis. *Adv Sci* **2023**, *10* (24), 2302568.
(175) Yuan, L.; Zhou, J.; Zhang, M.; Wen, X.; Martirez, J. M. P.; Robatjazi, H.; Zhou, L.; Carter, E. A.; Nordlander, P.; Halas, N. J. Plasmonic Photocatalysis with Chemically and Spatially Specific Antenna-Dual Reactor Complexes. *ACS Nano* **2022**, *16* (10), 17365−17375.
(176) Yuan, Y.; Deneen, S.; Bayles, A.; Yuan, L.; Lou, M.; Dhindsa, P.; Ahmad, A.; Chung, S.; Robatjazi, H.; Nordlander, P.; Halas, N. J. Enhancing Catalyst Stability with Plasmonic Hot Carriers for Nitrous Oxide Decomposition, Carbon Monoxide Oxidation, and Steam Methane Reforming. *ACS Energy Lett* **2025**, *10* (8), 3799−3807.
(177) Zhou, L.; Martirez, J. M. P.; Finzel, J.; Zhang, C.; Swearer, D. F.; Tian, S.; Robatjazi, H.; Lou, M.; Dong, L.; Henderson, L.; Christopher, P.; Carter, E. A.; Nordlander, P.; Halas, N. J. Light-Driven Methane Dry Reforming with Single Atomic Site Antenna-Reactor Plasmonic Photocatalysts. *Nat Energy* **2020**, *5* (1), 61−70.
(178) Zhan, C.; Yi, J.; Hu, S.; Zhang, X.-G.; Wu, D.-Y.; Tian, Z.-Q. Plasmon-Mediated Chemical Reactions. *Nat. Rev. Methods Primer* **2023**, *3* (1), 12.
(179) Tan, D.; Wei, T.; Xu, B.; Wang, W.; Li, H.; Zhou, Y.; Lin, B.; Yang, G. Ag-Au Antenna-Reactor System with Enhanced Superimposed LSPR-Induced Electric Fields for Plasmon-Mediated CO2 Photoreduction. *ACS Catal* **2025**, *15* (17), 15629−15639.
(180) Zhang, X.; Fan, Y.; You, E.; Li, Z.; Dong, Y.; Chen, L.; Yang, Y.; Xie, Z.; Kuang, Q.; Zheng, L. MOF Encapsulated Sub-Nm Pd Skin/Au Nanoparticles as Antenna-Reactor Plasmonic Catalyst for Light Driven CO2 Hydrogenation. *Nano Energy* **2021**, *84*, 105950.
(181) Verma, R.; Belgamwar, R.; Chatterjee, P.; Bericat-Vadell, R.; Sa, J.; Polshettiwar, V. Nickel-Laden Dendritic Plasmonic Colloidosomes of Black Gold: Forced Plasmon Mediated Photocatalytic CO2 Hydrogenation. *ACS Nano* **2023**, *17* (5), 4526−4538.
(182) Zhang, X.; Xie, W.; Wang, Z.; Liu, Y.; Wang, P.; Cheng, H.; Dai, Y.; Huang, B.; Zheng, Z. Highly Thermally Stable Au-Rh NRs for Plasmon-Enhanced Photothermal Catalytic CO2 Hydrogenation to C2. *Energy Fuels* **2025**, *39*, 17029.
(183) https://www.hartenergy.com/exclusives/startup-syzygy-sets-out-shake-refining-chemicals-210323/.
(184) Khan, S. I.; Houache, M. S. E.; Abu-Lebdeh, Y.; Baranova, E. A. Plasmonic Nanomaterials as Catalysts for CO2 Electroreduction. *ACS Electrochem* **2025**, *1* (10), 1924−1944.
(185) Lu, W.; Ju, F.; Yao, K.; Wei, X. Photoelectrocatalytic Reduction of CO2 for Efficient Methanol Production: Au Nanoparticles as Electrocatalysts and Light Supports. *Ind. Eng. Chem. Res.* **2020**, *59* (10), 4348−4357.
(186) Uthirakumar, P.; Son, H.; Dao, V.; Lee, Y.; Yadav, S.; Lee, I.-H. Accelerating Photoelectrochemical CO2RR Selectively of C2+ Products by Integrating Ag/Pd Cocatalysts on Cu/Cu2O/CuO Heterojunction Nanorods. *J Env. Chem Eng* **2024**, *12* (2), 112442.
(187) Zhang, Y.; Guo, W.; Zhang, Y.; Wei, W. D. Plasmonic Photoelectrochemistry: In View of Hot Carriers. *Adv. Mater.* **2021**, *33* (46), 2006654.
(188) Ali, M. M.; Hossen, M. A.; Abd Aziz, A. Progress in Prediction of Photocatalytic CO2 Reduction Using Machine Learning Approach: A Mini Review. *Mater* **2025**, *8*, 100522.
(189) Rabaey, K.; Rozendal, R. A. Microbial Electrosynthesis — Revisiting the Electrical Route for Microbial Production. *Nat. Rev. Microbiol.* **2010**, *8* (10), 706−716.
(190) Chen, H.; Simoska, O.; Lim, K.; Grattieri, M.; Yuan, M.; Dong, F.; Lee, Y. S.; Beaver, K.; Weliwatte, S.; Gaffney, E. M.; Minteer, S. D. Fundamentals, Applications, and Future Directions of Bioelectrocatalysis. *Chem. Rev.* **2020**, *120* (23), 12903−12993.
(191) Kumar, T.; Eswari J, S. Review and Perspectives of Emerging Green Technology for the Sequestration of Carbon Dioxide into Value-Added Products: An Intensifying Development. *Energy Fuels* **2023**, *37* (5), 3570−3589.
(192) Luo, D.; Zhang, K.; Song, T.; Xie, J. Improving Cell Permeability and Stimulating Biofilm to Release Extracellular Polymeric Substances with Lysozyme for Enhanced Acetate Production in Microbial Electrosynthesis. *J. CO2 Util.* **2022**, *64*, 102204.
(193) Cao, Q.; Zhang, C.; Zhang, J.; Zhang, J.; Zheng, Z.; Liu, H. Enhanced Microbial Electrosynthesis Performance with 3-D Algal Electrodes under High CO2 Sparging: Superior Biofilm Stability and Biocathode-Plankton Interactions. *Bioresour. Technol.* **2024**, *412*, 131381.
(194) Marshall, C. W.; Ross, D. E.; Fichot, E. B.; Norman, R. S.; May, H. D. Long-Term Operation of Microbial Electrosynthesis Systems Improves Acetate Production by Autotrophic Microbiomes. *Environ. Sci. Technol.* **2013**, *47* (11), 6023−6029.
(195) Lekshmi, G. S.; Bazaka, K.; Ramakrishna, S.; Kumaravel, V. Microbial Electrosynthesis: Carbonaceous Electrode Materials for CO2 Conversion. *Mater. Horiz.* **2023**, *10* (2), 292−312.
(196) Gupta, P.; Verma, N. Conversion of CO2 to Formate Using Activated Carbon Fiber-Supported g-C3N4-NiCoWO4 Photoanode in a Microbial Electrosynthesis System. *Chem. Eng. J.* **2022**, *446*, 137029.
(197) Wang, R.; Li, H.; Sun, J.; Zhang, L.; Jiao, J.; Wang, Q.; Liu, S. Nanomaterials Facilitating Microbial Extracellular Electron Transfer at Interfaces. *Adv. Mater.* **2021**, *33* (6), 2004051.
(198) Guo, W.; Chen, Y.; Wang, J.; Cui, L.; Yan, Y. Enhanced Electroactive Bacteria Enrichment and Facilitated Extracellular Electron Transfer in Microbial Fuel Cells via Polydopamine Coated Graphene Aerogel Anode. *Bioelectrochemistry* **2024**, *160*, 108769.
(199) Klein, E. M.; Knoll, M. T.; Gescher, J. Microbe-Anode Interactions: Comparing the Impact of Genetic and Material Engineering Approaches to Improve the Performance of Microbial Electrochemical Systems (MES). *Microb. Biotechnol.* **2023**, *16* (6), 1179−1202.
(200) Wang, Z.; Hu, Y.; Dong, Y.; Shi, L.; Jiang, Y. Enhancing Electrical Outputs of the Fuel Cells with Geobacter Sulferreducens by Overexpressing Nanowire Proteins. *Microb. Biotechnol.* **2023**, *16* (3), 534−545.
(201) Yang, C.; Zhang, J.; Zhang, B.; Liu, D.; Jia, J.; Li, F.; Song, H. Engineering Shewanella Carassii, a Newly Isolated Exoelectrogen from Activated Sludge, to Enhance Methyl Orange Degradation and Bioelectricity Harvest. *Synth. Syst. Biotechnol.* **2022**, *7* (3), 918−927.
(202) Prévoteau, A.; Carvajal-Arroyo, J. M.; Ganigué, R.; Rabaey, K. Microbial Electrosynthesis from CO2: Forever a Promise? *Curr. Opin. Biotechnol.* **2020**, *62*, 48−57.
(203) Jourdin, L.; Burdyny, T. Microbial Electrosynthesis: Where Do We Go from Here? *Trends Biotechnol.* **2021**, *39* (4), 359−369.
(204) Chen, X.; Chen, Y.; Song, C.; Ji, P.; Wang, N.; Wang, W.; Cui, L. Recent Advances in Supported Metal Catalysts and Oxide Catalysts for the Reverse Water-Gas Shift Reaction. *Front. Chem.* **2020**, *8*, 709.
(205) González-Castaño, M.; Dorneanu, B.; Arellano-García, H. The Reverse Water Gas Shift Reaction: A Process Systems Engineering Perspective. *React. Chem. Eng.* **2021**, *6* (6), 954−976.
(206) Baraj, E.; Ciahotný, K.; Hlinčík, T. The Water Gas Shift Reaction: Catalysts and Reaction Mechanism. *Fuel* **2021**, *288*, 119817.
(207) Pahija, E.; Panaritis, C.; Gusarov, S.; Shadbahr, J.; Bensebaa, F.; Patience, G.; Boffito, D. C. Experimental and Computational

https://doi.org/10.1021/acs.chemrev.5c00361
Chem. Rev. 2026, 126, 5028−5082

Synergistic Design of Cu and Fe Catalysts for the Reverse Water-Gas Shift: A Review. *ACS Catal.* **2022**, *12* (12), 6887−6905.
(208) Tommasi, M.; Degerli, S. N.; Ramis, G.; Rossetti, I. Advancements in CO2 Methanation: A Comprehensive Review of Catalysis, Reactor Design and Process Optimization. *Chem. Eng. Res. Des.* **2024**, *201*, 457−482.
(209) Schwiderowski, P.; Ruland, H.; Muhler, M. Current Developments in CO2 Hydrogenation towards Methanol: A Review Related to Industrial Application. *Curr. Opin. Green Sustain. Chem.* **2022**, *38*, 100688.
(210) Wang, X.; Liu, Y.; Li, X.; Liu, D. Heterogeneous Catalysts, Reaction Kinetics, and Reactor Designs for Methanol Production from Carbon Dioxide: A Critical Review. *Can. J. Chem. Eng.* **2024**, *102* (4), 1592−1629.
(211) Lappa, F.; Khalil, I.; Morales, A.; Léonard, G.; Dusselier, M. One Step Methanol-Mediated CO_2 Conversion to Gasoline: Comprehensive Review and Critical Outlook. *Energy Fuels* **2024**, *38* (19), 18265−18291.
(212) Zhou, W.; Cheng, K.; Kang, J.; Zhou, C.; Subramanian, V.; Zhang, Q.; Wang, Y. New Horizon in C1 Chemistry: Breaking the Selectivity Limitation in Transformation of Syngas and Hydrogenation of CO_2 into Hydrocarbon Chemicals and Fuels. *Chem. Soc. Rev.* **2019**, *48* (12), 3193−3228.
(213) Nan, Y.; Mao, Y.; Zha, F.; Yang, Z.; Ma, S.; Tian, H. ZrO2-ZnO-CeO2 Integrated with Nano-Sized SAPO-34 Zeolite for CO2 Hydrogenation to Light Olefins. *React. Kinet. Mech. Catal.* **2022**, *135* (6), 2959−2972.
(214) Li, L.; Li, H.; Li, H.; Ding, W.; Xiao, J. CO_2 Utilization for Aromatics Synthesis over Zeolites. *Catal. Sci. Technol.* **2025**, *15* (2), 234−248.
(215) Istadi, I.; Fani, F.; Riyanto, T.; Anggoro, D. D.; Jongsomjit, B.; Putranto, A. B. Fe-Based Catalysts in CO2 Conversion to Olefins: Navigating Challenges and Catalytic Advances. *J. Ind. Eng. Chem.* **2025**, *149*, 1−15.
(216) Garba, M. D.; Usman, M.; Khan, S.; Shehzad, F.; Galadima, A.; Ehsan, M. F.; Ghanem, A. S.; Humayun, M. CO2 towards Fuels: A Review of Catalytic Conversion of Carbon Dioxide to Hydrocarbons. *J. Environ. Chem. Eng.* **2021**, *9* (2), 104756.
(217) Li, X.; Zhang, L.; Zhang, C.; Wang, L.; Tang, Z.; Gao, R. The Efficient Utilization of Carbon Dioxide in a Power-to-Liquid Process: An Overview. *Processes* **2023**, *11* (7), 2089.
(218) Jung, H. S.; Kim, B. G.; Bae, J. W. Synthetic Routes of Clean Hydrocarbons Fuels and Oxygenates by Catalytic Conversions of Carbon Oxides. *Appl. Catal. B Environ.* **2024**, *343*, 123477.
(219) Shang, X.; Liu, G.; Su, X.; Huang, Y.; Zhang, T. A Review of the Recent Progress on Direct Heterogeneous Catalytic CO_2 Hydrogenation to Gasoline-Range Hydrocarbons. *EES Catal.* **2023**, *1* (4), 353−368.
(220) Li, T.; Zhao, H.; Guo, L.; Liu, G.; Wu, J.; Xing, T.; Li, T.; Liu, Q.; Sui, J.; Han, Y.; Liang, J.; He, Y.; Tsubaki, N. Construction of Highly Active Fe_5C_2 -FeCo Interfacial Sites for Oriented Synthesis of Light Olefins from CO_2 Hydrogenation. *ACS Catal.* **2025**, *15* (2), 1112−1122.
(221) Xu, M.; Liu, X.; Cao, C.; Sun, Y.; Zhang, C.; Yang, Z.; Zhu, M.; Ding, X.; Liu, Y.; Tong, Z.; Xu, J. Ternary Fe-Zn-Al Spinel Catalyst for CO_2 Hydrogenation to Linear α-Olefins: Synergy Effects between Al and Zn. *ACS Sustain. Chem. Eng.* **2021**, *9* (41), 13818−13830.
(222) Yang, X.; Song, G.; Li, M.; Chen, C.; Wang, Z.; Yuan, H.; Zhang, Z.; Liu, D. Selective Production of Aromatics Directly from Carbon Dioxide Hydrogenation over *n* Na-Cu-Fe_2O_3 /HZSM-5. *Ind. Eng. Chem. Res.* **2022**, *61* (23), 7787−7798.
(223) Li, Z.; Wu, W.; Wang, M.; Wang, Y.; Ma, X.; Luo, L.; Chen, Y.; Fan, K.; Pan, Y.; Li, H.; Zeng, J. Ambient-Pressure Hydrogenation of CO2 into Long-Chain Olefins. *Nat. Commun.* **2022**, *13* (1), 2396.
(224) Cheng, Y.; Chen, Y.; Zhang, S.; Wu, X.; Chen, C.; Shi, X.; Qing, M.; Li, J.; Liu, C.-L.; Dong, W.-S. High-Yield Production of Aromatics over $CuFeO_2$ /Hierarchical HZSM-5 *via* CO_2 Fischer−Tropsch Synthesis. *Green Chem.* **2023**, *25* (9), 3570−3584.
(225) Li, Y.; Zeng, L.; Pang, G.; Wei, X.; Wang, M.; Cheng, K.; Kang, J.; Serra, J. M.; Zhang, Q.; Wang, Y. Direct Conversion of Carbon Dioxide into Liquid Fuels and Chemicals by Coupling Green Hydrogen at High Temperature. *Appl. Catal. B Environ.* **2023**, *324*, 122299.
(226) Wang, C.; Jin, Z.; Guo, L.; Yamamoto, O.; Kaida, C.; He, Y.; Ma, Q.; Wang, K.; Tsubaki, N. New Insights for High-Through CO_2 Hydrogenation to High-Quality Fuel. *Angew. Chem., Int. Ed.* **2024**, No. e202408275.
(227) Li, C.; Yuan, X.; Fujimoto, K. Direct Synthesis of LPG from Carbon Dioxide over Hybrid Catalysts Comprising Modified Methanol Synthesis Catalyst and β-Type Zeolite☆. *Appl. Catal. Gen.* **2014**, *475*, 155−160.
(228) Fujiwara, M.; Sakurai, H.; Shiokawa, K.; Iizuka, Y. Synthesis of C2+ Hydrocarbons by CO2 Hydrogenation over the Composite Catalyst of Cu-Zn-Al Oxide and HB Zeolite Using Two-Stage Reactor System under Low Pressure. *Catal. Today* **2015**, *242*, 255−260.
(229) Fujiwara, M.; Satake, T.; Shiokawa, K.; Sakurai, H. CO2 Hydrogenation for C2+ Hydrocarbon Synthesis over Composite Catalyst Using Surface Modified HB Zeolite. *Appl. Catal. B Environ.* **2015**, *179*, 37−43.
(230) Nimlos, C. T.; Nash, C. P.; Dupuis, D. P.; To, A. T.; Kumar, A.; Hensley, J. E.; Ruddy, D. A. Direct Conversion of Renewable CO_2 -Rich Syngas to High-Octane Hydrocarbons in a Single Reactor. *ACS Catal.* **2022**, *12* (15), 9270−9280.
(231) To, A. T.; Arellano-Treviño, M. A.; Nash, C. P.; Ruddy, D. A. Direct Synthesis of Branched Hydrocarbons from CO2 over Composite Catalysts in a Single Reactor. *J. CO2 Util.* **2022**, *66*, 102261.
(232) van Ravenhorst, I. K.; Vogt, C.; Oosterbeek, H.; Bossers, K. W.; Moya-Cancino, J. G.; van Bavel, A. P.; van der Eerden, A. M. J.; Vine, D.; de Groot, F. M. F.; Meirer, F.; Weckhuysen, B. M. Capturing the Genesis of an Active Fischer−Tropsch Synthesis Catalyst with Operando X-ray Nanospectroscopy. *Angew. Chem., Int. Ed.* **2018**, *57* (37), 11957−11962.
(233) Van Ravenhorst, I. K.; Hoffman, A. S.; Vogt, C.; Boubnov, A.; Patra, N.; Oord, R.; Akatay, C.; Meirer, F.; Bare, S. R.; Weckhuysen, B. M. On the Cobalt Carbide Formation in a Co/TiO_2 Fischer−Tropsch Synthesis Catalyst as Studied by High-Pressure, Long-Term *Operando* X-Ray Absorption and Diffraction. *ACS Catal.* **2021**, *11* (5), 2956−2967.
(234) Melaet, G.; Ralston, W. T.; Li, C.-S.; Alayoglu, S.; An, K.; Musselwhite, N.; Kalkan, B.; Somorjai, G. A. Evidence of Highly Active Cobalt Oxide Catalyst for the Fischer−Tropsch Synthesis and CO_2 Hydrogenation. *J. Am. Chem. Soc.* **2014**, *136* (6), 2260−2263.
(235) Have, I. C. T.; Kromwijk, J. J. G.; Monai, M.; Ferri, D.; Sterk, E. B.; Meirer, F.; Weckhuysen, B. M. Uncovering the Reaction Mechanism behind CoO as Active Phase for CO2 Hydrogenation. *Nat. Commun.* **2022**, *13* (1), 324.
(236) Tian, G.; Li, Z.; Zhang, C.; Liu, X.; Fan, X.; Shen, K.; Meng, H.; Wang, N.; Xiong, H.; Zhao, M.; Liang, X.; Luo, L.; Zhang, L.; Yan, B.; Chen, X.; Peng, H.-J.; Wei, F. Upgrading CO2 to Sustainable Aromatics via Perovskite-Mediated Tandem Catalysis. *Nat. Commun.* **2024**, *15* (1), 3037.
(237) Tatsumi, T.; Muramats, A.; Tominaga, H. ALCOHOL SYNTHESIS FROM CO2/H2 ON SILICA-SUPPORTED MOLYBDENUM CATALYSTS. *Chem. Lett.* **1985**, *14* (5), 593−594.
(238) Xu, D.; Wang, Y.; Ding, M.; Hong, X.; Liu, G.; Tsang, S. C. E. Advances in Higher Alcohol Synthesis from CO2 Hydrogenation. *Chem* **2021**, *7* (4), 849−881.
(239) Zhang, S.; Wu, Z.; Liu, X.; Shao, Z.; Xia, L.; Zhong, L.; Wang, H.; Sun, Y. Tuning the Interaction between Na and Co2C to Promote Selective CO2 Hydrogenation to Ethanol. *Appl. Catal. B Environ.* **2021**, *293*, 120207.
(240) Zhang, F.; Zhou, W.; Xiong, X.; Wang, Y.; Cheng, K.; Kang, J.; Zhang, Q.; Wang, Y. Selective Hydrogenation of CO_2 to Ethanol over Sodium-Modified Rhodium Nanoparticles Embedded in Zeolite Silicalite-1. *J. Phys. Chem. C* **2021**, *125* (44), 24429−24439.

https://doi.org/10.1021/acs.chemrev.5c00361
Chem. Rev. 2026, 126, 5028−5082

(241) Ji, S.; Hong, F.; Mao, D.; Guo, Q.; Yu, J. Enhanced Ethanol Synthesis from CO2 Hydrogenation over Fe and Na Co-Modified Rh/CeO2 Catalysts. *Chem. Eng. J.* **2024**, *495*, 153633.
(242) Xu, D.; Ding, M.; Hong, X.; Liu, G. Mechanistic Aspects of the Role of K Promotion on Cu-Fe-Based Catalysts for Higher Alcohol Synthesis from CO_2 Hydrogenation. *ACS Catal.* **2020**, *10* (24), 14516−14526.
(243) Zhang, Q.; Wang, S.; Geng, R.; Wang, P.; Dong, M.; Wang, J.; Fan, W. Hydrogenation of CO2 to Higher Alcohols on an Efficient Cr-Modified CuFe Catalyst. *Appl. Catal. B Environ.* **2023**, *337*, 123013.
(244) Tan, A. F. J.; Isnaini, M. D.; Phisalaphong, M.; Yip, A. C. K. The Engineering of CO_2 Hydrogenation Catalysts for Higher Alcohol Synthesis. *RSC Sustain.* **2024**, *2* (12), 3638−3654.
(245) Wang, C.; Yu, H.; Lin, T.; Qi, X.; Yu, F.; Zhong, L.; Sun, Y. Direct Synthesis of Higher Alcohols from Syngas over Modified Mo 2 C Catalysts under Mild Reaction Conditions. *Catal. Sci. Technol.* **2022**, *12* (5), 1697−1708.
(246) Zhang, L.; Ball, M. R.; Rivera-Dones, K. R.; Wang, S.; Kuech, T. F.; Huber, G. W.; Hermans, I.; Dumesic, J. A. Synthesis Gas Conversion Over Molybdenum-Based Catalysts Promoted by Transition Metals. *ACS Catal.* **2020**, *10* (1), 365−374.
(247) Meng, S.; Gu, J.; Jiang, S.; Weng, Y.; Huang, C.; Ren, P.; Xue, X.; Sun, Q.; Zhang, Y.; Fan, M. Lignin Carbon-Initiated Ni/K/Mo2C Catalyst for Efficient Synthesis of Higher Alcohols from Syngas. *Chem. Eng. J.* **2024**, *481*, 148751.
(248) Yang, Z.; Luo, M.; Liu, Q.; Li, C.; Wang, Y.; Li, H.; Yao, L. Effect of K and Ni Promoters on Mo2C/Al2O3 Catalyst for Higher Alcohols Synthesis from Syngas. *Kinet. Catal.* **2024**, *65* (3), 251−260.
(249) Yangbin, R.; Yujing, W.; Yiqing, Z.; Chao, H.; Yulong, Z.; Qi, S. Recent Advances of Mo-Based Catalysts for Synthesizing Higher Alcohols from Syngas. *Mol. Catal.* **2024**, *568*, 114508.
(250) He, S.; Qu, H.; Liu, J.; Sun, J.; Su, Y.; Hu, R.; Zhang, Y.; Su, H. Remarkably Enhanced Catalytic Performance of Three-Dimensional Hierarchically Porous Mo2C Catalysts for Higher Alcohols Synthesis from Syngas. *Mol. Catal.* **2024**, *556*, 113941.
(251) Yang, Z.; Luo, M.; Liu, Q.; Yao, L.; Wang, Y.; Li, H.; Chen, L.; Shao, C. Effect of Transition and Alkali Metals on Mo2C/Al2O3 Catalysts for Syngas to Higher Alcohols. *J. Environ. Chem. Eng.* **2024**, *12* (6), 114455.
(252) Ye, X.; Ma, J.; Yu, W.; Pan, X.; Yang, C.; Wang, C.; Liu, Q.; Huang, Y. Construction of Bifunctional Single-Atom Catalysts on the Optimized β-Mo2C Surface for Highly Selective Hydrogenation of CO2 into Ethanol. *J. Energy Chem.* **2022**, *67*, 184−192.
(253) Baddour, F. G.; Roberts, E. J.; To, A. T.; Wang, L.; Habas, S. E.; Ruddy, D. A.; Bedford, N. M.; Wright, J.; Nash, C. P.; Schaidle, J. A.; Brutchey, R. L.; Malmstadt, N. An Exceptionally Mild and Scalable Solution-Phase Synthesis of Molybdenum Carbide Nanoparticles for Thermocatalytic CO_2 Hydrogenation. *J. Am. Chem. Soc.* **2020**, *142* (2), 1010−1019.
(254) Karadaghi, L. R.; To, A. T.; Habas, S. E.; Baddour, F. G.; Ruddy, D. A.; Brutchey, R. L. Activating Molybdenum Carbide Nanoparticle Catalysts under Mild Conditions Using Thermally Labile Ligands. *Chem. Mater.* **2022**, *34* (19), 8849−8857.
(255) Wang, L.; Yin, Q.; Zhai, X.; Yi, Y. Recent Progresses of Plasma-Catalytic CH4/CO2 Conversion to Oxygenates: A Short Review. *Curr. Opin. Green Sustain. Chem.* **2025**, *51*, 100989.
(256) Liu, S.; Winter, L. R.; Chen, J. G. Review of Plasma-Assisted Catalysis for Selective Generation of Oxygenates from CO2 and CH4. *ACS Catal.* **2020**, *10* (4), 2855−2871.
(257) Ray, D.; Ye, P.; Yu, J. C.; Song, C. Recent Progress in Plasma-Catalytic Conversion of CO2 to Chemicals and Fuels. *Catal. Today* **2023**, *423*, 113973.
(258) Shen, X.; Craven, M.; Xu, J.; Wang, Y.; Li, Z.; Wang, W.; Yao, S.; Wu, Z.; Jiang, N.; Zhou, X.; Sun, K.; Du, X.; Tu, X. Unveiling the Mechanism of Plasma-Catalytic Low-Temperature Water-Gas Shift Reaction over Cu/γ-Al2O3 Catalysts. *JACS Au* **2024**, *4* (8), 3228−3237.
(259) Kim, D.-Y.; Inagaki, Y.; Yamakawa, T.; Lu, B.; Sato, Y.; Shirai, N.; Furukawa, S.; Kim, H.-H.; Takakusagi, S.; Sasaki, K.; Nozaki, T. Plasma-Derived Atomic Hydrogen Enables Eley-Rideal-Type CO2 Methanation at Low Temperatures. *JACS Au* **2025**, *5* (1), 169−177.
(260) Zeng, Y.; Chen, G.; Liu, B.; Zhang, H.; Tu, X. Unraveling Temperature-Dependent Plasma-Catalyzed CO_2 Hydrogenation. *Ind. Eng. Chem. Res.* **2023**, *62* (46), 19629−19637.
(261) Carreon, M. L. Plasma-Driven Decentralized Production of Essential Chemicals. *Nat. Catal.* **2025**, *8* (1), 2−7.
(262) Zhu, H.; Huang, Y.; Yin, S.; Zhang, W. Microwave Plasma Setups for CO2 Conversion: A Mini-Review. *Green Energy Resour.* **2024**, *2* (1), 100061.
(263) Wang, Y.; Yang, J.; Sun, Y.; Ye, D.; Shan, B.; Tsang, S. C. E.; Tu, X. Engineering Ni-Co Bimetallic Interfaces for Ambient Plasma-Catalytic CO2 Hydrogenation to Methanol. *Chem* **2024**, *10* (8), 2590−2606.
(264) Sugiyama, H.; Miyazaki, M.; Sasase, M.; Kitano, M.; Hosono, H. Room-Temperature CO2 Hydrogenation to Methanol over Air-Stable Hcp-PdMo Intermetallic Catalyst. *J. Am. Chem. Soc.* **2023**, *145* (17), 9410−9416.
(265) Michiels, R.; Engelmann, Y.; Bogaerts, A. Plasma Catalysis for CO2 Hydrogenation: Unlocking New Pathways toward CH3OH. *J. Phys. Chem. C* **2020**, *124*, 25859.
(266) Cui, Z.; Meng, S.; Yi, Y.; Jafarzadeh, A.; Li, S.; Neyts, E. C.; Hao, Y.; Li, L.; Zhang, X.; Wang, X.; Bogaerts, A. Plasma-Catalytic Methanol Synthesis from CO2 Hydrogenation over a Supported Cu Cluster Catalyst: Insights into the Reaction Mechanism. *ACS Catal.* **2022**, *12* (2), 1326−1337.
(267) Li, Z.; Lin, Q.; Li, M.; Cao, J.; Liu, F.; Pan, H.; Wang, Z.; Kawi, S. Recent Advances in Process and Catalyst for CO2 Reforming of Methane. *Renew. Sustain. Energy Rev.* **2020**, *134*, 110312.
(268) Navascués, P.; Cotrino, J.; González-Elipe, A. R.; Gómez-Ramírez, A. Plasma Assisted Dry Reforming of Methane: Syngas and Hydrocarbons Formation Mechanisms. *Fuel Process. Technol.* **2023**, *248*, 107827.
(269) Bogaerts, A. Plasma Technology for the Electrification of Chemical Reactions. *Nat. Chem. Eng.* **2025**, *2* (6), 336−340.
(270) Wang, K.; Ren, X.; Yin, G.; Hu, E.; Zhang, H. Recent Advances in Plasma-Based Methane Reforming for Syngas Production. *Curr. Opin. Green Sustain. Chem.* **2024**, *50*, 100981.
(271) O'Modhrain, C.; Pajares, A.; Coutino-Gonzalez, E.; De Vos, Y.; Guardia, P.; Gorbanev, Y.; Michielsen, B.; Bogaerts, A. Dry Reforming of Methane in Gliding Arc Plasma: Bridging Thermal and Post-Plasma Catalysis. *EES Catal.* **2025**, *3* (5), 1087−1097.
(272) Kwon, H.; Kim, T.; Song, S. Dry Reforming of Methane in a Rotating Gliding Arc Plasma: Improving Efficiency and Syngas Cost by Quenching Product Gas. *J. CO2 Util.* **2023**, *70*, 102448.
(273) Kuijpers, L.; Van Deursen, C. F. A. M.; Shen, Q.; Bongers, W. A.; Devid, E. J.; Van De Sanden, M. C. M. Microwave Plasma-Assisted CO_2 Dissociation with Methane and Ethylene: Improved Conversion and Selectivity Controlled by Afterglow Chemistry. *ACS Sustain. Chem. Eng.* **2025**, *13* (32), 13085−13099.
(274) Martin-del-Campo, J.; Coulombe, S.; Kopyscinski, J. Influence of Operating Parameters on Plasma-Assisted Dry Reforming of Methane in a Rotating Gliding Arc Reactor. *Plasma Chem. Plasma Process.* **2020**, *40* (4), 857−881.
(275) Ceulemans, S.; Morais, E.; Loenders, B.; Bogaerts, A. Microkinetic Modelling of Post-Plasma Catalysis to Improve the Conversion of Dry Reforming of Methane in a Gliding Arc Plasmatron. *J. Catal.* **2026**, *453*, 116474.
(276) Thammakan, S.; Boonyawan, D.; Chimupala, Y.; Yimklan, S.; Tamman, A.; Tapangpan, P.; Opassuwan, T.; Nisoa, M.; Sawangrat, C. Mesoporous K- and Ca-Promoted Ni/Al_2O_3 Catalysts Derived from MIL-53(Al) for Microwave Plasma-Assisted Dry Reforming of Methane into Syngas. *Ind. Eng. Chem. Res.* **2025**, *64* (38), 18727−18738.
(277) Kelly, S.; Mercer, E.; De Meyer, R.; Ciocarlan, R.-G.; Bals, S.; Bogaerts, A. Microwave Plasma-Based Dry Reforming of Methane:

https://doi.org/10.1021/acs.chemrev.5c00361
Chem. Rev. 2026, 126, 5028−5082

Reaction Performance and Carbon Formation. *J. CO2 Util.* **2023**, *75*, 102564.
(278) Kuang, S. Recent Advances in Microwave-Assisted Dry Reforming of Methane: Catalyst, Performance, and Fundamentals. *Front. Chem.* **2025**, *13*, 1681282.
(279) Sun, J.; Chen, Q.; Qin, W.; Wu, H.; Liu, B.; Li, S.; Bogaerts, A. Plasma-Catalytic Dry Reforming of CH4: Effects of Plasma-Generated Species on the Surface Chemistry. *Chem. Eng. J.* **2024**, *498*, 155847.
(280) Dou, L.; Liu, Y.; Gao, Y.; Li, J.; Hu, X.; Zhang, S.; Ostrikov, K.; Shao, T. Disentangling Metallic Cobalt Sites and Oxygen Vacancy Effects in Synergistic Plasma-Catalytic CO2/CH4 Conversion into Oxygenates. *Appl. Catal. B Environ.* **2022**, *318*, 121830.
(281) Qin, W.; Wu, H.; Chen, Q.; Sun, J.; Liu, N.; Liu, B.; Zhang, M. From Electric Field Catalysis to Plasma Catalysis: A Combined Experimental Study and Kinetic Modeling to Understand the Synergistic Effects in Methane Dry Reforming. *Chem. Eng. J.* **2025**, *508*, 161015.
(282) Pinard, L.; Batiot-Dupeyrat, C. Non-Thermal Plasma for Catalyst Regeneration: A Review. *Catal. Today* **2024**, *426*, 114372.
(283) Winter, L. R.; Chen, J. G. Challenges and Opportunities in Plasma-Activated Reactions of CO2 with Light Alkanes. *J. Energy Chem.* **2023**, *84*, 424−427.
(284) Li, S.; Sun, J.; Gorbanev, Y.; van't Veer, K.; Loenders, B.; Yi, Y.; Kenis, T.; Chen, Q.; Bogaerts, A. Plasma-Assisted Dry Reforming of CH4: How Small Amounts of O2 Addition Can Drastically Enhance the Oxygenate Production—Experiments and Insights from Plasma Chemical Kinetics Modeling. *ACS Sustain. Chem. Eng.* **2023**, *11* (42), 15373−15384.
(285) Vieira, L. H.; da Silva, A. H. M.; Santana, C. S.; Assaf, E. M.; Assaf, J. M.; Gomes, J. F. Recent Understanding of Water-Assisted CO2 Hydrogenation to Alcohols. *ChemCatChem* **2024**, *16* (11), No. e202301390.
(286) Meng, S.; Cui, Z.; Chen, Q.; Zhang, H.; Li, S.; Neyts, E. C.; Vlasov, E.; Jenkinson, K.; Bals, S.; Yang, D.; Liu, M.; Liu, Y.; Bogaerts, A.; Lu, A.-H.; Yi, Y. Water-Promoted C-C Coupling Reaction in Plasma-Catalytic CO2 Hydrogenation for Ethanol Production. *ACS Catal.* **2025**, *15* (4), 3236−3246.
(287) Jiang, X.; Nie, X.; Gong, Y.; Moran, C. M.; Wang, J.; Zhu, J.; Chang, H.; Guo, X.; Walton, K. S.; Song, C. A Combined Experimental and DFT Study of H2O Effect on In2O3/ZrO2 Catalyst for CO2 Hydrogenation to Methanol. *J. Catal.* **2020**, *383*, 283−296.
(288) Knezevic, J.; Zhang, T.; Zhou, R.; Hong, J.; Zhou, R.; Barnett, C.; Song, Q.; Gao, Y.; Xu, W.; Liu, D.; Proschogo, N.; Mohanty, B.; Strachan, J.; Soltani, B.; Li, F.; Maschmeyer, T.; Lovell, E. C.; Cullen, P. J. Long-Chain Hydrocarbons from Nonthermal Plasma-Driven Biogas Upcycling. *J. Am. Chem. Soc.* **2024**, *146* (18), 12601−12608.
(289) Bogaerts, A.; Tu, X.; Whitehead, J. C.; Centi, G.; Lefferts, L.; Guaitella, O.; Azzolina-Jury, F.; Kim, H.-H.; Murphy, A. B.; Schneider, W. F.; Nozaki, T.; Hicks, J. C.; Rousseau, A.; Thevenet, F.; Khacef, A.; Carreon, M. The 2020 Plasma Catalysis Roadmap. *J. Phys. Appl. Phys.* **2020**, *53* (44), 443001.
(290) Xu, S.; Chen, H.; Hardacre, C.; Fan, X. Non-Thermal Plasma Catalysis for CO2 Conversion and Catalyst Design for the Process. *J. Phys. Appl. Phys.* **2021**, *54* (23), 233001.
(291) Kim, D.-Y.; Ham, H.; Chen, X.; Liu, S.; Xu, H.; Lu, B.; Furukawa, S.; Kim, H.-H.; Takakusagi, S.; Sasaki, K.; Nozaki, T. Cooperative Catalysis of Vibrationally Excited CO2 and Alloy Catalyst Breaks the Thermodynamic Equilibrium Limitation. *J. Am. Chem. Soc.* **2022**, *144* (31), 14140−14149.
(292) Zhang, H.; Li, L.; Xu, R.; Huang, J.; Wang, N.; Li, X.; Tu, X. Plasma-Enhanced Catalytic Activation of CO2 in a Modified Gliding Arc Reactor. *Waste Dispos. Sustain. Energy* **2020**, *2* (2), 139−150.
(293) Dong, Z.; Li, B.; Zhu, Y.; Guo, W. Metal Halide Perovskites for CO2 Photoreduction: Recent Advances and Future Perspectives. *EES Catal.* **2024**, *2* (2), 448−474.
(294) Feng, X.; Cao, L.; Fu, C.; Qi, F.; Zhang, N.; Pu, Y.; Liang, Z.; Tang, X.; Huang, Q. Enhanced CO2 Conversion in Dielectric Barrier Discharge Plasma Coupled with a Heterojunction Photocatalyst. *Chem. Commun.* **2024**, *60* (67), 8900−8903.
(295) Huang, Q.; Liang, Z.; Qi, F.; Zhang, N.; Yang, J.; Liu, J.; Tian, C.; Fu, C.; Tang, X.; Wu, D.; Wang, J.; Wang, X.; Chen, W. Carbon Dioxide Conversion Synergistically Activated by Dielectric Barrier Discharge Plasma and the CsPbBr3@TiO2 Photocatalyst. *J. Phys. Chem. Lett.* **2022**, *13* (10), 2418−2427.
(296) Shen, Y.; Fu, C.; Luo, W.; Liang, Z.; Wang, Z.-R.; Huang, Q. Machine Learning for CO2 Conversion Driven by Dielectric Barrier Discharge Plasma and Cs2TeCl6 Photocatalysts. *Green Chem.* **2023**, *25* (19), 7605−7611.
(297) Bogaerts, A.; Centi, G.; Hessel, V.; Rebrov, E. Perspectives and Emerging Trends in Plasma Catalysis: Facing the Challenge of Chemical Production Electrification. *ChemCatChem* **2025**, *17* (7), No. e202401938.
(298) Chawdhury, P.; Chansai, S.; Conway, M.; Parker, J.; Lindley, M.; Stere, C. E.; Sankar, M.; Haigh, S. J.; Dennis-Smither, B.; Filip, S. V.; Poulston, S.; Hinde, P.; Hawkins, C.; Hardacre, C. Enhancing the Reaction of CO_2 and H_2 O Using Catalysts within a Nonthermal Plasma. *ACS Catal.* **2025**, *15* (9), 7053−7065.
(299) Simon, J.; Winter, L. R. Plasma-Activated Co-Conversion of N2 and C1 Gases towards Value-Added Products. *Curr. Opin. Green Sustain. Chem.* **2025**, *51*, 100985.
(300) Biester, A.; Marcano-Delgado, A. N.; Drennan, C. L. Structural Insights into Microbial One-Carbon Metabolic Enzymes Ni-Fe-S-Dependent Carbon Monoxide Dehydrogenases and Acetyl-CoA Synthases. *Biochemistry* **2022**, *61* (24), 2797−2805.
(301) Kurt, E.; Qin, J.; Williams, A.; Zhao, Y.; Xie, D. Perspectives for Using CO2 as a Feedstock for Biomanufacturing of Fuels and Chemicals. *Bioengineering* **2023**, *10* (12), 1357.
(302) Heffernan, J. K.; Lai, C.-Y.; Gonzalez-Garcia, R. A.; Keld Nielsen, L.; Guo, J.; Marcellin, E. Biogas Upgrading Using *Clostridium Autoethanogenum* for Value-Added Products. *Chem. Eng. J.* **2023**, *452*, 138950.
(303) Ghadermazi, P.; Re, A.; Ricci, L.; Chan, S. H. J. Metabolic Engineering Interventions for Sustainable 2,3-Butanediol Production in Gas-Fermenting Clostridium Autoethanogenum. *mSystems* **2022**, *7* (2), No. e01111-21.
(304) Wan, S.; Lai, M.; Gao, X.; Zhou, M.; Yang, S.; Li, Q.; Li, F.; Xia, L.; Tan, Y. Recent Progress in Engineering *Clostridium Autoethanogenum* to Synthesize the Biochemicals and Biocommodities. *Synth. Syst. Biotechnol.* **2024**, *9* (1), 19−25.
(305) Bourgade, B.; Humphreys, C. M.; Millard, J.; Minton, N. P.; Islam, M. A. Design, Analysis, and Implementation of a Novel Biochemical Pathway for Ethylene Glycol Production in *Clostridium Autoethanogenum*. *ACS Synth. Biol.* **2022**, *11* (5), 1790−1800.
(306) Heffernan, J.; Garcia Gonzalez, R. A.; Mahamkali, V.; McCubbin, T.; Daygon, D.; Liu, L.; Palfreyman, R.; Harris, A.; Koepke, M.; Valgepea, K.; Nielsen, L. K.; Marcellin, E. Adaptive Laboratory Evolution of Clostridium Autoethanogenum to Metabolize CO2 and H2 Enhances Growth Rates in Chemostat and Unravels Proteome and Metabolome Alterations. *Microb. Biotechnol.* **2024**, *17* (4), No. e14452.
(307) Lee, S.; Rim Lee, Y.; Lee, W.-H.; Youn Lee, S.; Moon, M.; Woo Park, G.; Min, K.; Lee, J.; Lee, J.-S. Valorization of CO2 to β-Farnesene in *Rhodobacter Sphaeroides*. *Bioresour. Technol.* **2022**, *363*, 127955.
(308) Akroum-Amrouche, D.; Akroum, H.; Lounici, H. Green Hydrogen Production by Rhodobacter Sphaeroides. *Energy Sources Part Recovery Util. Environ. Eff.* **2023**, *45* (1), 2862−2880.
(309) Li, S.; Sakuntala, M.; Song, Y. E.; Heo, J.; Kim, M.; Lee, S. Y.; Kim, M.-S.; Oh, Y.-K.; Kim, J. R. Photoautotrophic Hydrogen Production of *Rhodobacter Sphaeroides* in a Microbial Electrosynthesis Cell. *Bioresour. Technol.* **2021**, *320*, 124333.
(310) Li, S.; Kim, M.; Kong, D. S.; Min, K.; Wu, G.; Cui, M.; Kim, C.; Oh, Y.-K.; Kim, S.; Lee, S. Y.; Kang, S. G.; Nygård, Y.; Kim, J. R. Electron Uptake from Solid Electrodes Promotes the More Efficient Conversion of CO2 to Polyhydroxybutyrate by Using *Rhodobacter Sphaeroides*. *Chem. Eng. J.* **2023**, *469*, 143785.

https://doi.org/10.1021/acs.chemrev.5c00361
Chem. Rev. 2026, 126, 5028−5082

(311) Panich, J.; Fong, B.; Singer, S. W. Metabolic Engineering of Cupriavidus Necator H16 for Sustainable Biofuels from CO2. *Trends Biotechnol.* **2021**, *39* (4), 412−424.
(312) Uekert, T.; Bleem, A. C.; Holmes, E. C.; Pal, A.; Johnson, C. W.; Beckham, G. T. Coupling Waste Feedstocks to Microbial Protein Production in a Circular Food System. *ACS Sustain. Chem. Eng.* **2025**, *13* (2), 709−724.
(313) Muñoz-Páez, K. M.; Buitrón, G. Bioconversion of H2 and CO2 from Dark Fermentation to Methane: Effect of Operating Conditions on Methane Concentration. *Chemosphere* **2022**, *308*, 136305.
(314) Xie, Z.; Huang, S.; Wan, Y.; Deng, F.; Cao, Q.; Liu, X.; Li, D. Power to Biogas Upgrading: Effects of Different H2/CO2 Ratios on Products and Microbial Communities in Anaerobic Fermentation System. *Sci. Total Environ.* **2023**, *865*, 161305.
(315) Ham, P.; Bun, S.; Painmanakul, P.; Wongwailikhit, K. Effective Analysis of Different Gas Diffusers on Bubble Hydrodynamics in Bubble Column and Airlift Reactors towards Mass Transfer Enhancement. *Processes* **2021**, *9* (10), 1765.
(316) Wang, Y.; Dong, Y.; Zhang, L.; Chu, G.; Zou, H.; Sun, B.; Zeng, X. Carbon Dioxide Capture by Non-Aqueous Blend in Rotating Packed Bed Reactor: Absorption and Desorption Investigation. *Sep. Purif. Technol.* **2021**, *269*, 118714.
(317) Qian, F.; Zhu, C.; Knipe, J. M.; Ruelas, S.; Stolaroff, J. K.; DeOtte, J. R.; Duoss, E. B.; Spadaccini, C. M.; Henard, C. A.; Guarnieri, M. T.; Baker, S. E. Direct Writing of Tunable Living Inks for Bioprocess Intensification. *Nano Lett.* **2019**, *19* (9), 5829−5835.
(318) Kundoch, J.-O.; Ohde, D.; Byström, E.; Liese, A. Screening Platform for Immobilized Biocatalysts Utilizing Miniature Rotating Bed Reactors. *Org. Process Res. Dev.* **2024**, *28* (12), 4264−4272.
(319) Hassanaly, M.; Parra-Alvarez, J. M.; Rahimi, M. J.; Municchi, F.; Sitaraman, H. Bayesian Calibration of Bubble Size Dynamics Applied to CO2 Gas Fermenters. *arXiv* **2025**, *215*, 312.
(320) Jung, H.; Park, N.; Lee, J. H. Evaluating the Efficiency and Cost-Effectiveness of RPB-Based CO2 Capture: A Comprehensive Approach to Simultaneous Design and Operating Condition Optimization. *arXiv* **2024**, *365*, 123251.
(321) Ozkan, A.; Dufour, T.; Silva, T.; Britun, N.; Snyders, R.; Reniers, F.; Bogaerts, A. DBD in Burst Mode: Solution for More Efficient CO2 Conversion? *Plasma Sources Sci. Technol.* **2016**, *25* (5), 055005.
(322) Puiman, L.; Abrahamson, B.; van der Lans, R. G. J. M.; Haringa, C.; Noorman, H. J.; Picioreanu, C. Alleviating Mass Transfer Limitations in Industrial External-Loop Syngas-to-Ethanol Fermentation. *Chem. Eng. Sci.* **2022**, *259*, 117770.
(323) *Climate Intervention: Carbon Dioxide Removal and Reliable Sequestration*; National Academies Press: Washington, D.C., 2015. DOI: 10.17226/18805.
(324) *Carbon Management Understood, Enabled, Deployed*. Global CCS Institute. https://www.globalccsinstitute.com/ (accessed 2025-04-16).
(325) Xu, Y.; Isom, L.; Hanna, M. A. Adding Value to Carbon Dioxide from Ethanol Fermentations. *Bioresour. Technol.* **2010**, *101* (10), 3311−3319.
(326) Freyman, M. C.; Huang, Z.; Ravikumar, D.; Duoss, E. B.; Li, Y.; Baker, S. E.; Pang, S. H.; Schaidle, J. A. Reactive CO2 Capture: A Path Forward for Process Integration in Carbon Management. *Joule* **2023**, *7* (4), 631−651.
(327) Janke, C.; Duyar, M. S.; Hoskins, M.; Farrauto, R. Catalytic and Adsorption Studies for the Hydrogenation of CO2 to Methane. *Appl. Catal. B Environ.* **2014**, *152*−*153*, 184−191.
(328) Duyar, M. S.; Treviño, M. A. A.; Farrauto, R. J. Dual Function Materials for CO 2 Capture and Conversion Using Renewable H 2. *Appl. Catal. B Environ.* **2015**, *168*−*169*, 370−376.
(329) Duyar, M. S.; Wang, S.; Arellano-Treviño, M. A.; Farrauto, R. J. CO 2 Utilization with a Novel Dual Function Material (DFM) for Capture and Catalytic Conversion to Synthetic Natural Gas: An Update. *J. CO2 Util.* **2016**, *15*, 65−71.
(330) Arellano-Treviño, M. A.; He, Z.; Libby, M. C.; Farrauto, R. J. Catalysts and Adsorbents for CO2 Capture and Conversion with Dual Function Materials: Limitations of Ni-Containing DFMs for Flue Gas Applications. *J. CO2 Util.* **2019**, *31*, 143−151.
(331) Arellano-Treviño, M. A.; Kanani, N.; Jeong-Potter, C. W.; Farrauto, R. J. Bimetallic Catalysts for CO2 Capture and Hydrogenation at Simulated Flue Gas Conditions. *Chem. Eng. J.* **2019**, *375*, 121953.
(332) Proaño, L.; Tello, E.; Arellano-Trevino, M. A.; Wang, S.; Farrauto, R. J.; Cobo, M. In-Situ DRIFTS Study of Two-Step CO2 Capture and Catalytic Methanation over Ru,"Na2O"/Al2O3 Dual Functional Material. *Appl. Surf. Sci.* **2019**, *479*, 25−30.
(333) Proaño, L.; Arellano-Treviño, M. A.; Farrauto, R. J.; Figueredo, M.; Jeong-Potter, C.; Cobo, M. Mechanistic Assessment of Dual Function Materials, Composed of Ru-Ni, Na2O/Al2O3 and Pt-Ni, Na2O/Al2O3, for CO2 Capture and Methanation by in-Situ DRIFTS. *Appl. Surf. Sci.* **2020**, *533*, 147469.
(334) Jeong-Potter, C.; Farrauto, R. Feasibility Study of Combining Direct Air Capture of CO2 and Methanation at Isothermal Conditions with Dual Function Materials. *Appl. Catal. B Environ.* **2021**, *282*, 119416.
(335) Merkouri, L.-P.; Reina, T. R.; Duyar, M. S. Closing the Carbon Cycle with Dual Function Materials. *Energy Fuels* **2021**, *35* (24), 19859−19880.
(336) Gharamaleki, S. B.; Reina, T. R.; Duyar, M. S. Taking Dual Function Materials (DFM) from the Laboratory to Industrial Applications: A Review of DFM Operation under Realistic Integrated CO_2 Capture and Utilization Conditions. *Prog. Energy* **2025**, *7* (1), 012001.
(337) Kim, S.; Lin, X.; Farrauto, R. J. Effect of Moisture (2 Mol%) on CO2 Enhanced Desorption from Nano-Dispersed Na2O/Al2O3 for Direct Air Capture. *Chem. Eng. J.* **2024**, *499*, 156238.
(338) McNeary, W. W.; Ellebracht, N. C.; Jue, M. L.; Rasmussen, M. J.; Crawford, J. M.; Yung, M. M.; To, A. T.; Pang, S. H. Application of Solid-Supported Amines for Thermocatalytic Reactive CO_2 Capture. *ACS Omega* **2025**, *10* (3), 2364−2371.
(339) Leick, N.; Halingstad, S.; Crawford, J. M.; Carroll, G. M.; Yung, M. M.; Cortright, R.; Braunecker, W. A. Photo-Swing CO2 Capture Using a Branched Polyethylenimine as Sorbents and TiN Light Absorber. *J Mater Chem A* **2025**, *13* (35), 29334−29342.
(340) Halingstad, S.; Leick, N.; Huang, Z.; Crawford, J. M.; Carroll, G. M.; Kliegle, G. A.; Young, J. L.; Hill, A. J.; Cortright, R.; Yung, M. M.; Braunecker, W. A. Photoreactive Capture and Conversion of Dilute Carbon Dioxide into Synthetic Natural Gas. *ACS Appl Energy Mater* **2025**, *8* (18), 13179−13184.
(341) Crawford, J. M.; Rasmussen, M. J.; McNeary, W. W.; Halingstad, S.; Hayden, S. C.; Dutta, N. S.; Pang, S. H.; Matthew, M. Yung. High Selectivity Reactive Carbon Dioxide Capture over Zeolite Dual-Functional Materials. *ACS Catal.* **2024**, *14* (11), 8541−8548.
(342) Le Saché, E.; Pastor-Pérez, L.; Haycock, B. J.; Villora-Picó, J. J.; Sepúlveda-Escribano, A.; Reina, T. R. Switchable Catalysts for Chemical CO_2 Recycling: A Step Forward in the Methanation and Reverse Water-Gas Shift Reactions. *ACS Sustain. Chem. Eng.* **2020**, *8* (11), 4614−4622.
(343) Merkouri, L.-P.; Ramirez Reina, T.; Duyar, M. S. Feasibility of Switchable Dual Function Materials as a Flexible Technology for CO_2 Capture and Utilisation and Evidence of Passive Direct Air Capture. *Nanoscale* **2022**, *14* (35), 12620−12637.
(344) Merkouri, L.-P.; Mathew, J.; Jacob, J.; Ramirez Reina, T.; Duyar, M. S. Switchable Catalysis for Methanol and Synthetic Natural Gas Synthesis from CO2: A Techno-Economic Investigation. *J. CO2 Util.* **2024**, *79*, 102652.
(345) Jeong-Potter, C.; Arellano-Treviño, M. A.; McNeary, W. W.; Hill, A. J.; Ruddy, D. A.; To, A. T. Modified Cu-Zn-Al Mixed Oxide Dual Function Materials Enable Reactive Carbon Capture to Methanol. *EES Catal.* **2024**, *2* (1), 253−261.
(346) Martin, J. A.; Tan, E. C. D.; Ruddy, D. A.; King, J.; To, A. T. Temperature-Pressure Swing Process for Reactive Carbon Capture and Conversion to Methanol: Techno-Economic Analysis and Life

Cycle Assessment. *Environ. Sci. Technol.* **2024**, *58* (31), 13737−13747.
(347) Li, S.; Gallucci, F. CO2 Capture and Activation with a Plasma-Sorbent System. *Chem. Eng. J.* **2022**, *430*, 132979.
(348) Li, S.; Ongis, M.; Manzolini, G.; Gallucci, F. Non-Thermal Plasma-Assisted Capture and Conversion of CO2. *Chem. Eng. J.* **2021**, *410*, 128335.
(349) Zhong, H.; Piriaei, D.; Liccardo, G.; Kang, J.; Wang, B.; Cargnello, M.; Cappelli, M. A. Cold Plasma Activated CO_2 Desorption from Calcium Carbonate for Carbon Capture. *RSC Sustain.* **2025**, *3* (2), 973−982.
(350) Fitriani, S. W.; Okumura, T.; Kamataki, K.; Koga, K.; Shiratani, M.; Attri, P. Capture and Conversion of CO2 from Ambient Air Using Ionic Liquid-Plasma Combination. *Plasma Chem. Plasma Process.* **2024**, *44* (6), 2153−2162.
(351) Attri, P.; Koga, K.; Razzokov, J.; Okumura, T.; Kamataki, K.; Nozaki, T.; Shiratani, M. Plasma-Ionic Liquid-Assisted CO2 Capture and Conversion: A Novel Technology. *Appl. Phys. Express* **2024**, *17* (4), 046001.
(352) Umeojiakor, C.; Merkouri, L.-P.; Griffin, A.; Duyar, M. S.; Qiang, Z.; Xiang, Y. Nonthermal Plasma Assisted Desorption and Conversion of Captured CO_2 from Atmospheric Air. *RSC Sustain.* **2025**, *3* (6), 2632−2643.
(353) Vertongen, R.; De Felice, G.; van den Bogaard, H.; Gallucci, F.; Bogaerts, A.; Li, S. Sorption-Enhanced Dry Reforming of Methane in a DBD Plasma Reactor for Single-Stage Carbon Capture and Utilization. *ACS Sustain. Chem. Eng.* **2024**, *12* (29), 10841−10853.
(354) Gorky, F.; Nambo, A.; Carreon, M. L. Cold Plasma-Metal Organic Framework (MOF)-177 Breathable System for Atmospheric Remediation. *J. CO2 Util.* **2021**, *51*, 101642.
(355) Henard, C. A.; Wu, C.; Xiong, W.; Henard, J. M.; Davidheiser-Kroll, B.; Orata, F. D.; Guarnieri, M. T. Ribulose-1,5-Bisphosphate Carboxylase/Oxygenase (RubisCO) Is Essential for Growth of the Methanotroph Methylococcus Capsulatus Strain Bath. *Appl. Environ. Microbiol.* **2021**, *87* (18), No. e00881-21.
(356) Krishnan, A.; Dahlin, L. R.; Guarnieri, M. T.; Weissman, J. C.; Posewitz, M. C. Small Cells with Big Photosynthetic Productivities: Biotechnological Potential of the Picochlorum Genus. *Trends Biotechnol.* **2025**, *43* (4), 759−772.
(357) Dahlin, L. R.; Gerritsen, A. T.; Henard, C. A.; Van Wychen, S.; Linger, J. G.; Kunde, Y.; Hovde, B. T.; Starkenburg, S. R.; Posewitz, M. C.; Guarnieri, M. T. Development of a High-Productivity, Halophilic, Thermotolerant Microalga Picochlorum Renovo. *Commun. Biol.* **2019**, *2* (1), 1−9.
(358) Zhao, T.; Li, Y.; Zhang, Y. Biological Carbon Fixation: A Thermodynamic Perspective. *Green Chem.* **2021**, *23* (20), 7852−7864.
(359) Xiao, L.; Liu, G.; Gong, F.; Zhu, H.; Zhang, Y.; Cai, Z.; Li, Y. A Minimized Synthetic Carbon Fixation Cycle. *ACS Catal.* **2022**, *12* (1), 799−808.
(360) Scafaro, A. P.; Posch, B. C.; Evans, J. R.; Farquhar, G. D.; Atkin, O. K. Rubisco Deactivation and Chloroplast Electron Transport Rates Co-Limit Photosynthesis above Optimal Leaf Temperature in Terrestrial Plants. *Nat. Commun.* **2023**, *14* (1), 2820.
(361) Bährle, R.; Böhnke, S.; Englhard, J.; Bachmann, J.; Perner, M. Current Status of Carbon Monoxide Dehydrogenases (CODH) and Their Potential for Electrochemical Applications. *Bioresour. Bioprocess.* **2023**, *10* (1), 84.
(362) Peng, J.-H.; Lo, S.-C.; Yu, Y.-N.; Yang, Y.-T.; Chen, Y.-C.; Tsai, A.-I.; Wu, D.-Y.; Huang, C.-H.; Su, T.-T.; Huang, C.-C.; Chiang, E.-P. I. Carbon Fluxes Rewiring in Engineered E. Coli via Reverse Tricarboxylic Acid Cycle Pathway under Chemolithotrophic Condition. *J. Biol. Eng.* **2025**, *19* (1), 20.
(363) Liang, B.; Zhao, Y.; Yang, J. Recent Advances in Developing Artificial Autotrophic Microorganism for Reinforcing CO2 Fixation. *Front. Microbiol.* **2020**, *11*. DOI: 10.3389/fmicb.2020.592631.
(364) Schwander, T.; Schada von Borzyskowski, L.; Burgener, S.; Cortina, N. S.; Erb, T. J. A Synthetic Pathway for the Fixation of Carbon Dioxide in Vitro. *Science* **2016**, *354* (6314), 900−904.
(365) Tommasi, I. C. The Biochemistry of Artificial CO2-Fixation Pathways: The Exploitation of Carboxylase Enzymes Alternative to Rubisco. *Catalysts* **2024**, *14* (10), 679.
(366) Cai, T.; Sun, H.; Qiao, J.; Zhu, Z.; et al. Cell-free chemoenzymatic starch synthesis from carbon dioxide. *Science* **2021**, *373*, 1523−1527.
(367) Scheffen, M.; Marchal, D. G.; Beneyton, T.; Schuller, S. K.; Klose, M.; Diehl, C.; Lehmann, J.; Pfister, P.; Carrillo, M.; He, H.; Aslan, S.; Cortina, N. S.; Claus, P.; Bollschweiler, D.; Baret, J.-C.; Schuller, J. M.; Zarzycki, J.; Bar-Even, A.; Erb, T. J. A New-to-Nature Carboxylation Module to Improve Natural and Synthetic CO2 Fixation. *Nat. Catal.* **2021**, *4* (2), 105−115.
(368) Satanowski, A.; Marchal, D. G.; Perret, A.; Petit, J.-L.; Bouzon, M.; Döring, V.; Dubois, I.; He, H.; Smith, E. N.; Pellouin, V.; Petri, H. M.; Rainaldi, V.; Nattermann, M.; Burgener, S.; Paczia, N.; Zarzycki, J.; Heinemann, M.; Bar-Even, A.; Erb, T. J. Design and Implementation of Aerobic and Ambient CO2-Reduction as an Entry-Point for Enhanced Carbon Fixation. *Nat. Commun.* **2025**, *16* (1), 3134.
(369) Badgett, A.; Brauch, J.; Thatte, A.; Rubin, R.; Skangos, C.; Wang, X.; Ahluwalia, R.; Pivovar, B.; Ruth, M. Updated Manufactured Cost Analysis for Proton Exchange Membrane Water Electrolyzers. *NREL* **2024**, NREL/TP-6A20−87625.
(370) Suri, D.; Aeshala, L. M.; Palai, T. Microbial Electrosynthesis of Valuable Chemicals from the Reduction of CO2: A Review. *Environ. Sci. Pollut. Res.* **2024**, *31* (25), 36591−36614.
(371) Cabau-Peinado, O.; Winkelhorst, M.; Stroek, R.; De Kat Angelino, R.; Straathof, A. J. J.; Masania, K.; Daran, J. M.; Jourdin, L. Microbial Electrosynthesis from CO2 Reaches Productivity of Syngas and Chain Elongation Fermentations. *Trends Biotechnol.* **2024**, *42* (11), 1503−1522.
(372) He, J.; Janáky, C. Recent Advances in Solar-Driven Carbon Dioxide Conversion: Expectations versus Reality. *ACS Energy Lett.* **2020**, *5* (6), 1996−2014.
(373) Rohlfs, J.; Bossers, K. W.; Meulendijks, N.; Valega Mackenzie, F.; Xu, M.; Verheijen, M. A.; Buskens, P.; Sastre, F. Continuous-Flow Sunlight-Powered CO2 Methanation Catalyzed by γ-Al2O3-Supported Plasmonic Ru Nanorods. *Catalysts* **2022**, *12* (2), 126.
(374) Chen, C.; Wu, M.; Xu, Y.; Ma, C.; Song, M.; Jiang, G. Efficient Photoreduction of CO_2 to CO with 100% Selectivity by Slowing Down Electron Transport. *J. Am. Chem. Soc.* **2024**, *146* (13), 9163−9171.
(375) Suppaso, C.; Nakazato, R.; Nakahata, S.; Kamakura, Y.; Ishiwari, F.; Saeki, A.; Tanaka, D.; Kamiya, K.; Maeda, K. Fibrous Pb(II)-Based Coordination Polymer Operable as a Photocatalyst and Electrocatalyst for High-Rate, Selective CO_2 -to-Formate Conversion. *Adv. Funct. Mater.* **2025**, *35* (28), 2417223.
(376) Ozden, A.; Li, J.; Kandambeth, S.; Li, X.-Y.; Liu, S.; Shekhah, O.; Ou, P.; Zou Finfrock, Y.; Wang, Y.-K.; Alkayyali, T.; Pelayo García De Arquer, F.; Kale, V. S.; Bhatt, P. M.; Ip, A. H.; Eddaoudi, M.; Sargent, E. H.; Sinton, D. Energy- and Carbon-Efficient CO2/CO Electrolysis to Multicarbon Products via Asymmetric Ion Migration-Adsorption. *Nat. Energy* **2023**, *8* (2), 179−190.
(377) Bhargava, S. S.; Azmoodeh, D.; Chen, X.; Cofell, E. R.; Esposito, A. M.; Verma, S.; Gewirth, A. A.; Kenis, P. J. A. Decreasing the Energy Consumption of the CO_2 Electrolysis Process Using a Magnetic Field. *ACS Energy Lett.* **2021**, *6* (7), 2427−2433.
(378) *Twelve announces plans to scale production of sustainable aviation fuel made from CO2 in Washington State.* Washington State Department of Commerce. https://www.commerce.wa.gov/twelve-announces-plans-to-scale-production-of-sustainable-aviation-fuel-made-from-co2-in-washington-state/ (accessed 2025-04-11).
(379) *OCO Chem - Technology.* https://ocochem.com/technology/ (accessed 2025-11-05).
(380) Ma, W.; Morales-Vidal, J.; Tian, J.; Liu, M.-T.; Jin, S.; Ren, W.; Taubmann, J.; Chatzichristodoulou, C.; Luterbacher, J.; Chen, H. M.; López, N.; Hu, X. Encapsulated Co-Ni Alloy Boosts High-Temperature CO2 Electroreduction. *Nature* **2025**, *641* (8065), 1156−1161.

(381) Baxter, S. J.; Rine, M.; Min, B.; Liu, Y.; Yao, J. Near 100% CO2 Conversion and CH4 Selectivity in a Solid Oxide Electrolysis Cell with Integrated Catalyst Operating at 450 °C. *J. CO2 Util.* **2022**, *59*, 101954.
(382) *Co production decarbonized | CO2 to CO | Convert CO2 into carbon monoxide | Topsoe.* https://www.topsoe.com/processes/carbon-monoxide (accessed 2025-04-30).
(383) Hermann, M.; Teleki, A.; Weitz, S.; Niess, A.; Freund, A.; Bengelsdorf, F. R.; Takors, R. Electron Availability in CO_2, CO and H_2 Mixtures Constrains Flux Distribution, Energy Management and Product Formation in *Clostridium Ljungdahlii*. *Microb. Biotechnol.* **2020**, *13* (6), 1831−1846.
(384) Davin, M. E.; Thompson, R. A.; Giannone, R. J.; Mendelson, L. W.; Carper, D. L.; Martin, M. Z.; Martin, M. E.; Engle, N. L.; Tschaplinski, T. J.; Brown, S. D.; Hettich, R. L. Clostridium Autoethanogenum Alters Cofactor Synthesis, Redox Metabolism, and Lysine-Acetylation in Response to Elevated H2:CO Feedstock Ratios for Enhancing Carbon Capture Efficiency. *Biotechnol. Biofuels Bioprod.* **2024**, *17* (1), 119.
(385) LanzaTech. *Technology.* LanzaJet. https://www.lanzajet.com/technology (accessed 2025-11-19).
(386) *Projects.* Electrochaea GmbH - Power-to-Gas Energy Storage. https://www.electrochaea.com/projects/ (accessed 2025-04-11).
(387) *The Shunli CO2-to-Methanol Production Plant.* CRI - Carbon Recycling International. https://carbonrecycling.com/projects/shunli (accessed 2025-04-11).
(388) *G2L™ eFuels technology | Process licensing | Products | Topsoe.* https://www.topsoe.com/our-resources/knowledge/our-products/process-licensing/g2ltm-efuels-technology (accessed 2025-04-28).
(389) Hecimovic, A.; Mayer, M. T.; De Haart, L. G. J.; Gupta, S.; Kiefer, C. K.; Navarrete, A.; Schulz, A.; Fantz, U. Benchmarking Microwave-Induced CO2 Plasma Splitting against Electrochemical CO2 Reduction for a Comparison of Promising Technologies. *J. CO2 Util.* **2024**, *83*, 102825.
(390) Jouny, M.; Luc, W.; Jiao, F. General Techno-Economic Analysis of CO2 Electrolysis Systems. *Ind. Eng. Chem. Res.* **2018**, *57* (6), 2165−2177.
(391) Lazard. *Lazard LCOE+ 2024.* https://www.lazard.com/media/xemfey0k/lazards-lcoeplus-june-2024-_vf.pdf (accessed 2025-02-06).
(392) International Energy Agency. *Renewables 2024.* https://iea.blob.core.windows.net/assets/17033b62-07a5-4144-8dd0-651cdb6caa24/Renewables2024.pdf (accessed 2025-02-06).
(393) Denholm, P.; Duraes De Faria, V.; Frost, J. How the U.S. Power Grid Kept the Lights on in Summer 2024. *NREL* **2024**, NREL/TP-6A40−91517.
(394) Shehabi, A.; Smith, S.; Sartor, D.; Brown, R.; Herrlin, M.; Koomey, J.; Masanet, E.; Horner, N.; Azevedo, I.; Lintner, W. United States Data Center Energy Usage Report. *Federal Energy Management Program of the U.S. Department of Energy* **2016**, LBNL-1005775.
(395) Mai, T. T.; Jadun, P.; Logan, J. S.; McMillan, C. A.; Muratori, M.; Steinberg, D. C.; Vimmerstedt, L. J.; Haley, B.; Jones, R.; Nelson, B. Electrification Futures Study: Scenarios of Electric Technology Adoption and Power Consumption for the United States. *NREL* **2018**, NREL/TP-6A20−71500.
(396) Li, Y.; Zhou, E.; Tao, L.; Baek, K.; Sun, P.; Elgowainy, A. Near-Term Electricity Requirement and Emission Implications for Sustainable Aviation Fuel Production with CO_2-to-Fuels Technologies. *NREL* **2023**, NREL/TP-6A20−84838.
(397) Grant, E.; Brunik, K.; King, J.; Clark, C. E. Hybrid Power Plant Design for Low-Carbon Hydrogen in the United States. *J. Phys. Conf. Ser.* **2024**, *2767* (8), 082019.
(398) *World Energy Outlook 2024 - Analysis.* IEA. https://www.iea.org/reports/world-energy-outlook-2024 (accessed 2025-04-30).
(399) *World Energy Transitions Outlook 2024.* https://www.irena.org/Publications/2024/Nov/World-Energy-Transitions-Outlook-2024 (accessed 2025-04-30).
(400) *Executive summary - Electricity 2024 - Analysis.* IEA. https://www.iea.org/reports/electricity-2024/executive-summary (accessed 2025-03-14).
(401) Kätelhön, A.; Meys, R.; Deutz, S.; Suh, S.; Bardow, A. Climate Change Mitigation Potential of Carbon Capture and Utilization in the Chemical Industry. *Proc. Natl. Acad. Sci.* **2019**, *116* (23), 11187−11194.
(402) Jeje, S. O.; Marazani, T.; Obiko, J. O.; Shongwe, M. B. Advancing the Hydrogen Production Economy: A Comprehensive Review of Technologies, Sustainability, and Future Prospects. *Int. J. Hydrog. Energy* **2024**, *78*, 642−661.
(403) U.S. Department of Energy Hydrogen Fuel Cell Technologies Office. *U.S. National Clean Hydrogen Strategy and Roadmap*; U.S. Department of Energy Hydrogen Fuel Cell Technologies Office, 2023. https://www.hydrogen.energy.gov/library/roadmaps-vision/clean-hydrogen-strategy-roadmap.
(404) Howe, C.; O'Dell, K.; Rustagi, N.; Christian, T. *Pathways to Commercial Liftoff: Clean Hydrogen*; U.S. Department of Energy, Office of Clean Energy Demonstrations, 2024. https://liftoff.energy.gov/wp-content/uploads/2025/01/Pathways-to-Commercial-Liftoff_Clean-Hydrogen_December-2024-Update.pdf.
(405) DOE HFTO. *Technical Targets for Proton Exchange Membrane Electrolysis.* Energy.gov. https://www.energy.gov/eere/fuelcells/technical-targets-proton-exchange-membrane-electrolysis (accessed 2023-08-26).
(406) Badgett, A.; Ruth, M.; Pivovar, B. Chapter 10 - Economic Considerations for Hydrogen Production with a Focus on Polymer Electrolyte Membrane Electrolysis. In *Electrochemical Power Sources: Fundamentals, Systems, and Applications*; Smolinka, T., Garche, J., Eds.; Elsevier, 2022; pp 327−364.
(407) Badgett, A.; Brauch, J.; Saha, P.; Pivovar, B. Decarbonization of the Electric Power Sector and Implications for Low-Cost Hydrogen Production from Water Electrolysis. *Adv. Sustain. Syst.* **2024**, *8*, 2300091.
(408) Patel, G. H.; Havukainen, J.; Horttanainen, M.; Soukka, R.; Tuomaala, M. Climate Change Performance of Hydrogen Production Based on Life Cycle Assessment. *Green Chem.* **2024**, *26* (2), 992−1006.
(409) *H2A-Lite: Hydrogen Analysis Lite Production Model | Hydrogen and Fuel Cells | NREL.* https://www.nrel.gov/hydrogen/h2a-lite (accessed 2025-10-10).
(410) *Inauguration of the world's largest PEM electrolyzer to produce decarbonized hydrogen | Air Liquide.* https://www.airliquide.com/stories/industry/inauguration-worlds-largest-pem-electrolyzer-produce-decarbonized-hydrogen (accessed 2025-04-01).
(411) *Affordable Clean Hydrogen Starts Here.* Bloom Energy. https://www.bloomenergy.com/bloomelectrolyzer/ (accessed 2025-04-01).
(412) Badgett, A.; Cooney, G.; Hoffmann, J.; Milbrandt, A. *2023 Billion-Ton Report*; Oak Ridge National Laboratory, 2023. Chapter 7.3: CO2 Emissions from Stationary Sources.
(413) Sievert, K.; Schmidt, T. S.; Steffen, B. Considering Technology Characteristics to Project Future Costs of Direct Air Capture. *Joule* **2024**, *8* (4), 979−999.
(414) Gale, J.; Bradshaw, J.; Chen, Z.; Garg, A.; Gomez, D.; Rogner, H.-H.; Simbeck, D.; Williams, R.; Toth, F.; van Vuuren, D. . *IPCC Special Report on Carbon Dioxide Capture and Storage*; 2025, pp 75−104.
(415) US Department of Energy: Bioenergy Technologies Office. *BETO: Billion-Ton 2023: Chapter 7 - Emerging Resources: Microalgae, Macroalgae, and Point-Source Carbon Dioxide Waste Streams.* https://www.energy.gov/eere/bioenergy/2023-billion-ton-report-assessment-us-renewable-carbon-resources (accessed 2025-04-02).
(416) *Haru Oni.* . https://hifglobal.com/haru-oni (accessed 2025-04-11).
(417) Habibic, A. *Slow-developing e-fuel market prompts Ørsted to terminate FlagshipONE project.* Offshore Energy. https://www.offshore-energy.biz/slow-developing-e-fuel-market-prompts-orsted-to-terminate-flagshipone-project/ (accessed 2025-04-11).

https://doi.org/10.1021/acs.chemrev.5c00361
Chem. Rev. 2026, 126, 5028−5082

(418) *Tianying Inc. Emissions-to-Liquids Technology*. CRI - Carbon Recycling International. https://carbonrecycling.com/projects/tianying-e-methanol (accessed 2025-04-11).
(419) *Jiangsu Sailboat - Chemical Products from Recycled CO2*. CRI - Carbon Recycling International. https://carbonrecycling.com/projects/sailboat (accessed 2025-04-11).
(420) *Liquid Wind's second eFuel facility granted environmental permit — Liquid Wind*. Liquid Wind - eMPowering our Future. https://www.liquidwind.com/news/liquid-winds-second-efuel-facility-granted-environmental-permit (accessed 2025-04-11).
(421) *Kassø e-methanol facility produces industry-grade e-methanol for the first time - European Energy*. https://europeanenergy.com/2025/04/03/kasso-e-methanol-facility-produces-industry-grade-e-methanol-for-the-first-time/, https://europeanenergy.com/2025/04/03/kasso-e-methanol-facility-produces-industry-grade-e-methanol-for-the-first-time/ (accessed 2025-04-11).
(422) *Umeå | eFuel facility — Liquid Wind*. Liquid Wind - eMPowering our Future. https://www.liquidwind.com/umea (accessed 2025-04-11).
(423) *TotalEnergies - Sunfire's SOEC Technology for the e-CO2 Met Project | Sunfire*. https://sunfire.de/en/cases/totalenergies-sunfires-soec-technology-for-the-e-co2-met-project/ (accessed 2025-04-11).
(424) *CO_2-based Polyesters & Chemicals*. Avantium Corporate. https://avantium.com/products-technologies/co2-based-polyesters-chemicals/ (accessed 2025-04-11).
(425) *JM and Reolum partnership*. matthey.com. https://matthey.com/media/2025/media/2025/jm-and-reolum-partnership (accessed 2025-04-23).
(426) *Infinium's Project Pathfinder is World's First Fully Operational eFuels Facility*. Infinium. https://www.infiniumco.com/news/infiniums-project-pathfinder-is-worlds-first-fully-operational-efuels-facility (accessed 2025-04-11).
(427) Kazmer, R. *Startup backed by Bill Gates turns air pollutant and water into clean fuel: "This has all the benefits of fuel as we know it."* The Cool Down. https://www.thecooldown.com/green-tech/infinium-startup-bill-gates-clean-fuel/ (accessed 2025-04-11).
(428) International, B. *HIF Global selects JM tech for South America's largest eFuels plant*. Bioenergy International. https://bioenergyinternational.com/hif-global-selects-jm-tech-for-south-americas-largest-efuels-plant/ (accessed 2025-04-23).
(429) Murer, C. *Pushing forward: Synhelion produces syncrude at plant DAWN*. https://synhelion.com/news/pushing-forward-synhelion-produces-syncrude-at-plant-dawn (accessed 2025-04-11).
(430) Johnson Matthey. *Renewable methanol production with eMERALD CO_2 to methanol technology*. https://matthey.com/products-and-markets/chemicals/methanol/co2-to-methanol (accessed 2025-04-24).
(431) Belsa, B.; Xia, L.; García De Arquer, F. P. CO_2 Electrolysis Technologies: Bridging the Gap toward Scale-up and Commercialization. *ACS Energy Lett.* **2024**, *9* (9), 4293−4305.
(432) Somoza-Tornos, A.; Guerra, O. J.; Crow, A. M.; Smith, W. A.; Hodge, B.-M. Process Modeling, Techno-Economic Assessment, and Life Cycle Assessment of the Electrochemical Reduction of CO2: A Review. *iScience* **2021**, *24* (7), 102813.
(433) Sisler, J.; Khan, S.; Ip, A. H.; Schreiber, M. W.; Jaffer, S. A.; Bobicki, E. R.; Dinh, C.-T.; Sargent, E. H. Ethylene Electrosynthesis: A Comparative Techno-Economic Analysis of Alkaline vs Membrane Electrode Assembly vs CO2-CO-C2H4 Tandems. *ACS Energy Lett.* **2021**, *6* (3), 997−1002.
(434) Gao, T.; Xia, B.; Yang, K.; Li, D.; Shao, T.; Chen, S.; Li, Q.; Duan, J. Techno-Economic Analysis and Carbon Footprint Accounting for Industrial CO2 Electrolysis Systems. *Energy Fuels* **2023**, *37* (23), 17997−18008.
(435) Osorio-Tejada, J. CO2 Conversion to CO via Plasma and Electrolysis: A Techno-Economic and Energy Cost Analysis. *Environ. Sci.* **2024**, *17*, 5833−5853.
(436) Da Cunha, S. C.; Resasco, J. Insights from Techno-Economic Analysis Can Guide the Design of Low-Temperature CO_2 Electrolyzers toward Industrial Scaleup. *ACS Energy Lett.* **2024**, *9* (11), 5550−5561.
(437) Detz, R. J.; van der Zwaan, B. Cost Projections for Microwave Plasma CO Production Using Renewable Energy. *J. Energy Chem.* **2022**, *71*, 507−513.
(438) Portillo, E.; Gandara-Loe, J.; Reina, T. R.; Pastor-Pérez, L. Is the RWGS a Viable Route for CO2 Conversion to Added Value Products? A Techno-Economic Study to Understand the Optimal RWGS Conditions. *Sci. Total Environ.* **2023**, *857*, 159394.
(439) Xavier Silva, C.; Moncada Botero, J.; Sastre, F.; van den Ham, J.; Buskens, P.; Meulendijks, N.; Detz, R. J. Techno-Economic Analysis for the Sunlight-Powered Reverse Water Gas Shift Process: Scenarios, Costs, and Comparative Insights. *Sustain. Energy Technol. Assess.* **2024**, *65*, 103768.
(440) Harris, K.; Grim, R. G.; Huang, Z.; Tao, L. A Comparative Techno-Economic Analysis of Renewable Methanol Synthesis from Biomass and CO2: Opportunities and Barriers to Commercialization. *Appl. Energy* **2021**, *303*, 117637.
(441) Bazmi, M.; Gong, J.; Jessen, K.; Tsotsis, T. Waste CO2 Capture and Utilization for Methanol Production via a Novel Membrane Contactor Reactor Process: Techno-Economic Analysis (TEA), and Comparison with Other Existing and Emerging Technologies. *Chem. Eng. Process. - Process Intensif.* **2024**, *201*, 109825.
(442) Zang, G.; Sun, P.; Elgowainy, A.; Wang, M. Technoeconomic and Life Cycle Analysis of Synthetic Methanol Production from Hydrogen and Industrial Byproduct CO2. *Environ. Sci. Technol.* **2021**, *55* (8), 5248−5257.
(443) De Luna, P.; Hahn, C.; Higgins, D.; Jaffer, S. A.; Jaramillo, T. F.; Sargent, E. H. What Would It Take for Renewably Powered Electrosynthesis to Displace Petrochemical Processes? *Science* **2019**, *364* (6438), No. eaav3506.
(444) Cordero-Lanzac, T.; Ramirez, A.; Navajas, A.; Gevers, L.; Brunialti, S.; Gandía, L. M.; Aguayo, A. T.; Mani Sarathy, S.; Gascon, J. A Techno-Economic and Life Cycle Assessment for the Production of Green Methanol from CO2: Catalyst and Process Bottlenecks. *J. Energy Chem.* **2022**, *68*, 255−266.
(445) Badgett, A.; Brauch, J.; Saha, P.; Pivovar, B. Decarbonization of the Electric Power Sector and Implications for Low-Cost Hydrogen Production from Water Electrolysis. *Adv. Sustain. Syst.* **2024**, *8* (9), 2300091.
(446) Rosental, M.; Fröhlich, T.; Liebich, A. Life Cycle Assessment of Carbon Capture and Utilization for the Production of Large Volume Organic Chemicals. *Front. Clim.* **2020**, *2*, 586199.
(447) Sadok, R.; Benveniste, G.; Wang, L.; Clavreul, J.; Brunot, A.; Cren, J.; Jegoux, M.; Hagen, A. Life Cycle Assessment of Power-to-Gas Applications via Co-Electrolysis of CO_2 and H_2 O. *J. Phys. Energy* **2020**, *2* (2), 024006.
(448) Khojasteh-Salkuyeh, Y.; Ashrafi, O.; Mostafavi, E.; Navarri, P. CO2 Utilization for Methanol Production; Part I: Process Design and Life Cycle GHG Assessment of Different Pathways. *J. CO2 Util.* **2021**, *50*, 101608.
(449) Lee, U.; R Hawkins, T.; Yoo, E.; Wang, M.; Huang, Z.; Tao, L. Using Waste CO2 from Corn Ethanol Biorefineries for Additional Ethanol Production: Life-cycle Analysis. *Biofuels Bioprod. Biorefining* **2021**, *15* (2), 468−480.
(450) De Kleijne, K.; De Coninck, H.; Van Zelm, R.; Huijbregts, M. A. J.; Hanssen, S. V. The Many Greenhouse Gas Footprints of Green Hydrogen. *Sustain. Energy Fuels* **2022**, *6* (19), 4383−4387.
(451) Ravikumar, D.; Keoleian, G.; Miller, S. The Environmental Opportunity Cost of Using Renewable Energy for Carbon Capture and Utilization for Methanol Production. *Appl. Energy* **2020**, *279*, 115770.

https://doi.org/10.1021/acs.chemrev.5c00361
Chem. Rev. 2026, 126, 5028−5082